UNDERSTANDING THE ROLE OF HEMATOPOIETIC PBX-INTERACTING PROTEIN (HPIP) IN TAXOL RESISTANCE USING BREAST CANCER AS A MODEL SYSTEM

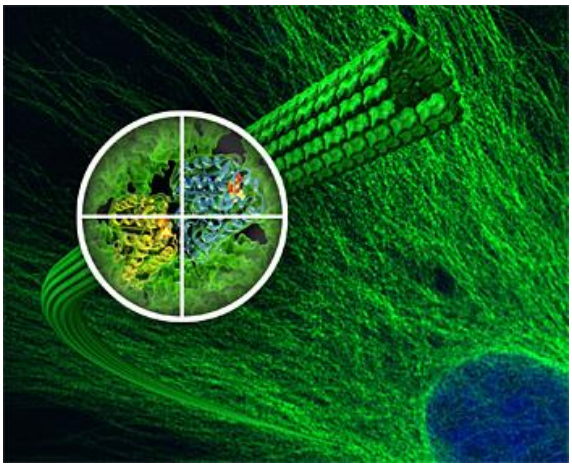

Thesis submitted for the degree of
DOCTOR OF PHILOSOPHY
In BIOCHEMISTRY
By

Oindrilla Dey
08LBPH05
Supervisor: Dr. Bramanandam Manavathi, PhD

Department of Biochemistry
School of Life Sciences
University of Hyderabad
Hyderabad-50004

Department of Biochemistry
School of Life Sciences
University of Hyderabad
Hyderabad 500 046
India

CERTIFICATE

This is to certify that this thesis entitled **"Understanding the role of Hematopoietic PBX-interacting Protein (HPIP) in taxol resistance using breast cancer as a model system"** submitted to the University of Hyderabad by **Ms Oindrilla Dey**, for the degree of Doctor of Philosophy, is based on the studies carried out by him under my supervision. I declare to the best of my knowledge that this has not been submitted earlier for the award or diploma from any other University or Institution.

Dr. Bramanandam Manavathi, Ph.D.,

Supervisor

Head

Department of Biochemistry

Dean

School of Life Sciences

Department of Biochemistry
School of Life Sciences
University of Hyderabad
Hyderabad 500 046
India

DECLARATION

I hereby declare that the work presented in this thesis is entirely original and was carried out by me in the Department of Biochemistry, University of Hyderabad, under the supervision of **Dr. Bramanandam Manavathi, Ph.D.** I further declare that this work has not been submitted earlier for the award of degree or diploma from any other University or Institution.

Dr. Bramanandam Manavathi, Ph.D., Ms Oindrilla Dey

Supervisor

Date:

Place: Department of Biochemistry

University of Hyderabad - 500 046

Department of Biochemistry
School of Life Sciences
University of Hyderabad
Hyderabad 500 046
India

DECLARATION

I, **Oindrilla Dey**, hereby declare that this thesis entitled **"Understanding the role of Hematopoietic PBX-interacting Protein (HPIP) in taxol resistance using breast cancer as a model system"** submitted by me under the supervision of **Dr. Bramanandam Manavathi, Ph.D.**, is a bonafide research work which is also free from plagiarism. I also declare that it has not been submitted previously in part or full to this university or any other university or institution for the award of degree or diploma. I hereby agree that my thesis can be deposited in shodganga/ INFLIBNET.

A report on plagiarism statistics from the university librarian is enclosed.

Dr. Bramanandam Manavathi, Ph.D. Ms Oindrilla Dey

Supervisor

Date:

Place: Department of Biochemistry

University of Hyderabad - 500 046

Acknowledgments

To all who have inspired and motivated me to pursue research in life science, I express my sincere gratitude.

I would like to thank my supervisor, Dr Bramanandam Manavathi, who has been a motivation himself. I am grateful for his invaluable guidance, advice, criticism and support at every stage of this work. I've learnt so much from him.

I am greatly thankful to my doctoral committee members, Dr. O.H Shetty and Dr. S Rajagopal for their invaluable insights and suggestions on my thesis work.

I would like to thank the present and former Heads of Department of Biochemistry (Prof. N. Siva Kumar, Prof. O.H. Setty, Prof. K.V.A Ramaiah, Prof. M. Ramanadham) and Deans of School of Life Sciences (Prof. Pallu Reddanna, Prof. A.S Raghavendra, Prof. R.P. Sharma, Prof. Aparna Dutta Gupta, Prof. M. Ramanadham) for allowing me to use all the central facilities of department and school.

I would like to thank Dr. Naresh Babu V Sepuri, Dr. S. Rajagopal, Dr. Suresh Yenugu, and Dr Sharmistha Banerjee, and their students for allowing me to use their lab facilities.

I thank Dr Roy for helping me with my FACS studies.

I thank all faculty members of School of Life Sciences and also all the non-teaching staff for their timely help.

I consider myself lucky to have lab mates like Suresh, Vijay, Raghav Singh, Saratchandra, Mythili, Srinadh, Subramanyam Kumar, Anita, Praveen, Azita, Vasu, Anju, and Naresh, who made my stay in the lab wonderful.

I thank Dr Barnali, Dr Merino, Dr Suneel, and Dr Sunilparthasarathy for their support and friendship.

I thank all my friends for their love, affection and support.

I greatly acknowledge UoH and CSIR for providing me financial assistance, and all the funding bodies (CSIR, DBT, CREBB, DST, FIST, UPE, and PURSE) for their financial aid to the department and school.

I am grateful to my mother and father, who instilled in me a curiosity and a desire to work hard that have proven to be invaluable during the entire course of PhD. I thank them for their love, kindness and support. I thank my brother, Dr Biplab, for inspiring and guiding me throughout my PhD.

Finally, I thank Rishiraj for being a part of my life.

…Oindrilla Dey

ACRONYMS

2ME2	2-methoxy-estradiol
7AAD	7- aminoactinomycin
Aa	**a**mino acid
APS	Ammonium persulphate
Bak	BCL2-Antagonist/Killer
Bcl2	B-cell lymphoma 2
BIM	B-cell lymphoma 2 interacting mediator of cell death
BSA	Bovine serum albumin
$CaCl_2$	Calcium chloride
Cdk1	Cyclin-dependent kinase1
cDNA	Complementary DNA
CLIP 170	Class II-associated invariant chain peptide
CO_2	Carbon Dioxide
CrEL	Cremophor EL
DAPI	4',6-diamidino-2-phenylindole
DCIS	Ductal carcinoma *in situ*
DEAE	Diethylaminoethanol
DEP domain	Dishevelled, Egl-10 and Pleckstrin domain
DMEM	Dulbecco's Modified Eagle's medium
DMSO	Dimethyl sulfoxide
dNTP	Deoxyribonucleotide triphosphate
dT	Deoxythymidine
DTT	Dithiothreitol

EB1	End binding protein 1
ECL	Enhanced chemiluminescence
EDTA	Ethylenediaminetetraacetic acid
Eg5	Kinesin 5
EGTA	Ethylene glycol tetraacetic acid
ER	Estrogen receptor
FACS	Fluorescence-activated cell sorting
FAK	Focal adhesion kinase
FBS	Fetal bovine serum
FDA	Food and Drug administration
FOXM1	Forkhead box protein M1
FtsZ	Filamenting temperature-sensitive mutant Z
GAPDH	Glyceraldehyde 3-phosphate dehydrogenase
GCP	Gamma-tubulin complex proteins
GDP	Guanosine diphosphate
GEO	Gene Expression Omnibus
GFP	Green fluorescent protein
GSK-3β	Glycogen synthase kinase 3 beta
GST	Glutathione S-transferase
GTP	Guanosine-5'-triphosphate
HDAC6	Histone deacetylase 6
HEK293T	Human Embryonic Kidney 293 T cells
HER2	Human epidermal growth factor receptor 2
HPIP	Hematopoietic PBX interacting protein
HRP	Horseradish peroxidase

IC_{50}	Half maximal inhibitory concentration
IDC	Invasive Ductal Carcinoma
IgG	Immunoglobulin G
JNK	c-Jun N-terminal kinase
KCl	Potassium Chloride
kD	kilo Daltons
KSP	Kinesin spindle protein
LCIS	Lobular carcinoma *in situ*
M	Molar
MAPK	Mitogen-activated protein kinases
MAPs	Microtubule associated proteins
MBC	Metastatic breast cancer
MCF7	Michigan Cancer Foundation-7 cells
MDR	Multidrug resistance
$MgCl_2$	Magnesium chloride
M-MuLV	Moloney Murine Leukemia Virus
MPF	Maturation promoting factor
MT	Microtubules
MTOC	Microtubule organisation centre
NaCl	Sodium chloride
NES	Nuclear export signal
NF-κB	Nuclear factor-κB
Nlp	Ninein-like protein
NLS	Nuclear localisation signal
NMR	Nuclear magnetic resonance

NP40	Nonidet P-40
Op18	Stathmin/oncoprotein 18
Opti-MEM	Opti- Minimum Essential Medium
PARP	Poly (ADP-ribose) polymerase
PBS	Phosphate-buffered saline
PBX1	Pre-B-cell leukemia homeobox 1
PCM	Pericentriolar material
Pgp	P- glycoprotein
PI	Propidium iodide
PI3K	Phosphoinositide 3-kinase
PIPES	Piperazine-N, N′-bis (2-ethanesulfonic acid
PMG	Phosphate Magnesium chloride GTP
PMSF	Phenylmethylsulfonyl fluoride
RIPA	Radio-immunoprecipitation assay
Rpm	Revolutions per minute
RT-PCR	Reverse transcriptase Polymerase Chain Reaction
SAC	Spindle assembly checkpoint
SDS-PAGE	Sodium dodecyl sulphate polyacrylamide gel
shRNA	Small or short hairpin RNA
SIRT2	Sirtuin 2
TAZ	Transcriptional coactivator with PDZ-binding motif
TBA	Microtubule binding agents
TBS	Tris buffered solution
TEM	Transmission electron microscopy
TEMED	Tetramethylethylenediamine

TTL	Tubulin tyrosine ligase
VBL	Vinblastine
VCR	Vincristine
VDS	Vindesine
VRL	Vinorelbine
WHO	World Health Organisation
WST-1	Water soluble tetrazolium 1
α-TAT	α-tubulin acetyl transferase
γ-TuRCs	Gamma-tubulin ring complex

Table of Contents

CHAPTER I

GENERAL INTRODUCTION

CHAPTER II

ROLE OF HPIP IN TAXOL RESISTANCE IN BREAST CANCER CELLS

Chapter 1

General Introduction

1.1 BREAST CANCER

According to International Agency for Research on Cancer, 1.7 million women were diagnosed with breast cancer in 2012 alone and about 6.3 million women are alive with breast cancer diagnosed in the previous five years (Ferley *et al.,* 2015). The GLOBOCAN 2012 report published by WHO indicates a 20% rise in breast cancer incidence compared to 2008, and a 14% increase in mortality rate. Breast cancer is the second most common cancer and the leading cause of cancer death among women (522,000 deaths in 2012). The incidence rates vary widely across the world from 27 per 100,000 in Asian and Middle African countries to 96 in Western Europe, US, Canada and Australia. It now represents one in four of all cancers in women. With such high incidence, one out of every eight women now has a chance of developing breast cancer during their lifetime.

Breast cancer can originate in different areas of the breast — the ducts, lobules, or in some cases, the tissue in between. Histologically, breast cancer can be classified into the following types:

1) Ductal carcinoma *in situ* (DCIS) which is a non-invasive form,
2) Invasive Ductal Carcinoma (IDC) which can be again of different types based on histology, e.g., tubular, medullary, mucinous, papillary, cribriform
3) Lobular carcinoma *in situ* (LCIS)
4) Invasive Lobular Carcinoma
5) Inflammatory breast cancer

Another major way of defining breast cancer type is by hormonal receptor profiling of the tumour.

- Estrogen or progesterone receptor positive
- HER2 positive

- Triple negative (TNBC), negative to estrogen, progesterone, or HER2 receptors
- Triple positive, positive to estrogen, progesterone and HER2 receptors

The most common treatment includes surgery, radiotherapy and chemotherapy. Most patients with breast cancer surgically remove the cancerous tissue from the breast. It can be either partial or total mastectomy. Surgery is mostly accompanied by radiotherapy or chemotherapy to kill the remaining cancer cells which could not be removed at the time of surgery. Chemotherapy includes administration of a wide range of drugs that has been approved for breast cancer treatment. Anti-microtubule agents form an integral component of cancer chemotherapy. Based on their effect on microtubule polymerization these agents are classified into two types: those destabilizing polymerization, such as vinca alkaloids and those stabilizing polymerization such as the taxanes. Both these types however serve the same purpose of disrupting the equilibrium between microtubule polymers and soluble tubulin subunits, and results in mitotic arrest followed by apoptosis. Although these drugs have different mechanisms of action, eventually acquired or *de novo* resistance fails most cancer treatments. Hormone therapy is a type of cancer treatment given to hormone-receptor positive breast cancers mostly at early stages or if the cancer has metastasized, to remove hormones or attenuate their action by blocking their receptors and inhibiting cancer cells from growing. Hormone therapy with aromatase inhibitors inhibits the enzyme called aromatase from turning androgens to estrogens and, is the preferred line of treatment for postmenopausal women. Another type of treatment is targeted therapy which includes monoclonal antibodies and tyrosine kinase inhibitors that specifically identifies and attacks cancer cells keeping normal cells unharmed. PARP inhibitors forms a type of targeted therapy used in the treatment of TNBC. Trastuzumab is a monoclonal antibody that targets and blocks HER2. Trastuzumab combined with chemotherapy is highly effective and is prescribed for about one out of four breast cancer patients. Often, Pertuzumab, another monoclonal antibody is used in combination with trastuzumab and chemotherapy to treat HER2

positive breast cancer patients. In case, trastuzumab treatment fails and cancer progresses, patients are treated with Lapatinib, a tyrosine kinase inhibitor that blocks HER2 and other proteins in tumour cells.

1.2 MICROTUBULES

1.2.1. Microtubule structure

Microtubules consist of long, hollow filaments of about 25 nm in diameter, which forms the key components of the eukaryotic cytoskeleton (Wade and Hyman 1997; Downing and Nogales, 1998; Kavallaris, 2010). They play important roles in diverse cellular functions including development and maintenance of cell shape, localization of organelles, intracellular trafficking, cell signalling and segregation of chromosomes during mitosis (Hoenger *et al.*, 1994; Jordan and Wilson, 2004; Kalinina *et al.*, 2013).

Microtubules are made up of tubulin monomers that are globular proteins of 50 kD each and consist of 5 distinct families, the alpha (α), beta (β), gamma (γ), delta (δ), epsilon (ε) and zeta (ζ) tubulin that are encoded in different chromosomes (Dutcher, 2003; Kaur *et al*,. 2014). All tubulins share a common ancestor with the distantly related prokaryotic cell division protein, FtsZ (Pilhofer *et al.,* 2011). Of these tubulins, α- and β- tubulins associate in a head to tail manner to form a protofilament. Thirteen such protofilaments are sealed by lateral interactions to form a single hollow microtubule (Tilney *et al.,* 1973). This arrangement of the tubulin heterodimer gives the polymer a polarity with one end having α-tubulin (minus end) and the other end having an exposed β-tubulin (plus end; Fig 1). Each tubulin (~450 amino acids) monomer consists of three functional domains; the N-terminal domain (residues 1-206) which is involved in nucleotide binding (GTP/GDP), a central domain (residues 207-384) involved in lateral/longitudinal association between α and β-tubulin monomers to form protofilaments, and

a C-terminal domain (starting from residue 385) which is involved in binding to microtubule associated proteins (MAPs) and mitotic kinesin Eg5 (Orr *et al.*, 2003; Sui and Downing, 2010). Although highly conserved, α- and β- tubulins show extensive molecular heterogeneity in their C- terminal domains giving rise to multiple isotypes. Each α- and β- tubulin have 6 isotypes encoded by distinct genes located on different chromosomes. These tubulin isotypes show specific tissue and cell expression patterns, and undergo various post-translational modifications, e.g., phosphorylation, acetylation, detyrosination and glutamylation that alter the interaction of microtubules with MAPs and therefore, their function. This results in a unique 'tubulin code' (Bhalla, 2003; Janke, 2014; Sirajuddin *et al.*, 2014).

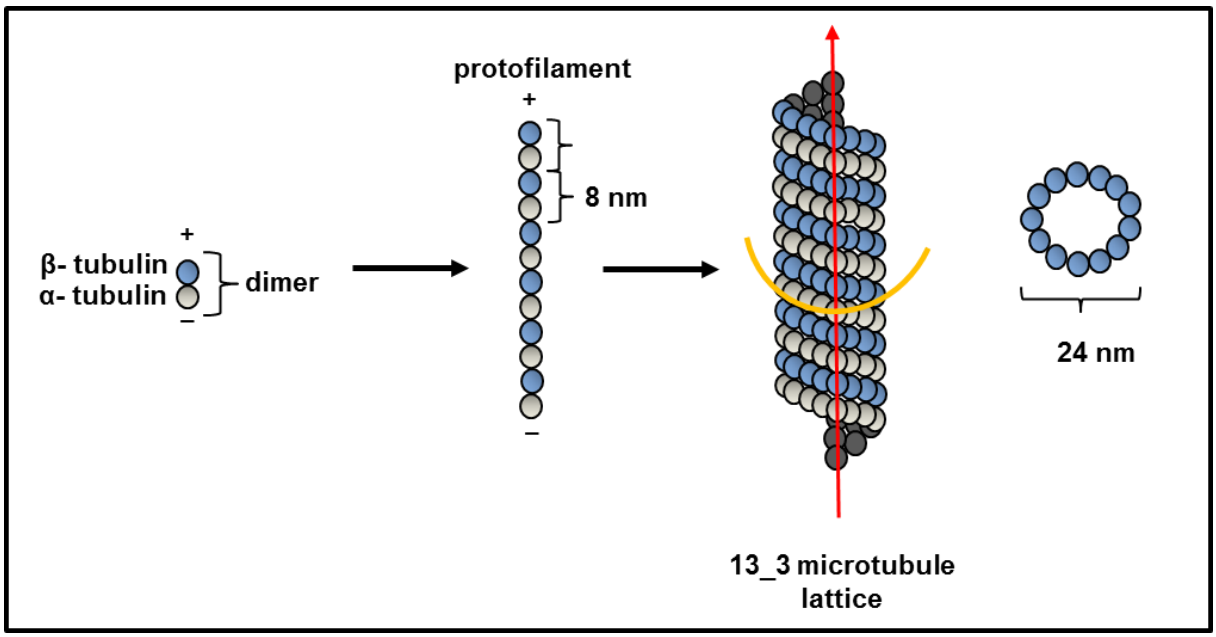

Figure 1. Microtubule structural organisation. Microtubules consist of polymers of α- and β- tubulins which associate to form protofilaments. 13 such protofilaments together form a hollow microtubule of ~25 nm diameter. The arrangement of α- and β- tubulins in a head to tail manner gives the microtubule a 'plus' end with β- tubulin exposed and a 'minus' end with α-tubulin exposed.

1.2.2 Microtubule dynamics

Microtubules are highly dynamic cytoskeletal structures that switch between cycles of polymerisation and depolymerisation. A precise control over microtubule dynamics has led the

cells to organize and reorganize the cytoskeleton for various cellular functions. The polymerization of microtubules occurs by a nucleation-elongation mechanism (Voter and Erickson, 1984; Tassin and Bornens, 1999). *In vivo*, formation of new microtubules is nucleated in a region called centrosome or microtubule organisation centre (MTOC). The centrosome consists of a pair of centriole surrounded of a complex of proteins called pericentriolar material (PCM) (Moritz *et al.,* 1995). The MT (-) end remains anchored to the centrosome whereas the (+) ends radiate out into the cytoplasm, towards the cell periphery (Gorbsky *et al.*,, 1988). However, higher plant cells lacks such centrosome. The most important structural component of the centriole is the γ-tubulin which form complexes with additional proteins, termed γ-tubulin complex proteins (GCPs).

Several models have been proposed so far for microtubule nucleation mechanism. The two most widely accepted models are the 'template model' and the 'protofilament model'. In the template model, γ-tubulin molecules laterally interact forming a ring complex, upon which αβ-tubulin heterodimers gets added to grow into a hollow tube. On the other hand, the protofilament model proposes that γ-tubulin ring complexes (γ-TuRCs) are short protofilaments formed by longitudinal association of γ-tubulin molecules that curl up due to the intrinsic curvature of the GTP bound γ-tubulin monomers, similar to GDP-bound, unpolymerized αβ-tubulin. Unlike α- and β-tubulin heterodimers, GTP-bound γ-tubulin can associate laterally in the γ-TuRC even with their curved conformation providing a template for weak lateral interaction between αβ-tubulin heterodimers. The protofilaments can then grow rapidly by continuous reversible non-covalent addition of α/β-tubulin heterodimers at their open plus-end. Concomitantly, lateral association of multiple protofilaments (>11) then leads to closure of a microtubule. However, microtubule lengthening only occurs when an energetically lattice is formed, e.g., 13_3 lattice, else it undergoes immediate catastrophe.

However, experimental proof for both models has been found making both models equally accepted (Aldaz *et al.,* 2005).

Microtubules exhibit two kinds of non-equilibrium dynamics, both *in vitro* and *in vivo*, and require energy in the form of GTP to mediate such dynamicity. One is called 'dynamic instability' proposed by Mitchison and Kirschner in 1984 and the other is called 'treadmilling' (Fig 2; Mitchison and Kirschner, 1984b). In dynamic instability, microtubules exist either in a slow elongation state or a rapid shortening state, with intermittent periods of constricted dynamics or pause, with no net growth in the microtubules. Polymerization of microtubules occur when GTP binds to the nucleotide exchangeable site (E-site) in β-tubulin and the non-exchangeable site (N-site) in α-tubulin. During or soon after polymerization, GTP at the exchangeable or E-site of β-tubulin is hydrolyzed (David-Pfeuty *et al.,* 1977, MacNeal & Purich, 1978) resulting in a nonexchangeble GDP at the β-tubulin E-site. Thus, the β-tubulin in the polymer has a GDP at E-site. Only upon depolymerization, the released β-tubulin subunits exchange GDP for GTP at E-site for another round of polymerization. On the other hand, α-tubulin also binds to GTP but at a non-exchangeable site (N-site), which during polymerization remains unhydrolysed. Although β-tubulin has an exchangeable GTP, it is the α- tubulin that triggers GTP hydrolysis to GDP+ Pi at the E-site β-tubulin, following which β-tubulin changes to a curved conformation locking the tubulin-GDP to the core of the microtubule and maintains association between the protofilaments (Carlier *et al.,* 1984; O'Brien *et al.,* 1987; Alushin *et al.,* 2014). Dynamic instability requires a β-tubulin-GTP cap at the end of the growing MTs that stabilizes the MTs (Mitchison & Kirschner 1984a). Thus, stoichiometrically microtubules are polymers of (GTP: α-tubulin /GDP: β-tubulin)$_n$, with a GTP (or GDP- Pi): β-tubulin cap at the growing end which accommodates continuous addition of tubulin heterodimers (Nogales, 1999). In the presence of the GTP cap, the microtubule plus end is stabilized and grows rapidly, whereas, once the cap is lost, the GDP-containing polymers

get unstabilised and the protofilaments peel off outwardly (Panda *et al.*, 2002). Also, the growing (+) end of microtubule can generate high force by converting chemical energy from GTP hydrolysis to mechanical force, which is required for various forms of cellular motility (Dogterom and Yurke, 1997).

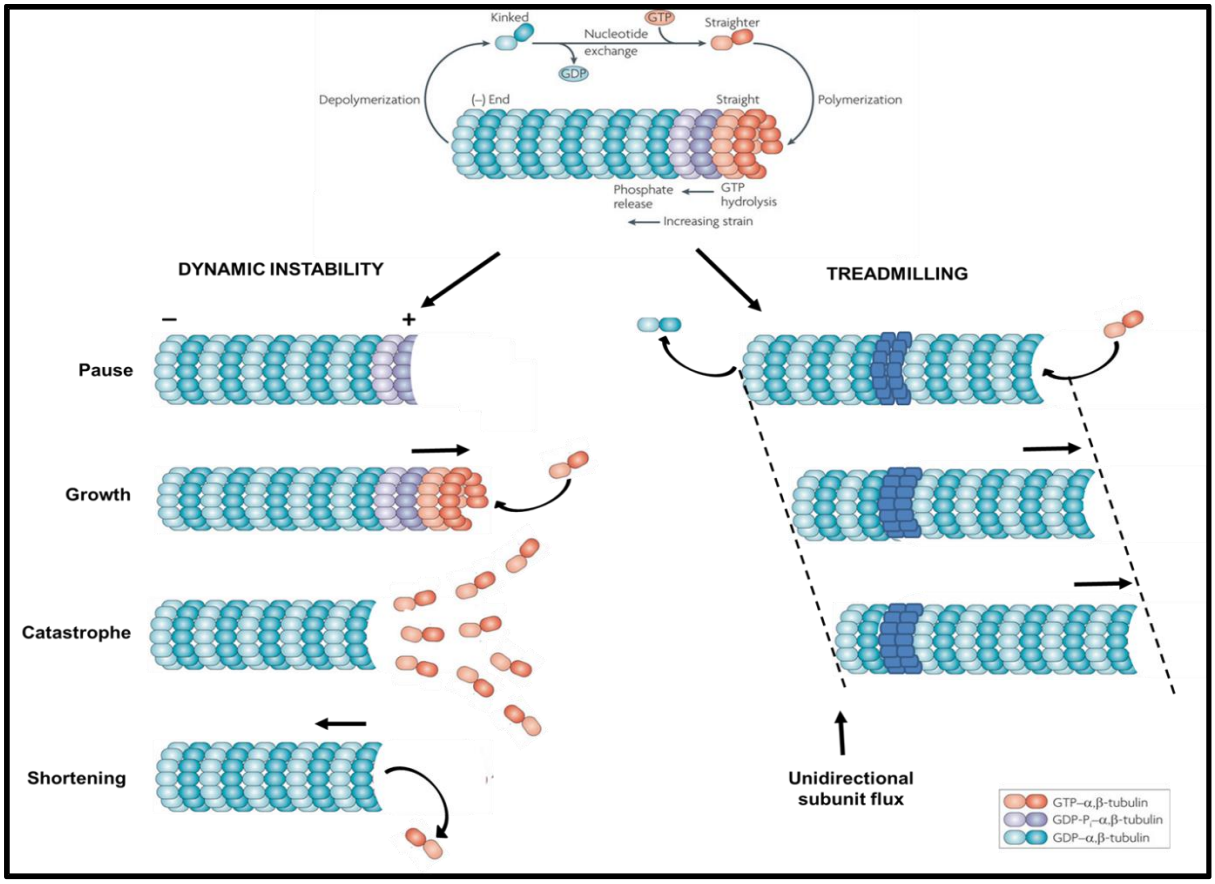

Figure 2. Microtubule assembly dynamics and organization. Microtubules shows two kinds of GTP-dependant dynamic behaviour, dynamic instability and treadmilling. During dynamic instability, tubulin subunits associate and dissociate from the plus end of the protofilaments, resulting in either growth or shortening of the microtubules. Treadmilling, on the other hand, occurs when one end of a filament grows in length while the other end shrinks. Though net growth remains same, it appears like a section of filament "moving" across a stratum or the cytosol.

The second dynamic behaviour is called ‘treadmilling’. At steady state treadmilling, the MT polymer has constant addition of tubulin heterodimers at one end balanced with simultaneous loss at the other end, keeping constant net growth (Margolis and Wilson, 1978). This occurs

due to difference in the critical tubulin subunit concentrations at the two ends of the microtubule (Fig 2; Rodionov and Borisy, 1997). Treadmilling is particularly observed during mitosis. At a particular time, a specific microtubule population can display either treadmilling, dynamic-instability or even both, depending on the composition of the microtubule population, i.e., isotype composition, posttranslational modifications and composition of its associated proteins.

1.2.3 Role of microtubules in mitosis

The highly dynamic nature of microtubules is crucial for their role in cell division and chromosomal segregation during mitosis. This, in turn, regulates cell proliferation and cell migration in tumor progression. During interphase, microtubules grows out from the MTOC and function as stable protein scaffolds for cellular protein and vesicle transport. Microtubule turn over, i.e., the exchange rate between the polymerised tubulin with the soluble tubulin pool, is relatively slow during interphase, with half-times ranging from several minutes to several hours (Kline-Smith and Walczac, 2004). During G1 to S phase, the two centrosomal centrioles separate and duplicate. They enlarge in size by late G2 phase and remain attached together till the beginning of mitosis. With the onset of mitosis, the interphase microtubule network starts depolymerizing and is replaced by highly dynamic microtubules (Sharp *et al.,* 2000). In eukaryotic cells, mitosis is initiated when cyclin B1 complexes with the cyclin-dependent kinase (cdk1) to form maturation promoting factor (MPF). In early prophase, centrosomes separate to form the spindle poles, and DNA condenses into chromosomes. This is mediated by kinesin spindle proteins, kinesin Eg5. Based on their roles in mitosis, MTs can be characterized into three subsets. Firstly, the kinetochore MTs (kMTs), which remain attached to sister chromatids at the kinetochore by its plus ends. Secondly, interpolar MTs which extends from the opposite pole and interdigitate at the spindle midzone. Thirdly, astral MTs which

extends out from the spindle. During early prophase, MT are highly dynamic and nucleation rate at the centrosomes increases by 4-fold. The MT (+) ends starts emanating radially from the spindle poles. Since the nuclear envelope is still intact, the growth of these MTs is stabilized by nuclear envelope proteins. Thus, the initial events are regulated by cytoplasmic factors. Once the nuclear envelope breaks down, chromosomes and nuclear factors are released into the cytoplasm resulting in a dramatic increase in microtubule (MT) dynamics (Wittman *et al.*, 2001). During prometaphase, plus ends of kinetochore MTs grows as long as 5-10 µm, dissociates completely and then re-grow till it probes the cytoplasm to establish a link with a chromosomal kinetochore, as proposed by the 'Search-and-Capture' model of spindle assembly. The sister chromatid kinetochores can associate with the spindle MTs in a various ways. The most stable being the 'amphitelic attachment' or biorientation, in which both sister kinetochores simultaneously attach to microtubules emanating from opposite centrosomes (Channels *et al.*, 2008).

1.2.4 Microtubule binding agents

The significance of microtubules in the process of mitosis and cell division makes them easy targets for anticancer drugs. These drugs inhibit cancer cell proliferation by interfering with the correct formation of the mitotic spindle, delayed G2-M phase transition, impaired chromosome congression and segregation and subsequent initiation of mitochondrial apoptotic pathway. Microtubule binding agents (TBAs) are classified into two types: those inhibiting polymerization, such as vinca alkaloids and colchicine, and those stabilizing polymerization such as the taxanes. TBAs interfere in MT dynamics by either binding to the β-tubulin subunit of αβ-tubulin on the tubulin heterodimer (MT-destabilizing agents) or the MT wall (MT-stabilizing agents) causing disruption of MT dynamics (Fig 3; Zhou *et al.*, 2005). They mostly function by disrupting the equilibrium between polymerised microtubules and soluble tubulin monomers.

1.2.4.1 Microtubule destabilizing agents

Vinca alkaloids are naturally occurring or semi synthetic nitrogenous bases. They were first isolated in the 1950's by Canadian scientists, Robert Noble and Charles Beer from pink periwinkle (*Catharanthus roseus).* Phytochemical analysis of these compounds initially allowed them to be used for their hypoglycemic activity. Later they were used in medical research for their cytotoxic effects. Vinca drugs have been used for treating diabetes, reduce high blood pressure and also as a sterilizer. However, they have been used greatly as cancer fighters. The four major vinca alkaloids used in medical applications are vinblastine (VBL), vinorelbine (VRL), vincristine (VCR) and vindesine (VDS), out of which only VCR, VBL and VRL have been approved for use by the FDA (USA). From 2008, Europe has approved a new synthetic vinca alkaloid, vinflunine for medicinal treatment (McGrogan *et al.*, 2008). The vinca alkaloids bind with high affinity to the vinca domain located adjacent to the E-site on β-tubulin at the plus (+) end of the microtubule and with low affinity to the sides of the microtubule (Kiselyov *et al.* 2007). This disrupts the GTP cap at the plus end of microtubule leading to its destabilization.

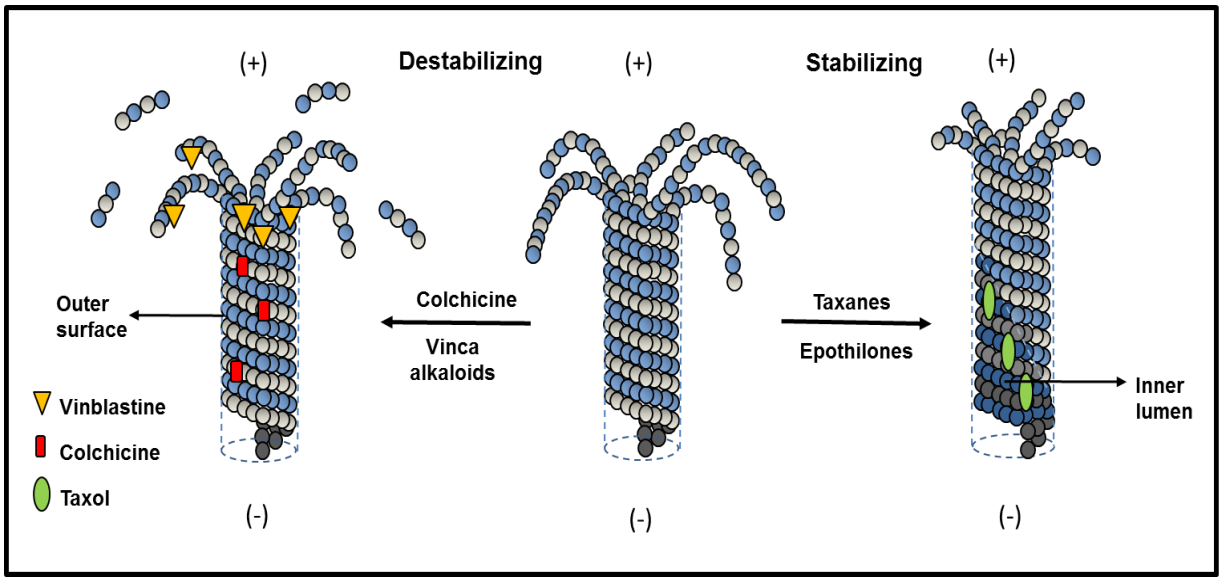

Figure 3. Microtubules binding agents. Microtubule binding agents can be either destabilizing, colchicine and vinca alkaloids, or stabilizing, taxanes and epothilones.

Colchicine was originally extracted from the meadow saffron, *Colchicum autumnale* (Borisy and Taylor, 1967). Due to its high cytotoxicity to normal tissue, it is not used in the treatment of cancer. However, it is used extensively in exploring the functional properties of microtubules and development of drugs against cancer cells. Colchicine binds to a domain located at the β-tubulin and α-tubulin interface (Kaur *et al.,* 2014*).* Other drugs, combretastatin and 2-methoxy-estradiol (2ME2), can also bind to the colchicine site. Combretastatin (isolated from the South African willow *Combretum caffrum*) binds to tubulin, destabilizes microtubule and leads to mitotic arrest with subsequent apoptosis, whereas, 2ME2 is a metabolite of estradiol, which inhibits cancer cell growth *in vitro* (McGrogan *et al.,* 2008).

1.2.4.2 Microtubule stabilizing agents

Paclitaxel is the most commonly used MT-stabilizing drug in anticancer therapy. It was originally isolated from the bark of the Pacific yew tree, *Taxus brevifolia* in 1971. It was only in 1992 that the Food and Drug administration (FDA, USA) approved it for the treatment of advanced ovarian cancer and subsequently for metastatic breast cancer treatment in 1994. Electron crystallography revealed that paclitaxel binds within a hydrophobic cleft of β-tubulin and laterally interact with the tubulin subunits via hydrogen bonding and hydrophobic contact. The binding of paclitaxel results in lateral polymerization and enhanced microtubule stability leading to G2-M phase arrest followed by apoptosis (Yared and Tkaczuk, 2012). Details of paclitaxel action will be discussed in the latter sections.

Epothilones belongs to a new class of MT- stabilizing agent that, were isolated from myxobacterium *Sorangium cellulosum.* Like paclitaxel, epothiones stabilizes microtubules by binding to the β-tubulin, and induces mitotic arrest followed by apoptosis. Although epothilones and taxanes share overlapping binding sites on β-tubulin, but they are not identical (Nettles *et al.,* 2004). Clinical trials with epothilone B (Patupilone; Novartis) and an analogue

of epothilone B (Ixabepilone; Bristol-Myers squibb), have been successful in treating metastatic breast cancer patients who are resistant to both taxanes and anthracyclines (Sabbatini and Spriggs, 2009). A clear advantage of epothilones over paclitaxel is that they are undetected by P-glycoproteins and can bypass the resistance mechanisms associated with drug efflux pumps in cell lines (Lee and Kelly, 2009).

1.3 TAXOL

1.3.1 History and derivatives

Paclitaxel was discovered as a result of a large-scale screening of plant extracts with anti tumor properties initiated by the National Cancer Institute in the 1960s (Kumar et al., 2010). It was originally extracted from a slow growing coniferous Pacific yew tree (*Taxus brevifolia)* by Wani and Wall (Wani *et al.*, 1971). The drug underwent slow developmental changes, until in 1979, Peter Schiff and Susan Horwitz discovered that paclitaxel stimulated microtubule polymerization *in vitro,* unlike the previously discovered microtubule binding vinca drugs (Schiff *et al.,* 1979). Eventually, Bristol-Myers Squibb (USA) developed and commercialized Cremophor EL (CrEL), a polyoxyethylated castor oil, combined with dehydrated alcohol formulation of paclitaxel. Due to scarcity of naturally occurring paclitaxel, a semisynthetic more water soluble derivative, docetaxel, was developed from European yew tree (*Taxus baccata)*. By 1995, both paclitaxel and docetaxel were approved for clinical use and since then they have been the first line of therapy for treatment of advanced breast and ovarian cancer, non-small-cell lung cancer and Kaposi's sarcoma. Presently, for metastatic breast cancer, the dose and schedule of paclitaxel approved by the FDA (USA) is 175 mg/m^2 given as 3-hour infusion every 3 weeks, and docetaxel is 60-100 mg/m^2 given as a 1-hour infusion every 3 weeks (Sparano, 2000). However, the solvents used for these drug formulations, CrEL for

paclitaxel and polysorbate 80 (Tween 80) for docetaxel, result in various side effects specifically the acute hypersensitivity and peripheral neuropathy. Therefore, over the last decade, various taxane formulations based on albumin nanoparticles (nab-Paclitaxel), drug analogs (tesetaxel), prodrugs (DHA-paclitaxel), polyglutamate emulsions (Paclitaxel poliglumex) etc have been developed and even undergoing clinical trials (Fig 4; Yared and Tkaczuk, 2012).

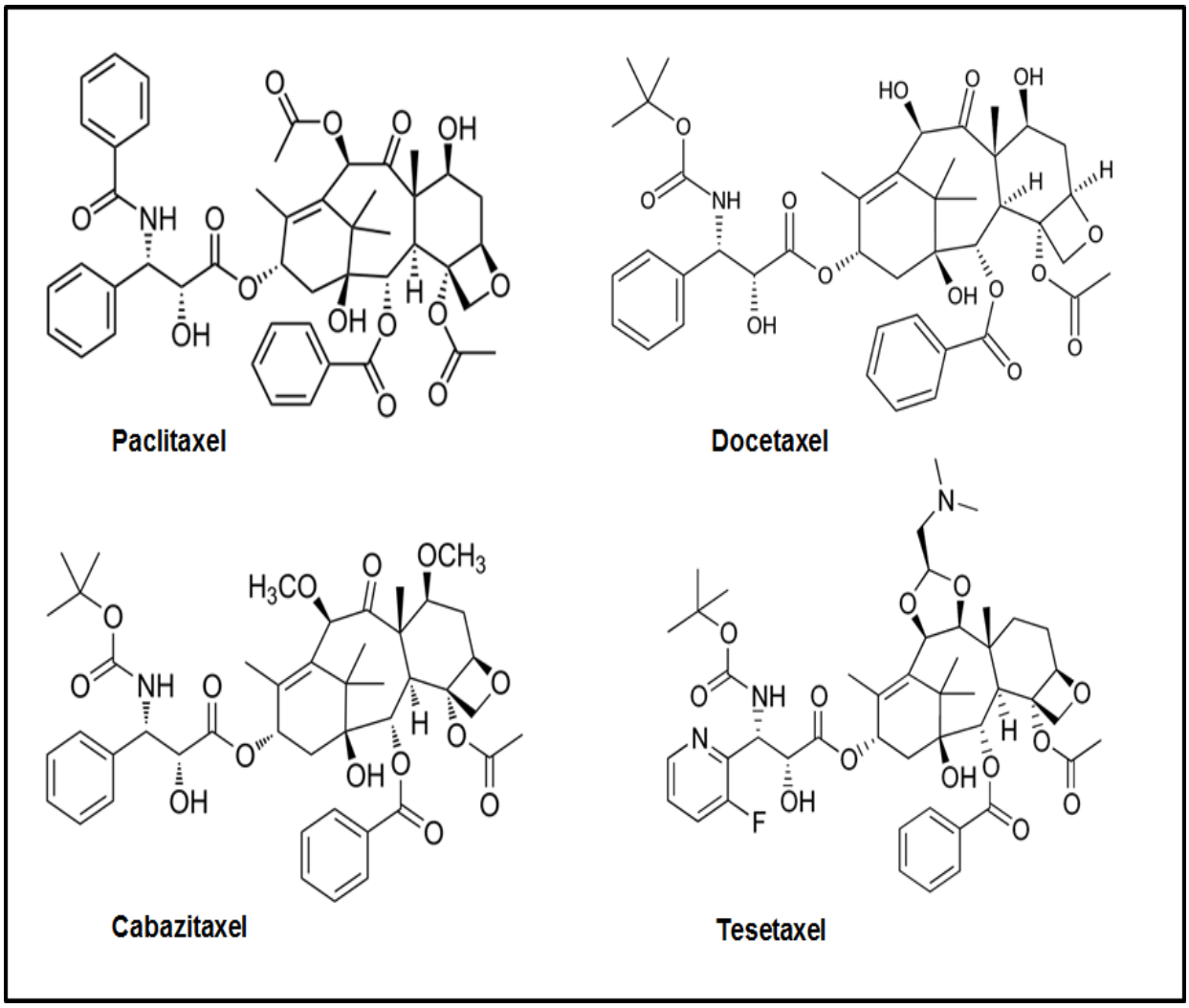

Figure 4. Structure of Paclitaxel and its derivatives. Paclitaxel structure consists of a diterpene core which forms the taxane skeleton, 3 phenyl ring-bearing side chains and 2 acetoxy moieties. Docetaxel, cabazitaxel and tesetaxel has a tert-butoxy group different at C3 position. At C10 position, docetaxel has a hydroxyl group, cabazitaxel has an acetyl group, and tesetaxel has dimethylaminomethyl group.

1.3.2 Pharmacokinetics

The uptake and elimination of paclitaxel depend on dose and administration rate. Paclitaxel uptake is found to be homogenous in liver, spleen, heart, lung and muscles but minimal in brain and testes, as demonstrated by radiolabeled drug studies (Lesser *et al.,* 1995). Oral administration of paclitaxel lead to poor bioavailability due to the drug either being effluxed by the enterocyte P-glycoprotein (P-gp) or being metabolised in the liver before reaching target cancer cells, therefore requiring parental administration. Early clinical trials with prolonged slow infusions of paclitaxel (24-hour infusions) showed more linear pharmacokinetics, whereas, studies with high plasma concentrations or shorter infusions (3-hour infusions) showed high nonlinearity (Michaud *et al.,* 2000). This nonlinearity can be due to the plasma concentration of the drug exceeding the eliminating capacity of the body, thereby disproportionately increasing the area under the plasma-time curve (Walle *et al.,* 1995).

Paclitaxel is majorly eliminated by the liver followed by bile excretion either as unchanged paclitaxel or metabolites. Renal excretion is as minimal as only 10% of the injected taxol when recovered in urine over a 24-hour period (Monsarrat *et al.,* 1990). Major metabolites of paclitaxel are 6α-hydroxy-paclitaxel, formed by hydroxylation of C6 in the taxane ring by cytochrome P450 2C8, and 3'-para-hydroxypaclitaxel, formed by cytochrome P450 3A4 (Walle *et al.,* 1995; Kumar *et al.,* 2010).

1.3.3 Effect of taxol in vitro and in vivo

Ever since the discovery of taxol and its derivatives as microtubule stabilizing agents, numerous studies have been carried out to elucidate its mechanism of action. *In vitro,* taxol decreases the lag time required for microtubule assembly by shifting the equilibrium towards microtubule polymers and decreases critical concentration of tubulins required for assembly.

The microtubules formed are stable and resistant to depolymerisation by cold (4°C) and $CaCl_2$ (4 mM) (Schiff *et al.,* 1979). Taxol binds along the surfaces of microtubules, with a maximum stoichiometry of 1 mol of taxol per 1 mol of tubulin in microtubules (Derry *et al.,* 1995). The binding is reversible, since [^{3}H] Taxol bound to polymerised microtubules can be easily replaced by unlabelled taxol. Taxol also leads to a decrease in number of protofilaments of a microtubule from an average of 13 to 12 (Diaz *et al.,* 1998).

In vivo, at high concentrations, taxol causes extensive microtubule bundling and increase in polymer mass along with G2-M block followed by apoptosis (Fig 5). However, at low concentrations taxol acts differently at opposite microtubule ends. Taxol potently block mitosis, with no change in microtubule polymer mass and no microtubule bundling. This results from stabilization of growing and shortening dynamics of microtubules at the plus ends by the binding of very few taxol molecules. At the minus ends however, same substoichiometric ratios of taxol bound to tubulin did not affect growing, shortening, or dynamicity. Thus, in blocked mitotic cells, taxol potently suppresses dynamics at plus ends of spindle microtubules, whereas at minus ends permits continued microtubule depolymerisation at the spindle poles (Derry *et al.,* 1995). This has led to the observation that centrosomal components that are normally located at the minus ends of microtubules in the mitotic spindle often become disorganized in the presence of taxol (DeBrabander *et al.,* 1981).

1.3.4 Taxol binding sites on microtubule

Each tubulin (~450 amino acids) monomer consists of three functional domains. The N-terminal domain (residues 1-206) has a Rossman fold which is involved in nucleotide binding (GTP/GDP). The central domain (residues 207-384) is formed by two antiparallel helices (H11 and H12) that fold across to the other two domains. This domain is involved in

lateral/longitudinal association between α and β-tubulin monomers to form protofilaments by interacting between the microtubule loop (M-loop; residues 271–286) and the helix H3 and loop H1-S2. The C-terminal domain (starting from residue 385) is involved in binding to microtubule associated proteins (MAPs) (Orr *et al*, 2003).

Taxol has a large complex structure comprising of an oxetene core, three phenyl ring-bearing side chains and two acetoxy moieties. Some studies suggest that the side chains are responsible for its effect on microtubules (Miller and Ojima, 2001), whereas, other studies imply that if not an absolute requirement, these side chains enhances the potency of taxol (Downing, 2000). Photoaffinity studies with [^{3}H] Taxol revealed that taxol binds to β-tubulin on the inner surface of the microtubule. Taxol binds to assembled tubulins with greater affinity than soluble tubulin monomer. It enters the inner lumen through small pores present on the walls of microtubule polymer. Binding of taxol to the β-tubulin causes conformational changes in the β-tubulin lattice. Several residues have been identified that make direct contacts with taxol, e.g., Val23 makes hydrophobic contacts with paclitaxel's *N*' and 3' phenyl rings. Asp 26 forms hydrogen bonding to the nitrogen in paclitaxel's C13 side chain. Other residues, Leu 215, Leu 217, Leu 228 and His 227 are involved in hydrophobic contacts with the 2-phenyl ring, while Ala 231 and Ser 234 contact the 3' phenyl group of taxol (Lowe *et al.*, 2000).

Snyder *et al* has proposed a model based on molecular docking studies, X-ray crystallography and NMR studies that, taxol binding to tubulin takes T- shape or a butterfly structure (Synder *et al.*,2001). This T-shaped or butterfly structure of taxol mimics a portion of the B9-B10 loop of α-tubulin and even shows functional similarity. In this model, the binding pocket of taxol resides in a hydrophobic cleft near the surface of β-tubulin formed by Pro358, Arg 359, Gly 360 and Leu 361. From this pocket, taxol can make hydrogen bondings and hydrophobic contacts with segments of helices H1, H6, H7, and the loop between H6 and H7. The taxol-binding site is close to the M-loop (residues 271-286), which participates in lateral interactions

with the H3 helix of the adjacent β-tubulin monomer in the microtubule. It has been proposed that on taxol binding, a conformational change occurs in the M-loop which mediates stronger lateral contacts between the protofilaments leading to a rigid taxol bound microtubule (Nogales, 2000).

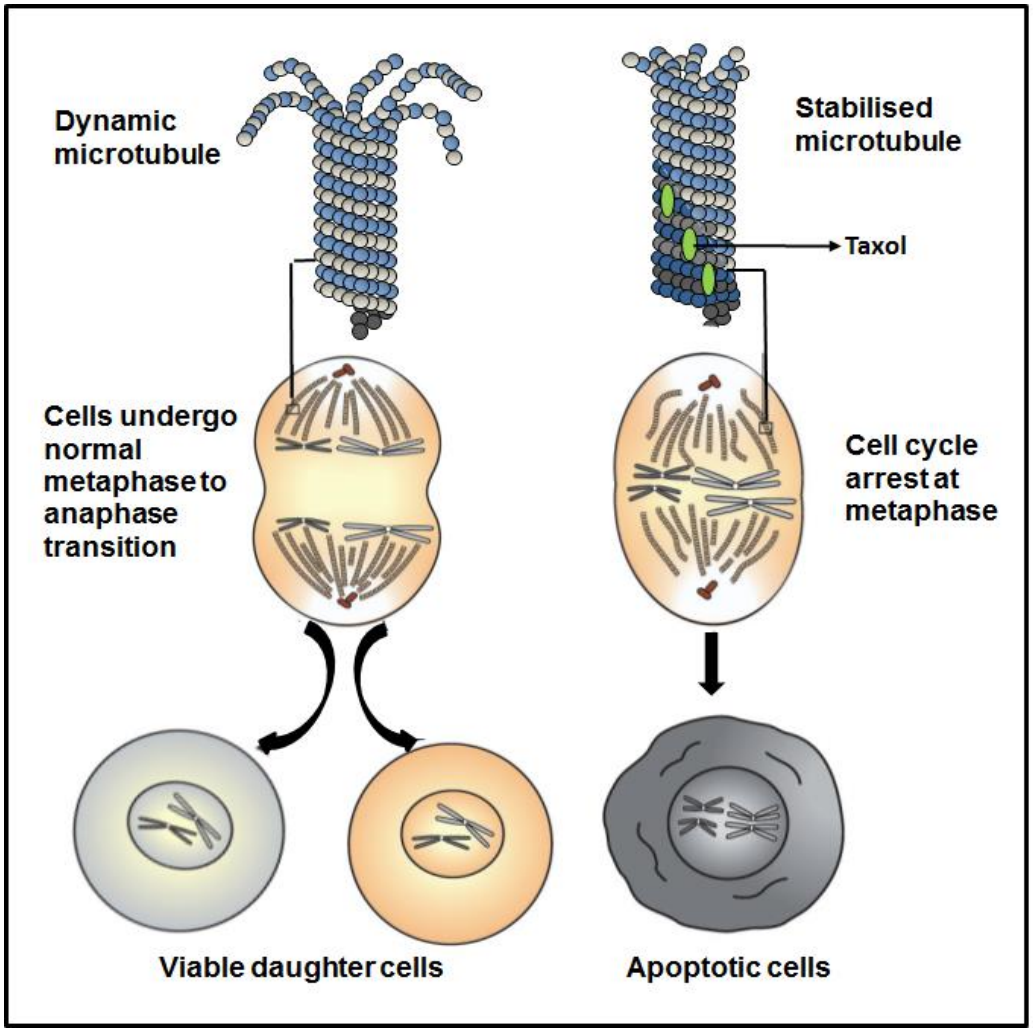

Figure 5: Mechanism of taxol. During cell division, microtubules are highly dynamic. It undergoes disassembly to form new networks of spindle microtubules, mitotic asters and kinetochore microtubules in a tightly regulated mechanism. Taxanes bind to the inner surface and stabilizes the spindle microtubules, such that the chromosomes fail to segregate at metaphase leading to mitotic arrest and finally triggering apoptosis.

1.3.5 Mechanisms of taxol resistance

Intrinsic and acquired drug resistance to taxanes are a major threat to the success of anticancer chemotherapy. Various factors underlying taxane resistance include mutations in both α and β tubulin, altered β-tubulin isotype expression, P-glycoprotein (P-gp), overexpression and altered expression of microtubule-associated proteins (MAPs). Moreover, functional aberrations in multiple molecular pathways, such as cell cycle control, growth promotion and apoptosis can all contribute to chemoresistance (Jordan and Wilson, 2004).

1) Mutations

Mutations in β-tubulin can cause alteration in microtubule dynamics and stability and affect taxol binding leading to resistance. Several studies have reported mutations in the β I-tubulin isotype taxol-resistant cell lines. However, their clinical implication has not yet been proved (Berrieman *et al.*, 2004). For example, taxol resistant Chinese hamster ovary cells show alterations in a cluster of leucine residues in the H6-H7 loop region of β- tubulin, an area close to the paclitaxel-binding site. It was further identified that mutations at L215 confers enhanced taxol sensitivity (Wang *et al.*, 2006). In another study, epidermoid tumor line KB-3-1 when exposed to increasing concentrations of paclitaxel resulted in a paclitaxel-resistant clone having a mutation in the paclitaxel-binding region of β-tubulin (Asp26Glu) and less stable microtubules (Hari *et al.*, 2006). In another report, mutational analysis of the class I beta-tubulin in breast cancer patients led to the identification of a somatic mutation codon 306 [Arg (CGC) to Cys (TGC)], and 2 genetic polymorphisms, codon 217 [Leu (CTG) to Leu (CTA)] and (C to T) at 57 bases downstream from exon 4 (Hasegawa *et al.*, 2002). However, mutation of the class I β-tubulin gene is found to unlikely to be instrumental in conferring resistance to paclitaxel in breast cancer (Maeno *et al.*, 2003).

2) β-tubulin isotype

The α- and β-tubulin have multiple isotypes that have tissue and cell-specific expression (Ludueña, 1998, Dozier *et al.*, 2003). The tubulin isotypes highly homologous but are unique by their last 20–27 amino acids, carboxy-terminal tails, which forms the putative site for binding many MAPs. Post-translational modifications of these tubulin can alter the interaction of microtubules with MAPs and change their functions. Taxol resistance in breast cancer has been associated with variations in tubulin isotype expression, especially increased expression of β III-tubulin (Shalli *et al.,* 2005).

Interestingly, dimers composed of βIII-tubulin are found to be less stable and depolymerise more easily than other β-tubulin isotypes. They also showed increased dynamicity with an overall increase in rate of exchange of tubulin dimers at the microtubule ends (Panda *et al*., 1994). Taxol reaches its binding site on β-tubulin by diffusion through small openings in the microtubule wall. This requires a transitional step of binding of paclitaxel to an intermediate site within a nanopore, from which it moves directly to its binding site in the inner surface of microtubule. Targeted molecular dynamics revealed that paclitaxel utilizes the H6/H7 loop as a hinge to move directly from this intermediate binding site to its final position in the luminal binding site. This movement involves formation of a hydrogen bond by serine 275 in all β-tubulin isotypes, except βIII-tubulin and βVI-tubulin, in which this residue is replaced by alanine. Thus the difference in taxol binding to different tubulin isotypes is due to the kinetic effect of this residue (Freedman *et al.,* 2009). The putative role of βIII-tubulin in taxol resistance and as a cellular survival factor is supported by the fact that βIII-tubulin is induced under conditions of cellular stress such as hypoxia and glucose deprivation (Raspaglio *et al.,* 2008; Cicchillitti *et al.,* 2008). Thus, βIII-tubulin can also protect cells from the genotoxic stress induced by cytotoxic drugs. *In silico* analysis of *Tubb3* promoter identified binding sites for several transcription factors that are components of cell survival pathways, e.g., HIF1α,

p53, nuclear factor-κB and the Wilms'tumour protein (Dennis *et al.,* 2002). miR200c downregulates βIII-tubulin in endometrial cancer cells and sensitises them to taxol. Thus, βIII-tubulin is a downstream regulator of various cell signalling pathways that play a potential role in cell survival.

3) MAPS

A plethora of proteins interact with microtubules and regulates microtubule dynamics. Some of them stabilize microtubules structure (MAP2, MAP4, Tau, STOP, Mip-90 and stathmin), others modulate microtubule space arrangement (MAP1, MAP2 and Tau) or enable the organelle migration among microtubules (kinesin, dynein and dynamin). Therefore, aberrant expression of microtubule associated proteins could impact the sensitivity of cancer cells to microtubule targeting drugs like taxol.

Stathmin/oncoprotein 18 (op18) is a major cell signaling phosphoprotein. Structurally, stathmin has two functional domains consisting of an N-terminal domain which stimulates microtubule plus end catastrophe, and a C-terminal domain, which sequesters tubulin and lowers the concentration of soluble tubulin resulting in slow microtubule growth (Cassimeris, 2002). Stathmin is overexpressed in breast cancer and is associated with disease progression and taxol resistance (Alli *et al*., 2002). Stathmin inhibition in ER-positive and ER-negative breast cancer cell lines resulted in inhibition of proliferation associated with increased G2/M arrest and apoptosis (Miceli *et al,* 2013). Stathmin overexpression in BT549 breast cancer cells resulted in decreased microtubule dynamics and paclitaxel sensitivity by 29% and 44%, respectively (Balasubramani *et al.,* 2011). The activity of stathmin can also be regulated at the transcriptional level by p53 and E2F (Ahn *et al.,* 1999; Polager and Ginsberg, 2003).

Microtubule associated proteins (MAPs) consist of several subtypes MAP1A, MAP1B, MAP2, MAP4 and tau proteins. MAP2, MAP4 and Tau have three or four structural repeats in their C-

terminal microtubule-binding domain. Each MAP has several isoforms reflecting differences in the number of microtubule-binding repeats (Honore *et al.,* 2005). Tau/MAP2 is predominantly a neuronal MAP and a key culprit in Parkinson's disease. However, high Tau expression is observed in taxol resistant breast cancer (Andre *et al.*, 2007; Rouzier *et al.*, 2005). Tau has either three- or four-repeat microtubule-binding domains. It strongly binds longitudinally along the inner and outer surface of the microtubule, between two adjacent tubulin dimers on the protofilaments, and dissociates slowly (Kar *et al.,* 2003a). *In vitro* polymerisation assay of tubulin pre-incubated with Tau resulted in decreased paclitaxel binding probably due to increased competition for the binding site on β-tubulin. Down regulation of Tau by siRNA leads microtubules more vulnerable to paclitaxel and makes breast cancer cells hypersensitive to this drug (Rouzier *et al.,* 2005). Phosphorylation of the microtubule- binding domain of Tau by various kinases, such as, type 2A phosphatases and GSK-3β can regulated its microtubule binding activity (Credle *et al.*,2015), which may in turn may play a key role in taxol resistance.

MAP4, on the other hand, is a predominant human non-neuronal MAP, ubiquitously found in all cell types. MAP4 binding to microtubules brings about conformational changes in α- and β-tubulin that results in stabilization of MT (Xiao *et al.,* 2012). It alters microtubule dynamics by increasing the rescue frequency, without affecting the catastrophe frequency. MAP4 overexpression has been correlated with increased resistance to paclitaxel. In taxol-resistant ovarian cells, phosphorylation of MAP4 results in its dissociation from the microtubule allowing mitosis to proceed, thereby, decreasing taxol sensitivity (Poruchynsky *et al.*, 2001). Thus, microtubule associated proteins are instrumental is causing taxol resistance in cancer cells and poses a major hurdle in chemotherapy.

4) Multidrug resistance (MDR)

A major factor causing resistance to antimitotic drugs is multidrug resistance (MDR) phenomenon, whereby, resistance to one drug can result in cross-resistance to other structurally unrelated drugs. The key mechanism of MDR is the overexpression of a class of membrane transporter proteins known as ABC-transporters (ATP-dependent drug efflux pumps). The first of many identified was P-glycoprotein, the product of the human MDR1 gene, on chromosome 7 (Safa, 2004). These P-gp can bind to a wide spectrum of hydrophobic drugs including paclitaxel, doxorubicin, vincristine and vinblastine. On drug-binding, the ATP-binding domain of P-gp is activated causing hydrolysis of ATP. This results in a conformational change in P-gp, causing drugs to be effluxed out of the cell limiting their activity (Ramachandra *et al.,* 1998). Therefore, new microtubule targeting drugs that are being developed requires circumventing this common mode of resistance. Several analogues are being developed including TPI-287, cabazitaxel and sagopilone, that are poor substrates of P-gp or drugs that can covalently link to microtubules and therefore would not be effluxed by P-gp e.g., zampanolide, cyclostreptin and the taccalonolides (Rohena and Mooberry, 2014).

Another class of drug efflux pumps implicated in taxanes resistance is the multi resistance-associated protein (MRP) family of transport proteins also referred to as ABCC (adenosine triphosphate-binding cassette C group) transporters, which include several subfamily members (Borst *et al.,* 2000). These have been implicated in imparting drug resistance in epithelial ovarian cancer and lung cancers (Cole *et al.*, 1992; Bagnoli *et al.,* 2013).

5) Post translational modifications

Microtubules undergo various post-translational modifications e.g., polyglutamylation, polyglycylation, phosphorylation, acetylation, and detyrosination/tyrosination, which regulates the binding of various MAPs, resulting in a signature ‘tubulin code’ (Verhey and Gaertig,

2007). This in turn, regulates the dynamic property of microtubules. All of the post-translational modifications, except acetylation, occur within carboxy tail of α- and β-tubulin.

Microtubules undergo detyrosination of the C-terminal tyrosine of α-tubulin by an unidentified carboxypeptidase (Westermann and Weber, 2003). However, the Nna1/CCP1 family of cytosolic carboxypeptidases share some similarities with this tubulin carboxypeptidase (Kalinina *et al.,* 2007). The reverse tyrosination reaction of the C-terminal glutamate residue of α-tubulin is catalyzed by tubulin tyrosine ligase (TTL) (Verhey and Gaertig, 2007). The detyrosination/tyrosination cycle differentially recruits two types of microtubule-binding proteins, molecular motors and plus-end tracking proteins (+TIPs). Multiple studies have shown that TTL is downregulated in human cancers, and correlate with increased tumorigenisis, tumor invasiveness, and poor prognosis (Mialhe *et al.,* 2001; Soucek *et al.,* 2006).

Glutamylation and glycylation occurs at glutamate residues in the C-terminal tails of both α- and β-tubulin. However, these modifications has not yet been implicated for cancer propagation and taxol resistance. Glycylation is mainly observed in axonemes of cilia and flagella, whereas glutamylation is commonly seen in neuronal cells, centrioles, axonemes, and the mitotic spindles. These modifications has been implicated in the intra-flagellar transport of structural and membrane components within cilia and flagella (Hammond *et al.,* 2008).

Microtubules get acetylated at Lys 40 of α-tubulin on the luminal side. The enzymes deacetylating tubulins are histone deacetylase 6 (HDAC6) and Sirtuin 2 (SIRT2), and acetylating tubulin is α-tubulin acetyl transferase (α-TAT, also termed MEC-17). MTs are highly acetylated in mitotic cells and acetylation results in stable microtubules. During metaphase, acetylated tubulin (Ac-tubulin) is enriched at interpolar and kinetochore MTs, but not at astral MTs, and Ac-tubulin becomes concentrated on the midbody during telophase and cytokinesis. Increased acetylation of α-tubulin was observed in taxol resistant small lung cell

carcinoma (Ohta *et al*., 1994). Elevated levels of α-tubulin acetylation is observed in metastatic and basal- like breast cancer, and is associated with promotion of microtentacles and invasiveness (Boggs *et al.,* 2015). To date, however, there is little or confirmed evidence that altered post-translational modifications is a major determinant of cellular sensitivity towards taxol or any tubulin-directed antimitotic agent.

1.4 HEMATOPOIETIC PBX-INTERACTING PROTEIN

Hematopoietic PBX interacting protein, also known as pre B-cell leukemia homeobox interacting protein (PBXIP1), was initially identified as a non-homeodomain containing interacting partner of PBX1 in a yeast two-hybrid screening of a foetal hematopoietic cDNA library using PBX1 as a bait (Abramovich *et al*., 2000). It contains a nuclear export signal and two functional nuclear localization signals, which accounts for its localisation mostly in the cytosol and in few amounts in the nucleus (Fig 6). This also implies that HPIP can act as a shuttle protein and is responsible for repressing the transcriptional activity of PBX, by inhibiting the ability of PBX-HOX complexes to bind to their target DNA sequences and also the transactivation activity of E2A-PBX (Abramovich *et al*., 2000). Recent studies revealed that HPIP induces erythroid differentiation in K562, a multipotent erythro-megaloblastic leukemia cell line, and displays stem cell property by activating the PI3K/AKT/GSK3β signaling pathway. Furthermore, the erythroid lineage-specific transcription factor, GATA1, binds to the HPIP promoter and activates HPIP gene transcription in a CTCF-dependent manner (Manavathi *et al*., 2012). HPIP has also been shown to involve in germ cell proliferation by inhibiting functional interaction between ERβ and Tex11 (Yu *et al*., 2012). Although HPIP was initially discovered in context of embryonic development, a number of studies have implicated its role in cancer scenario. HPIP is overexpressed in astrocytoma and is responsible for promoting tumor growth and migration (van Vuurden *et al*, 2014). HPIP

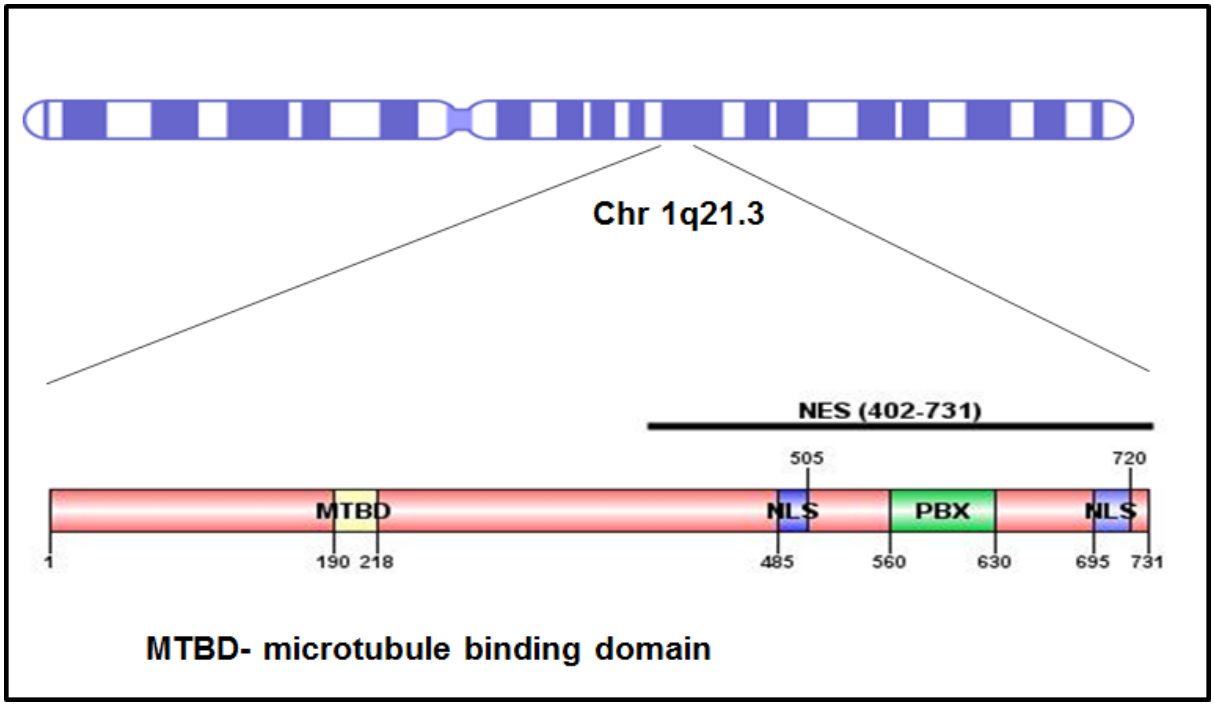

Figure 6. Structural domains of HPIP. HPIP has a nuclear export signal (NES) from 402-731 aa. It has two nuclear localisation signals (NLS) from 485-505 aa and 695-720 aa. The 560-630 aa region is the Pbx-interacting domain (PBX). HPIP binds to the microtubules by its 190-218 aa region (MTBD)

promotes liver cancer cell proliferation through activation of G2/M checkpoint by increasing the cyclin B1 and inhibiting GADD45α levels in liver cancer cells (Xu *et al.*, 2013). HPIP over expression is also found in various cancer tissues including breast, ovarian, and endometrial cancers (Uhlen *et al*., 2005). In breast cancer, Manavthi *et al.* has identified HPIP as a novel estrogen receptor (ERα) interacting protein that also binds to microtubules and tethers ERα to the microtubules and thereby triggering cytoplasmic signaling by activation of AKT and MAPK pathways (Manavathi *et al*, 2006). The activated AKT and MAPK further leads to ERα phosphorylation and estrogen-responsive gene expression (Wang *et al.*, 2008). Recent studies also revealed that in breast cancer cells HPIP is phosphorylated by estrogen-activated kinase TBK1, and it leads to MDM2-dependent HPIP degradation in breast cancer cells. In addition, HPIP is identified as a novel downstream target of P53 transcription factor (Shostak *et al*.,

2014). Furthermore, over expression of HPIP in breast cancer cells promotes adenocarcinomas in mice (Manavathi *et al*., 2006). Cellular functions of HPIP has been summarised in Figure 7.

HPIP is involved in cancer cell proliferation, migration and invasion in various cancers, and that HPIP activates AKT on paclitaxel treatment (Manavathi *et al*, 2006*)*. HPIP localises with the microtubules in the cytosol, via its N-terminal leucine–rich region between 190-218 amino acids. Based on these facts, we have examined whether HPIP can act as a microtubule associated protein, and whether it has any impact on taxol resistance in breast cancer.

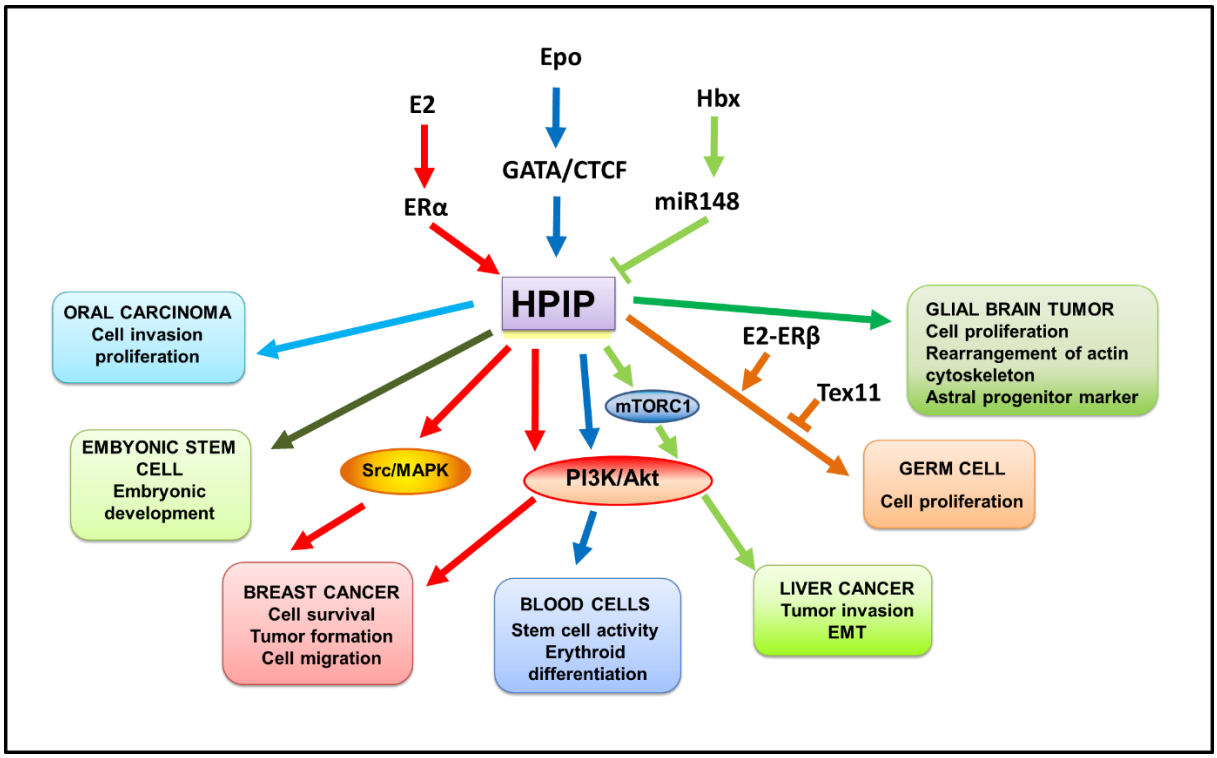

Figure 7. Functions of HPIP in various cell types. HPIP interacts with various cell signalling molecules, e.g., ER in breast cancer, mTORC1 in liver cancer, Tex11 in germ cells, and GATA1 and CTCF in blood cells. Under normal physiological conditions it plays a role in erythroid differentiation in blood cells and cell proliferation in germ cells. In cancerous cells, it can cause cell migration and proliferation.

Chapter 2

HPIP confers taxol resistance in breast cancer cells

2.1 HYPOTHESIS AND OBJECTIVE

From previous literature, it is established that HPIP is an oncoprotein (Manavathi *et al.,* 2006; Feng *et al.,* 2015 a and b). Microtubules, on the other hand, play an instrumental role in tumourogenic property of cancer cells (Ertych *et al.,* 2014). HPIP is known to interact with microtubules, however, its role in microtubule dynamics is still unknown. Manavathi *et al.,* have shown that breast cancer cells overexpressing HPIP were found to activate AKT on treatment with taxol, indicating that HPIP can trigger an intricate cell signalling pathway on taxol treatment (Manavathi *et al.,* 2006). We have further checked for reports of HPIP expression in taxol resistant cancer patients in publicly available databases through NCBI based Gene Expression Omnibus (GEO) profiles. We found out that in a dataset of 61 breast cancer patients, 41 patients who were taxol resistant and had recurrent invasive breast cancer exhibited a higher expression of HPIP in their tumours than patients sensitive to taxol (Fig 8A).

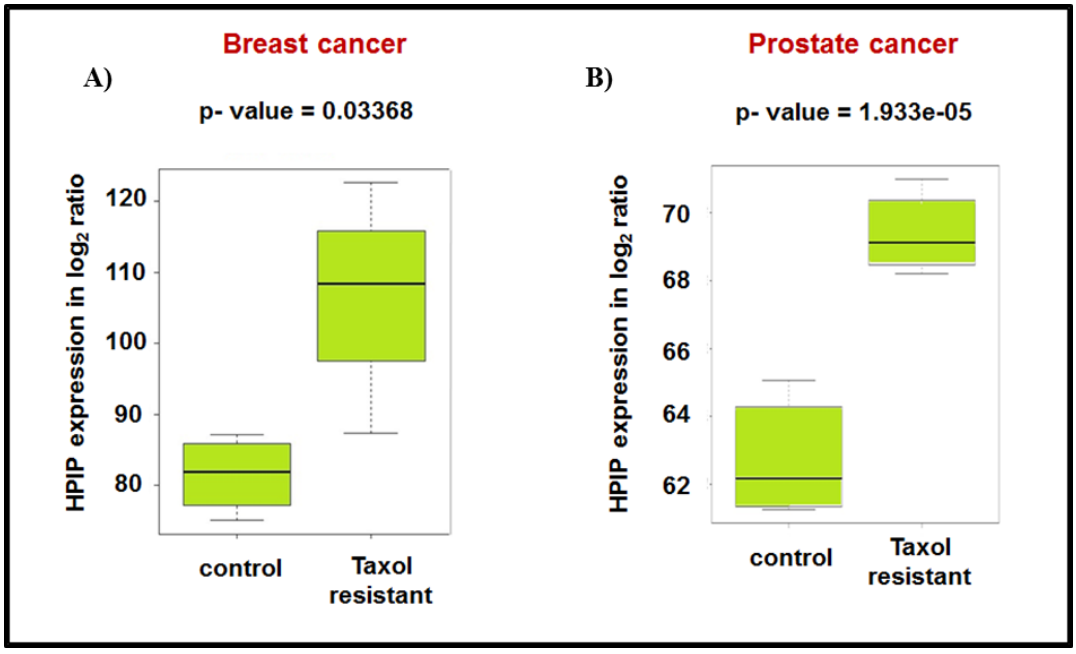

Figure 8: HPIP expression in GEO datasets. A) NCBI based GEO profile microarray of taxol resistant (n=41) and taxol sensitive (n=20) breast cancer patients were used to analyse HPIP mRNA expression (GEO profile ID: 77509457). B) Microarray data of taxol resistant prostate cancer cells (n=6) and untreated prostate cancer cells (n=6) (GEO profile ID: 74575277). HPIP expression was represented as log_2ratio of fold change and were graphed by a box plot.

Similarly, from GEO profiles we found a data set of taxol resistant prostate cancer cell lines DU-145 and PC-3, wherein HPIP expression was higher in the taxol resistant samples (Fig 8B). From these facts we hypothesize a putative role for HPIP conferring taxol resistance in breast cancer.

2.2 INTRODUCTION

Breast cancer treatment currently requires various alternative treatments integrating chemotherapy, hormone therapy and immunotherapy along with surgery and radiotherapy, considering the patient and the clinical and molecular characteristics of the tumour. In 90% of primary breast cancers and 50% of metastases, these systemic agents are effective at the initial stages of therapy. However, cancer recurs resulting in poor survival rates after a period of time (Gonzalez-Angulo *et al.*, 2007).

Taxanes, both paclitaxel and docetaxel, have been an integral part of breast cancer chemotherapy ever since its approval by the FDA, USA in 1995. They are used extensively either as single agents or in combination with anthracyclines or trastuzumab, or radiotherapy for the treatment of breast cancer patients, particularly those unsuitable for hormone therapies as well as metastatic patients. During mitosis, microtubules undergo massive reorganisation leading to the formation of spindle fibres, mitotic asters and kinetochore, which is essential for chromosomal attachment and segregation. Taxanes bind preferentially to polymerized microtubules rather than tubulin dimers. It functions by reducing depolymerisation and suppressing spindle microtubule dynamics. This fails to satisfy the spindle assembly checkpoint (SAC) that surveys the bipolar attachment of chromosomes to the mitotic spindle before the onset of anaphase. This leads to a delay or block at the metaphase–anaphase transition during mitosis that eventually results in cell death (Kallavaris, 2010).

Today, due to the drug resistance associated with taxanes and other systemic agents, approximately 30% of early-stage breast cancer have recurrent disease, and in most cases it is metastatic in nature. Taxane resistance is acquired by multiple mechanisms including altered intracellular drug levels resulting from overexpression of drug efflux proteins including P-glycoprotein (P-gp) and multidrug resistance-associated protein 1 (MRP-1) (Safa, 2004), mutations in α- and β-tubulin and overexpression of β-III tubulin I isotype (Kamath *et al.,* 2005) leading to unstable microtubule formation, altered signal transduction and apoptotic pathways (Fig 9; Fojo, 2007). Microtubule dynamics is regulated precisely by a battery of proteins collectively known as microtubule-associated proteins (MAPs) (Cassimeris, 1993; Szakács *et al.,* 2006). For instance, MAP2, MAP4, Tau (Dehmelt and Halpain, 2005), STOP (Margolis, 1990), and Mip-90 are known to stabilize microtubules, whereas, Op18/stathmin (Cassimeris, 2002; Walczak, 2000) and katanin (McNally, 2000) destabilizes the microtubules. There are others such as kinesin, and dynein, which restrict organelle migration on the microtubules (Wang *et al.,* 2015; Asthana *et al.,* 2012). Thus, it is possible that resistance to taxanes is the result of malfunctioning of any of these proteins.

HPIP has been implicated as an oncoprotein in various cancer e.g., hepatoma (Xu *et al*., 2013), colorectal cancer (Feng *et al.,* 2015a and b), oral carcinoma (Okada *et al.,* 2015), pleomorphic sarcomas and leiomyosarcomas (Silveira *et al.,* 2013) and breast cancer (Manavathi *et al.,* 2006; Wang *et al.,*2008; Uhlen *et al.,*2010; Shostak *et al.,*2014). Although, HPIP is known to bind to the microtubules (Abramovich *et al.,* 2002; Manavathi *et al.,* 2006), its role in microtubule dynamics and microtubule related cell signalling is largely unknown. It is found that HPIP tethers ERα to the cytosol in the presence of microtubule stabilizers, taxol and inhibits its translocation into the nucles, thereby interrupting its nuclear transcriptional activity. However, in the presence of microtubule destabilizers, nocodazole, this property of HPIP is greatly interrupted (Manavathi *et al.,* 2006). This indicates the interaction between

microtubules and HPIP. Also, cancer cells overexpressing HPIP were found to activate AKT on treatment with taxol. Activation of PI3K/AKT pathway is known to cause taxol resistance. For example, PARP inhibition triggers PI3K/AKT pathway leading to ineffectiveness of taxol (Szanto *et al.*, 2009). TWIST, a basic helix-loop-helix transcription factor, induced taxol resistance due to the positive involvement of AKT pathway (Zhang *et al.*, 2007). Again, ecotropic viral integration site 1 (Evi1) confers resistance to both TGFβ and taxol-induced cell death by activating AKT pathway in intestinal epithelial and colon cancer cells (Liu *et al.*, 2006). This implicates that HPIP could play a role in taxol activity on microtubules. In this part of the study we determine whether HPIP expression can confer taxol resistance like other MAPs, e.g., Tau.

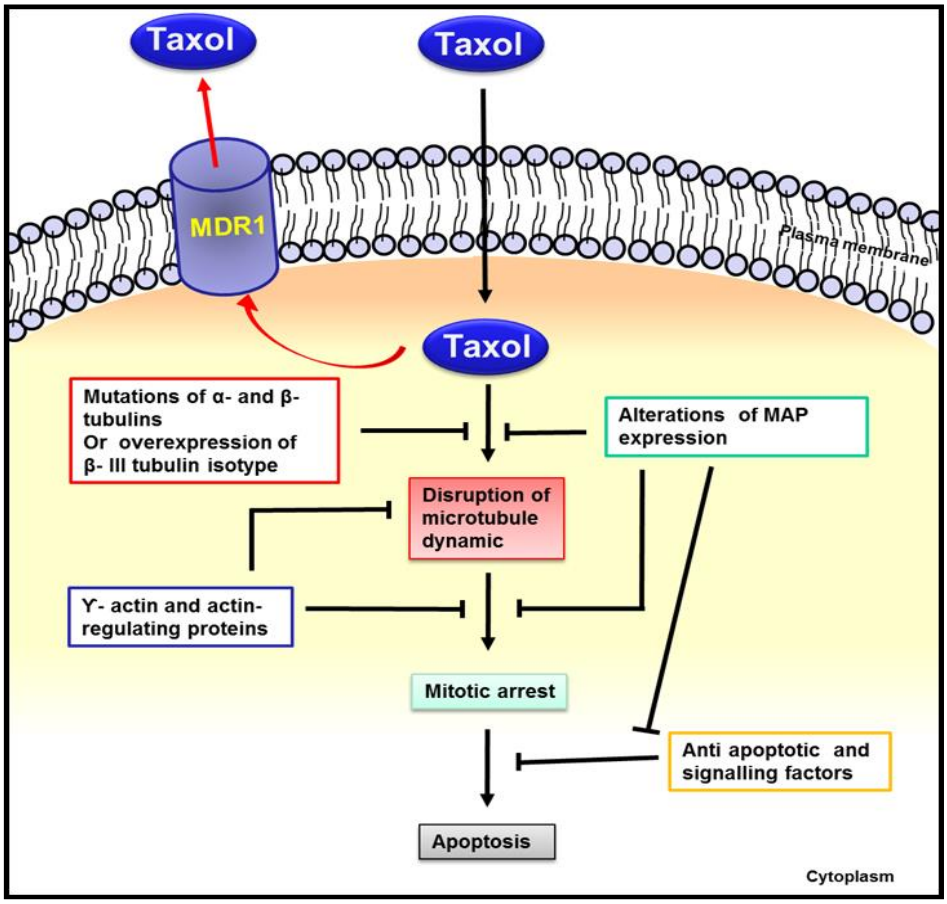

Figure 9. Mechanisms of taxol resistance. Taxol resistance can arise due to efflux of the drug as a result of overexpression of membrane bound P-glycoproteins, mutations in α- and β- tubulins and β-III tubulin isotype that prevents the drug from binding to tubulin subunits of the microtubule, alterations in MAPs, defects in other cytoskeletal proteins and apoptotic regulators.

2.3 METHODOLOGY

2.3.1 Plasmid constructs

The full length HPIP in T7-tagged mammalian expression vector, pcDNA 3.1A and Flag-tagged retroviral expression vector, pMIG were generated as previously described (Manavathi *et al.,* 2006, 2012). HPIP shRNA 5'-AAGGCTGAGCACTGGAAACATAAGAAGGA-3' in pGIPz vector was used. For generation of HPIP silencing in MCF7, *HPIP* shRNA in pGIPz vector was provided by Dr. Sam Aparicio, University of British Columbia, Canada. Plasmids used in this chapter is summarised in Table 1.

Name	**Description**	**Insert size**	**Reference**
BM 023	pcDNA 3.1	-	Manavathi *et al*., 2006
BM 022	pcDNA3.1/T7-HPIP	2196 bp	Manavathi *et al*., 2006
BM 250	pMIG control vector	-	Manavathi *et al*., 2012
BM 119	pMIG/flag-mHPIP	2196 bp	In this study
BM 123	pGIPZ-control shRNA	-	Dr. Sam Aparicio, Canada
BM 255	pGIPz-HPIP shRNA	29 bp	Dr. Sam Aparicio, Canada

Table 1. Plasmids used in this chapter

2.3.2 *Cell culture*

Immortalized, non-transformed breast epithelial cells, MCF-10A were a kind gift from Dr. Srigiridhar, IICT, Hyderabad, India, and breast metastatic adenocarcinoma cells, MCF7 were procured from National Centre for Cell Science (NCCS), Pune, India. HEK293T cells were used to produce packaging virus for viral transduction of plasmid constructs and were also procured from NCCS, Pune. All cell lines were cultured in humidified incubators with 5% CO_2 and maintained at 37^{o}C. MCF7 and HEK293T cells were cultured in Dulbecco's Modified Eagle's medium (DMEM) supplemented with 10% fetal bovine serum (FBS), 10 units/ml

penicillin and 10 μg/ml streptomycin. MCF10A were cultured in a growth medium of Ham's F12:DMEM (50:50) (GIBCO, USA), supplemented with 2.5 mM l-glutamine, 20 ng/ml epidermal growth factor (EGF) (Sigma), 0.1 μg/ml cholera toxin (CT) (Sigma), 10 μg/ml insulin (Sigma), 500 ng/ml hydrocortisone (Sigma) and 5% horse serum (GIBCO, USA). For passaging, cells were harvested by removing the culture medium and washing with phosphate-buffered saline (PBS), pH 7.2-7.4, followed by incubating with trypsin-EDTA (0.05% trypsin) with constant monitoring under microscope. Over-incubation was avoided to prevent degradation of membrane bound proteins. Once cells started detaching from the culture plate, trypsinisation was stopped by addition of fresh growth medium and cells were transferred into 15 ml tubes for 2-3 minutes at 1500 rpm. The supernatant was removed and cell pellet was suspended in fresh growth medium and split in a 1:3 ratio. Cryopreservation or freezing of cells were carried out by harvesting the cells by trypsinisation and then suspending them in their respective growth medium containing 20% FBS and 10% dimethyl sulfoxide (DMSO). The cryovials were stored in a cryo box containing isopropanol in -80^{o}C freezer overnight before storing permanently in liquid nitrogen tanks.

2.3.3 Transient transfection and viral transduction of MCF-7 cells

Packaging virus was produced for pMIG vector, pMIG-HPIP, pGIPz control shRNA vector, and pGIPz-*HPIP* shRNA using a standard four-plasmid packaging system by calcium phosphate transfection method in HEK293T cells. Virus-containing supernatants were harvested and concentrated by ultracentrifugation at 25,000 rpm for 90 minutes each to achieve titers of $0.5x10^9$ to $1x10^9$ infectious units/ml. The resultant virus concentrated soup was added to the MCF7 cells along with fresh growth medium. For achieving higher transduction efficiency, aliquots of viral titers was added to the cells for next three days. Transduction efficiency was verified by checking for green fluorescence under Olympus F100 microscope. Positively transduced cells were further selected with puromycin (Sigma).

Transfection was carried out using 5 µg of plasmids using Lipofectamine™ 2000 (Invitrogen, USA) following the manufacturer's protocol. The cells were seeded onto plates one day before transfection such that 70-80% growth confluency is reached at the time of transfection. Transfection complexes were prepared by mixing DNA (µg) and Lipofectamine™ 2000 (µl) at a ratio of 1:1 for most of the cell lines used. The plasmids and the appropriate amount of lipofectamine reagent were diluted in 100 µl of Opti- Minimum Essential Medium (Opti-MEM; GIBCO, USA) separately. After 5 minutes of incubation, the plasmid and the lipofectamine were mixed gently and incubated for 20 minutes at room temperature. Following incubation, transfection mix was added to culture plates containing serum and antibiotic- free growth medium. Cells were incubated in a humidified atmosphere containing 5% CO_2 at 37ºC for 6 hours following which the medium was replaced with fresh medium containing serum and antibiotics. Expression of transfected plasmids were verified after 48 hours.

2.3.4 Western blotting

Cell lysate preparation: Cells were scraped from culture plates and lysed with Radio-immunoprecipitation assay buffer (RIPA buffer; 20 mM Tris, pH 7.5, 150 mM NaCl, 1 mM EDTA, 1% Nonidet P-40) containing 1% sodium deoxycholate, 1 mM phenylmethylsulfonyl fluoride (PMSF), and complete mini protease inhibitor mixture (Roche Applied Science). The cell lysate was centrifuged at 12000 rpm for 15 minutes in a cold centrifuge to remove cell debris. When probing for phosphorylated proteins, RIPA buffer was supplemented with phosphatase inhibitors e.g, 10 mM sodium fluoride, 0.2 mM sodium orthovanadate and phosphatase inhibitor cocktails 1 and 2 (Sigma Aldrich, USA). The protein concentration was estimated by RC-DC assay kit (Bio-Rad). Approximately 100 µg of protein was used for loading onto SDS polyacrylamide gel (SDS-PAGE).

Casting SDS-PAGE gel: SDS-polyacrylamide gel was casted following Sambrook and Russell's Molecular cloning: a laboratory manual. 10 ml of 10% resolving SDS-polyacrylamide gel was prepared by adding 3.33 ml of 30% acrylamide, 2.5 ml of 1.5 M Tris (pH 8.8), 0.1 ml of 10% SDS and 10% ammonium persulphate (APS), 0.004 ml of tetramethylethylenediamine (TEMED) and 4 ml of double-distilled water. A stacking gel of 3 ml (0.51 ml of 30% acrylamide, 0.375 ml of 1.5 M Tris (pH 8.8), 0.3 ml of 10% SDS and 10% APS, 0.003 ml of TEMED and 2 ml of double-distilled water) was layered on the resolving gel and was allowed to solidify.

Running protein samples: Equal concentrations of protein ~100 µg were prepared in 4x loading buffer (50 mM Tris pH 6.8, 400 mM dithiothreitol (DTT), 8% SDS, 0.4% bromophenol blue, 40% glycerol) and denatured for 8-10 minutes at 95^{o}C before loading in the gel. The SDS-PAGE was run at 100 V in a buffer containing 25 mM Tris, 250 mM glycine, 0.1% SDS.

Blotting: Proteins separated on the SDS-PAGE gel were blotted onto a nitrocellulose membrane (Pal Lifesciences, USA) by wet transfer by using Towbin transfer buffer (3.03 g of 25 mM Tris, 14.4 g 192 mM glycine) at 30V, overnight. The quality of transfer was verified by Ponceau S in 5% (v/v) acetic acid.

Immunoblotting: The blot was washed with TBS buffer (20 mM Tris pH 7.5, 150 mM NaCl) to remove ponceau stains and then blocked for 1 hour with 5% of skimmed milk or 3% of BSA in TBS in case of phosphoproteins at room temperature. It was probed with specific primary antibodies in 3% BSA in TBS containing 10% sodium azide (NaN_3), overnight at 4^{o}C. After washing the blot thrice for 15 minutes with TBST (TBS containing 0.1% Tween 20), it was incubated with Horseradish Peroxidase (HRP) conjugated secondary antibodies (GE Healthcare, USA) for an hour at room temperature. Finally, blot was developed with enhanced

chemiluminescence (ECL) detection reagents (GE Healthcare, USA) and visualized by Chemidoc imaging system (Bio-Rad, USA).

2.3.5 *Cytotoxicity assay*

Cells were seeded in 96-well plate (Corning, USA) at a density of 1x 10^5 and incubated at 37^{o}C. Cells in triplicate wells were treated with increasing concentrations of paclitaxel (Sigma) ranging from 0.01-5 µM and DMSO as vehicle control in a final volume of 100 µl for 48 hours. After drug treatment, 10 µl of WST-1 (Clonetech, USA) was added to each well and incubated for 30 minutes to 4 hours at 37^{o}C, depending on intensity of colour development. The formation of formazan product was quantified by measuring absorbance at wavelength between 420-480 nm (maximum absorbance at 440 nm) and at a reference wavelength of >600 nm. The 50% inhibitory concentration (IC_{50}) was calculated by using Sigma Plot software.

2.3.6 Annexin V Apoptosis assay

Cellular apoptosis was analysed by Annexin V kit (Clontech, USA) as per the manufacturer's protocol. MCF7 cells were plated on 60 mm dish at a density of 1x10^6 cells. On reaching 70-80% confluency, indicating an exponential growth phase, the cells were treated with 100 nM of paclitaxel for 24 hours. Cells were harvested and washed twice with cold PBS to remove paclitaxel and then diluted with a binding buffer to a concentration of 1 x 10^6 cells/ml. 100 µl of the cell suspension (1 x 10^5 cells) were taken in a 5 ml culture tube and treated with phycoerythrin-labelled Annexin V and 7-aminoactinomycin. Cells were vortexed and incubated at room temperature for 15 minutes in the dark. The final volume of the cell mixture was made up to 500 µl and subjected to FACS analysis. Based on appropriate gating of the cells with respect to control samples, percentages of cell population at early apoptosis stage (Annexin V positive, 7-AAD negative) and late apoptosis stage (Annexin V positive, 7-AAD positive) of apoptosis were determined.

2.3.7 Cell cycle analysis by FACS

The percentage of cells in various stages of the cell cycle was determined by quantifying their cellular DNA content in a flow cytometric analysis of propidium iodide (PI)-labelled cells. MCF-7 cells were seeded at a density of $1x10^6$ cells in 60-mm dish, and cultured till they reached a confluency of 70-80%. Cells were treated with 100 nM of paclitaxel (Sigma) and harvested after 24 hours of incubation. Cells were fixed in ice-cold 70% ethanol and stored at 4^{o}C overnight. The next day, cells were washed with PBS twice, treated with 25 mg/ml RNase A at 37^{o}C for 1 hour, and stained with 50 mg/ml PI for 20 minutes. For flow cytometric analysis, a BD LSR Fortessa flow cytometer (Becton Dickinson, USA) equipped with 4 argon ion laser was used. For PI, the yellow/green laser with excitation wavelength of 561 nm was used, and the emission filter was 610/20 nm. A minimum of 10,000 cells were monitored per analysis. Using CellQuest software, appropriate size gates were established on the basis of forward light scatter, which is correlated with the size of the cell, and side scatter, which is correlated with the complexity of the cytoplasm. Cellular debris was excluded and not taken into account. Different stages of the cell cycle were analysed based on the DNA content of the cells which is indicated by the PI fluorescence intensity.

2.3.8 RNA isolation by Trizol method

Total RNA was extracted from cells by TRIzol Reagent (Life technologies, USA). TRIzol® Reagent is a monophasic solution of phenol, guanidine isothiocyanate, and maintains the integrity of the RNA by effectively inhibiting RNase activity while disrupting cells. The growth medium was removed from culture dishes and the cell monolayer was rinsed once with ice cold PBS. Cells were lysed directly in the culture plates by adding 1ml of TRIzol reagent and pipetting the cells up and down several times. Phase separation was carried out by adding 200 µl of chloroform and incubating the samples at room temperature for 5 minutes. The cell

suspension was centrifuged at 12000 rpm for 15 minutes at 4^{o}C so that the mixture separates into lower red phenol- chloroform phase, an interphase and an upper aqueous layer containing RNA. The aqueous upper layer was carefully removed and transferred into fresh tubes, followed by RNA precipitation with 0.5 ml of isopropanol for 15 minutes at room temperature. Samples were centrifuged at 12000 rpm for 20 minutes at 4^{o}C and the supernatant was discarded. The pellet was washed with 70% ethanol and traces of ethanol was removed by air drying. The pellet was then dissolved in RNase free, DNase free ultra-pure water (Life technologies, USA). The quality of RNA extracted was verified by running 1-2 µl of sample in 1% agarose gel.

2.3.9 Quantitative Reverse Transcriptase Polymerase Chain Reaction (RT-PCR)

First strand cDNA synthesis was carried out using 1 µg of RNA by using First Strand cDNA Synthesis Kit from Takara Bio Inc, Japan which uses a MMLV (Moloney Murine Leukemia virus)-derived reverse transcriptase. In the first step, RNA was incubated with 0.5 mM dNTP, 2.5 µM of oligo dT for 5 minutes at 65^{o}C. The second step involves incubation with 20 units of RNase inhibitor and 200 units of M-MuLV Reverse Transcriptase for 90 minutes at 42 ^{o}C followed by enzyme inactivation at 95 ^{o}C for 5 minutes. PCR reactions were setup using 1 µl of the synthesized cDNA using FastStart SYBR Green Master kit from Roche Life Sciences, USA in Roche LightCycler® 96 instrument. The primers used for amplification were, *HPIP* forward, 5'-GTCCCCTCGAGGAGTTGTGT-3' and reverse 5'-ATCTTCCATCATCTGAG GGC-3', *GAPDH* forward 5'- GTCCCCTCGAGGGAGTTGTGT-3' and reverse, 5'- ATCTT CCATCATCTGAGGGC-3′. The data was analysed by using $2^{\Delta\Delta Ct}$ method in which median cycle threshold value was considered for analysis, and all cycle threshold values were normalized to the expression of the housekeeping gene, *GAPDH*. The normalized mRNA level in control sample is arbitrarily given as 1, and the relative mRNA levels in test samples were compared to the levels in the control sample.

2.3.10 Biostatistical analysis

Microarray data of taxol resistant breast cancer patients and prostate cancer cell lines were obtained from NCBI based GEO profiles. Box plot was used to show HPIP expression in taxol sensitive vs taxol resistant samples. All results are expressed as means ±standard deviation, and differences between groups were analyzed by either t-test or one-way ANOVA using GraphPad Prism software.

2.4 RESULTS

2.4.1 Correlation of HPIP expression in mammary cells

Previously, HPIP overexpressing MCF7 cells when treated with taxol was found to activate AKT (Manavathi *et al,* 2006). Several studies have correlated the activation of AKT pathway to taxol resistance (Yun *et al.,* 2015; McCubrey *et al.,* 2006), therefore we hypothesize that HPIP expression may play a role in taxol resistance in cancer. Previous reports have shown that taxol resistant breast cancer patients show overexpression of a number of proteins, e.g., Tau (Rouzier *et al.,* 2005), Nlp (Zhao *et al.,* 2012), whereas patients sensitive to taxol showed a higher expression of proteins e.g., EB1 (Luo *et al.,* 2014), FOXM1, KIF20A (Khongkow *et al.,* 2015), Clip-170 (Sun *et al.,* 2012) and Parkin (Wang *et al.,* 2009). HPIP is found to be overexpressed in infiltrative ductal breast carcinoma (Bugide *et al.,* 2014), however, its status in taxol resistant breast cancer patients have not been reported. To verify our hypothesis that HPIP can cause taxol resistance, we analysed its expression in mammary epithelial cell lines. We have utilised MCF10A, an immortalized non-tumorigenic epithelial mammary cell line, and MCF7, a metastatic breast adenocarcinoma cell line, for HPIP expression. Western blot analysis of HPIP shows that the normal MCF10A has a lower expression than MCF7 breast

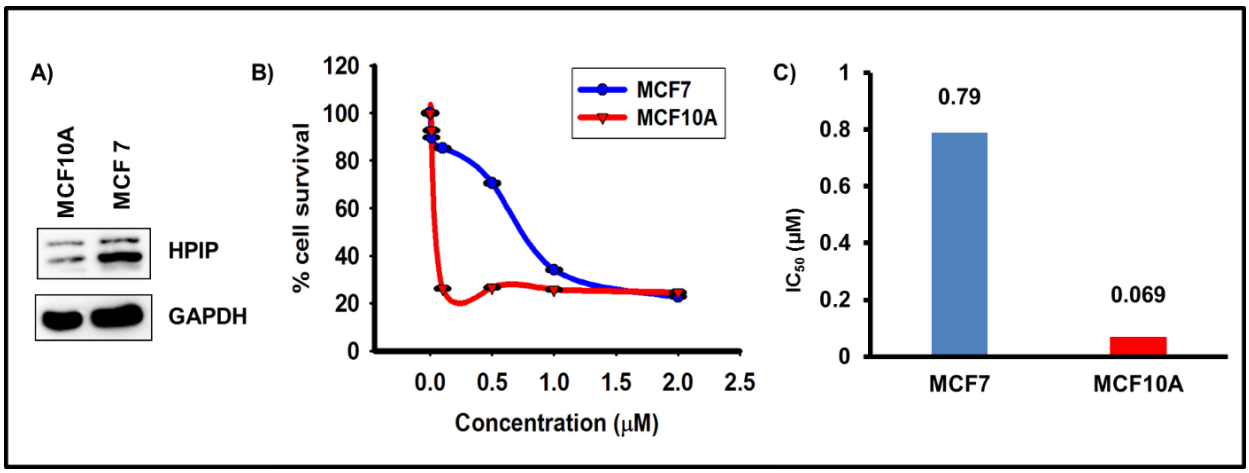

Figure 10. Correlation between HPIP expression and taxol sensitivity in mammary cells. A) Western blot analysis of HPIP expression in non-tumorigenic mammary cells, MCF10A versus metastatic mammary adenocarcinoma, MCF7. B) Cell viability assay of MCF10A and MCF7 cells on treatment with increasing concentration gradient of paclitaxel. The percentage of cell survival was plotted as a function of drug concentration. C) The 50% inhibitory concentration (IC_{50}) was calculated with Sigma Plot software.

cancer cells (Figure 10A). To check the sensitivity of both the cell lines to taxol, we checked cell viability with WST-1 reagent on treatment with increasing concentrartions of paclitaxel ranging as low as 0.01 μM to 2.0 μM. The MCF7 cells having a higher HPIP are more viable and shows greater resistance to taxol than non-cancerous MCF10A (Fig 10B). The IC_{50} value of taxol in MCF7 cells was determined to be 0.79 μM, almost 11 folds greater than that of MCF10A, IC_{50} value is 0.069 μM (Fig 10C). These results indicates that expression of HPIP correlates with taxol sensitivity in breast cancer.

2.4.2 HPIP alters taxol sensitivity in breast cancer cells, MCF7

In the recent past, several reports have identified different proteins involved in taxol resistance. The best strategy followed by these researchers has been to check the functionality of the protein on taxol resistance by either ectopically overexpressing them in a taxol sensitive cell line or silence them in a taxol resistant cell line, and vice versa. Lai *et al.* has identified Taz, a transcription factor to mediate taxol resistance. Therefore, for most of their studies they have

overexpressed Taz in taxol sensitive MCF10A and knocked down Taz in taxol resistant MCF7 (Lai *et al.*, 2011). We have utilised a similar strategy to check how taxol resistance varies with alteration in HPIP expression. To address this, we have silenced HPIP with shRNA in MCF7 by lentiviral transduction. pGIPz control shRNA vector, and pGIPz-*HPIP* shRNA constructs were used for this purpose. The percentage of transduced cells were observed under immunoflourescent microscope (Fig 11A). The silencing of HPIP was confirmed by western blotting using human anti-HPIP antibody (Sigma, USA) and was found to be more than 50% (Fig 11B). To test whether HPIP silencing affects the resistance of breast cancer cells to paclitaxel, HPIP silenced and control shRNA clones of MCF-7 were treated with increasing concentrations (0, 0.01, 0.1, 0.5, 1 and 2 μM) of paclitaxel for 48 hours and cell viability was determined by tetrazolium salt based WST-1 reagent. HPIP silenced cells were found to be more sensitive to the drug than the control cells (Fig 12A). HPIP silencing significantly reduced the IC_{50} value from 0.25 μM in control shRNA cells to 0.059 μM in HPIP shRNA transfected MCF7 cells which accounts for almost a ~4.2 fold change (Fig 12B). Similarly to

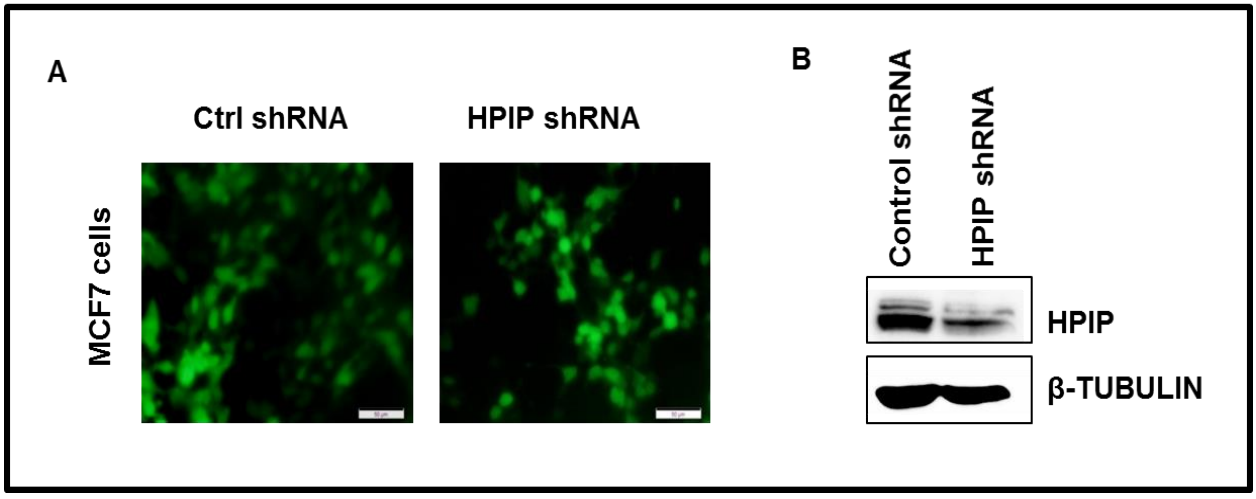

Figure 11. Effect of HPIP silencing on taxol resistance in MCF7 cells. A) Fluorescence of the inherent GFP tag in pGIPz vector and pGIPz-HPIP shRNA showing the rate of successful transduction. B) Western blot analysis of HPIP silencing in MCF7 cells.

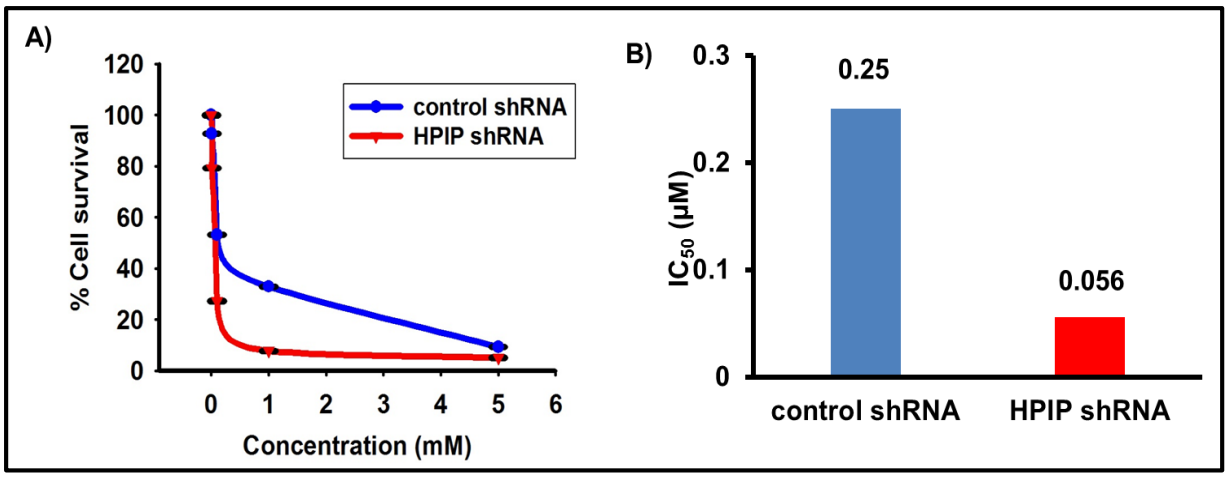

Figure 12. Effect of HPIP silencing on taxol resistance in MCF7 cells. A) Cell viability assay of control and HPIP shRNA stable MCF7 cells on treatment with gradient concentrations of paclitaxel. The percentage of cell survival was plotted as a function of drug concentration. B) The 50% inhibitory concentration (IC_{50}) was calculated with Sigma Plot software.

understand the effect of ectopic overexpression HPIP in MCF-7 cells, lentiviral transfection of either pMIG control vector or pMIG-HPIP was carried out to generate stable clones. Successful transduction was observed under immunoflourescent microscope (Fig 13A) and overexpression of HPIP in MCF-7 cells was confirmed with human anti-HPIP antibody in western blot analysis (Fig 13B).

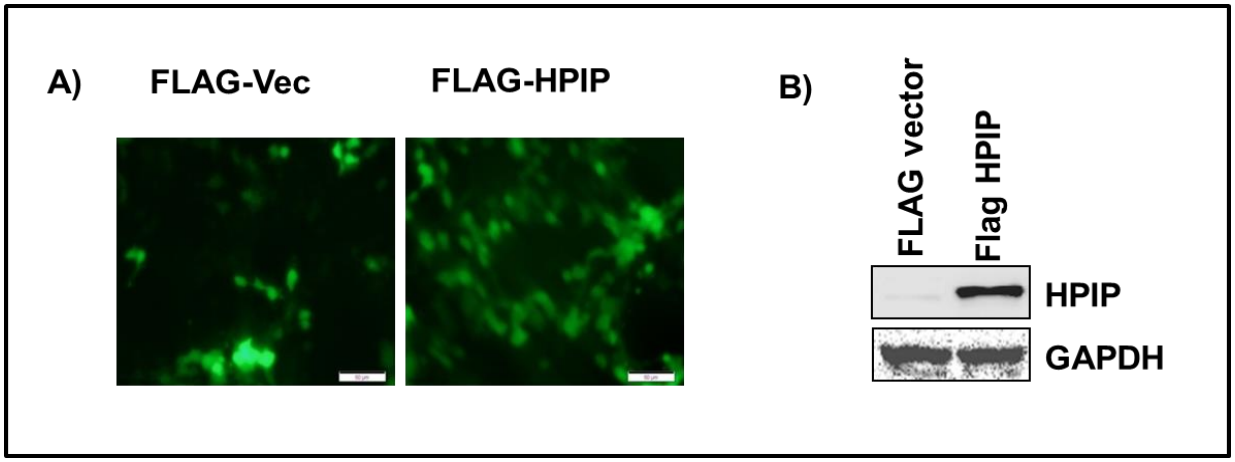

Figure 13. Effect of HPIP overexpression on taxol resistance in MCF7 cells. A) Fluorescence of the inherent GFP tag in pMIG vector and pMIG-HPIP showing successful transduction. B) Western blot analysis of HPIP silencing in MCF7 cells

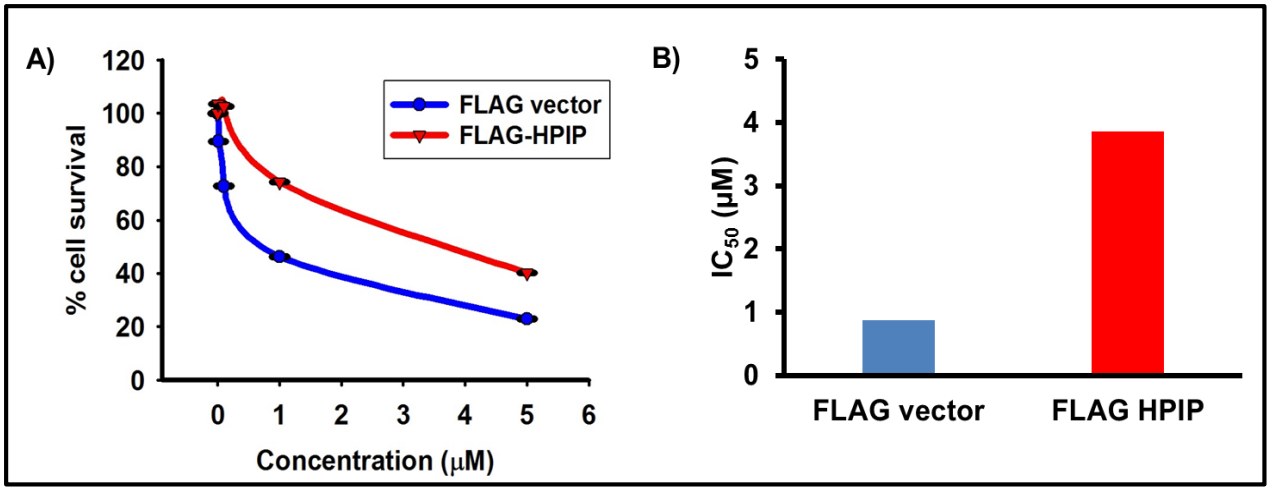

Figure 14. Effect of HPIP overexpression on taxol resistance in MCF7 cells. A) Cell viability assay of control and HPIP overexpressed MCF7 cells on treatment with increasing concentration of paclitaxel. The percentage of cell survival was plotted as a function of drug concentration. B) The 50% inhibitory concentration (IC_{50}) was calculated with Sigma Plot software.

Cell viability assay with increasing concentrations of paclitaxel shows that HPIP overexpression made the MCF7 cells more robust and resistant to paclitaxel (Fig 14A). The IC_{50} value increased by ~4.5 folds from 0.87 μM in control cells to 3.86 μM in HPIP overexpressing stable MCF7 clones (Fig 14B). These results confirm that HPIP is instrumental in causing taxol resistance in breast cancer cells.

2.4.3 *HPIP knockdown in MCF7 cells enhances paclitaxel induced apoptosis*

Taxol mediates its antitumor effect by promoting tubulin polymerisation and formation of stable non-functional microtubules. This disrupts the spindle microtubules dynamics resulting in chronic activation of spindle-assembly checkpoint causing a delay or block at the metaphase–anaphase transition during mitosis (Kavallaris, 2010). The exact mechanism by which taxol induced mitotic arrest results in cell death is still unclear.

Yeung *et al.* has proposed that depending upon taxol concentration, cells undergo apoptosis or necrosis (Yeung *et al.*, 1999). Therefore, to understand the possible mechanism by which HPIP causes taxol resistance and hence evade cell death, we treated HPIP silenced MCF7 cells with

100 nM of paclitaxel for 24 hours and assessed for apoptosis using Annexin V-PE/7 amino actinomycin D (7-AAD) staining by flow cytometry. This assay can distinguish necrotic cells from apoptotic cells. Annexin V binds to the phosphatidyl serine of plasma membrane when it loses its symmetry during early apoptosis, whereas, 7AADs bind to the cleaved DNA marking late apoptosis. The percentage of apoptotic cells that stained positive for both Annexin V and 7AAD increased from 14.0 % in shRNA-control group to 31.4 % in shRNA-HPIP group (Fig.15 A and B). Therefore, at low paclitaxel concentration apoptosis is induced and HPIP silencing results in induction of apoptosis.

2.4.4 HPIP knockdown in MCF7 cells causes paclitaxel induced cell cycle arrest

Taxol is previously known to stabilize microtubules and thereby, interfere in spindle microtubule dynamics leading to cell cycle arrest between metaphase and anaphase. This prolonged mitotic block finally triggers the apoptotic signalling pathway leading to cell death. Mitotic arrest is due to the chronic activation of SAC and degradation of cyclin B1 (Brito and Reider, 2006). We, therefore, investigated if this apoptosis is a result of mitotic arrest. As implicated in previous literature we compared the DNA content of paclitaxel-treated control and HPIP silenced MCF7 cells by flow cytometry, as a function of the propidium iodide retained by them. In order to evaluate actively dividing cells before the onset of extensive apoptosis, we harvested cells at 24 hours, rather than at 48 hours. Paclitaxel-treated HPIP silenced MCF7 cells exhibited an increase in the number of cells at G2/M (55.5%) compared to the control cells (36.9%). Concomitantly, the number of these paclitaxel treated HPIP silenced cells entering into G0/G1 has decreased to 23.3% (Fig 16A and B). This implies that on silencing HPIP, MCF7 cells are more susceptible to taxol mediated G2/M cell cycle arrest and fails to enter the G1 phase.

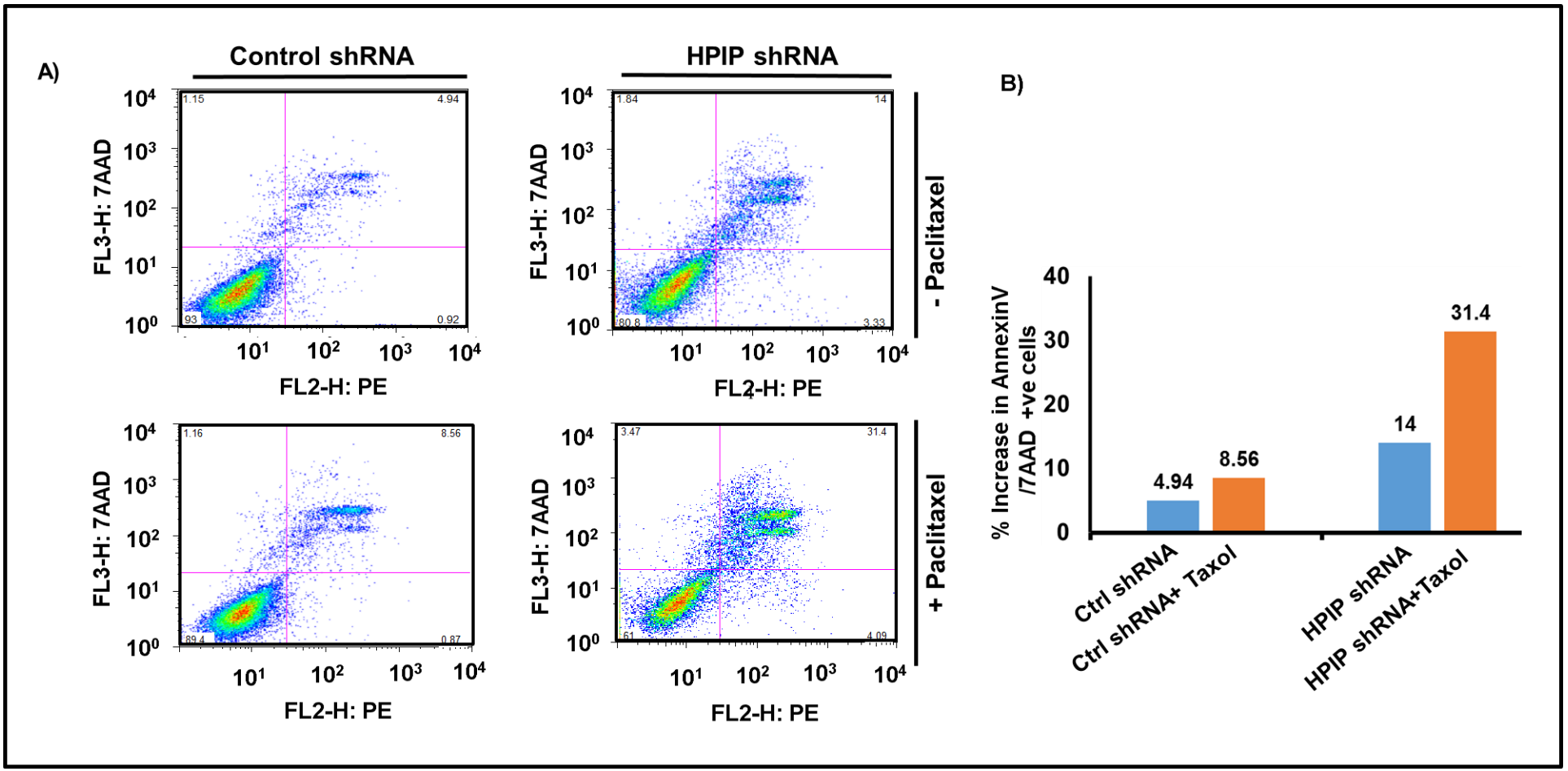

Figure 15. Effect of HPIP expression or knock down on paclitaxel-mediated apoptosis. A) ANNEXIN V and 7AAD staining followed by FACS analysis show the loss of HPIP expression increases number of apoptic cells in response to paclitaxel in MCF7. B) The number of apoptic cells (Annexin V/7AAD stained) were expressed qualitatively in a bar graph.

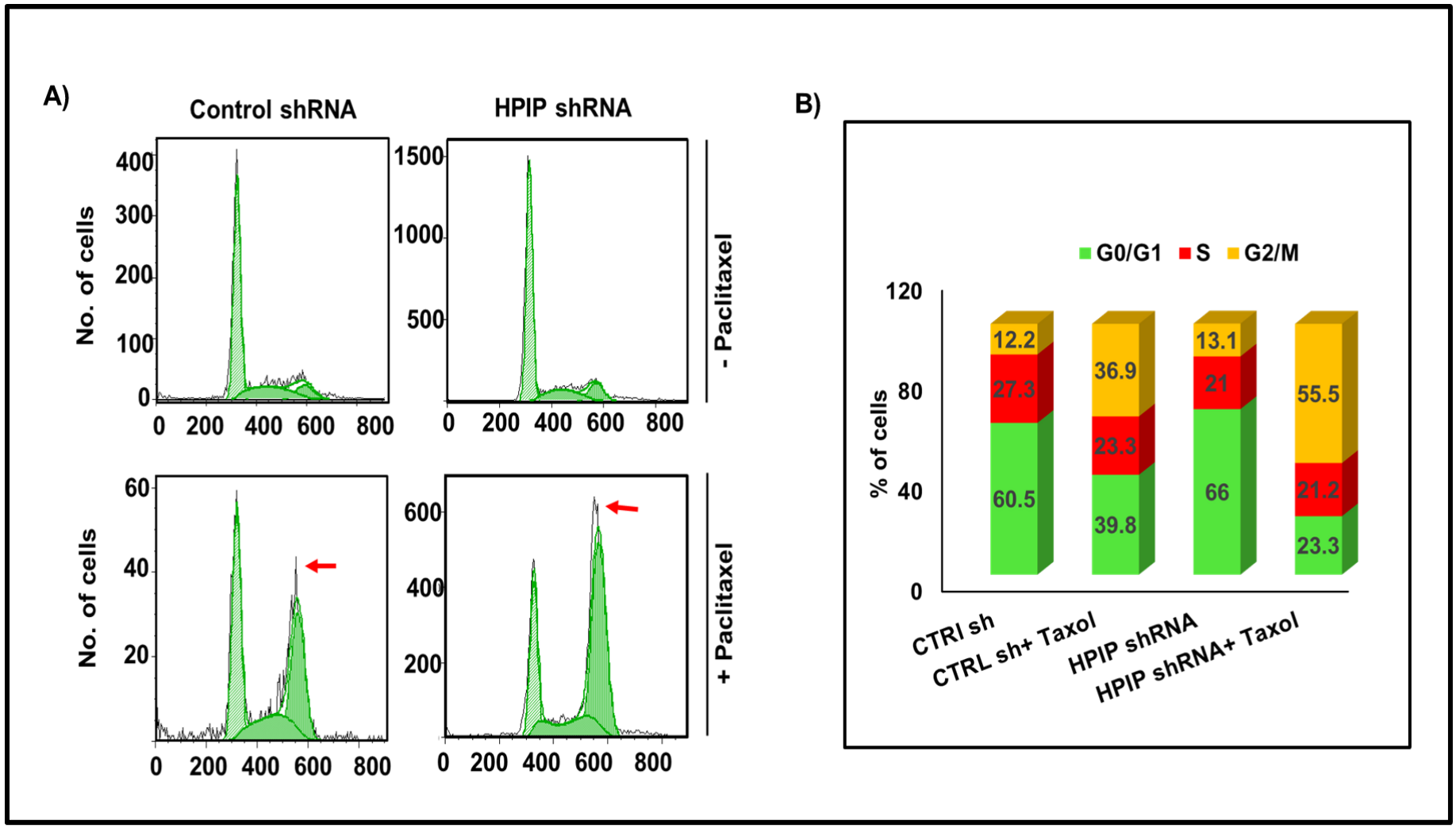

Figure 16. Effect of HPIP silencing on paclitaxel-mediated mitotic (G2/M) arrest in MCF7 cells. A) FACS analysis show the increase in number of cells arrested at G2/M upon HPIP knock down in response to paclitaxel in MCF7 cells compare to control cells. Propidium Iodide stained cells were subjected to analyze different stages of cell cycle. B) Bar graph representation of percentage of cells at different stages of cell cycle.

2.4.5 *HPIP alters β-tubulin III isotype expression in MCF7 cells*

Abnormal and high levels of β III-tubulin expression has been related to more aggressive and taxane-resistant cancers (Sève and Dumontet, 2008). Microtubules formed of these β-III tubulin are unstable and even on drug binding to the microtubules, these cells succeed to surpass the mitotic arrest checkpoint. Here, we have utilised this fact to determine whether alterations in HPIP can alter taxol sensitivity. We have ectopically over expressed HPIP by transient transfection. Quantitative RT-PCR was carried out for both HPIP overexpressing and HPIP silencing cells. Results were analysed by $2^{\Delta\Delta Ct}$ method and expressed in terms of relative folds. Indeed we found a 1.5 fold increase in HPIP overexpressed cells and silencing of HPIP resulted in decrease in β-tubulin III expression by ~5 folds compared to the control cells (Fig 17).

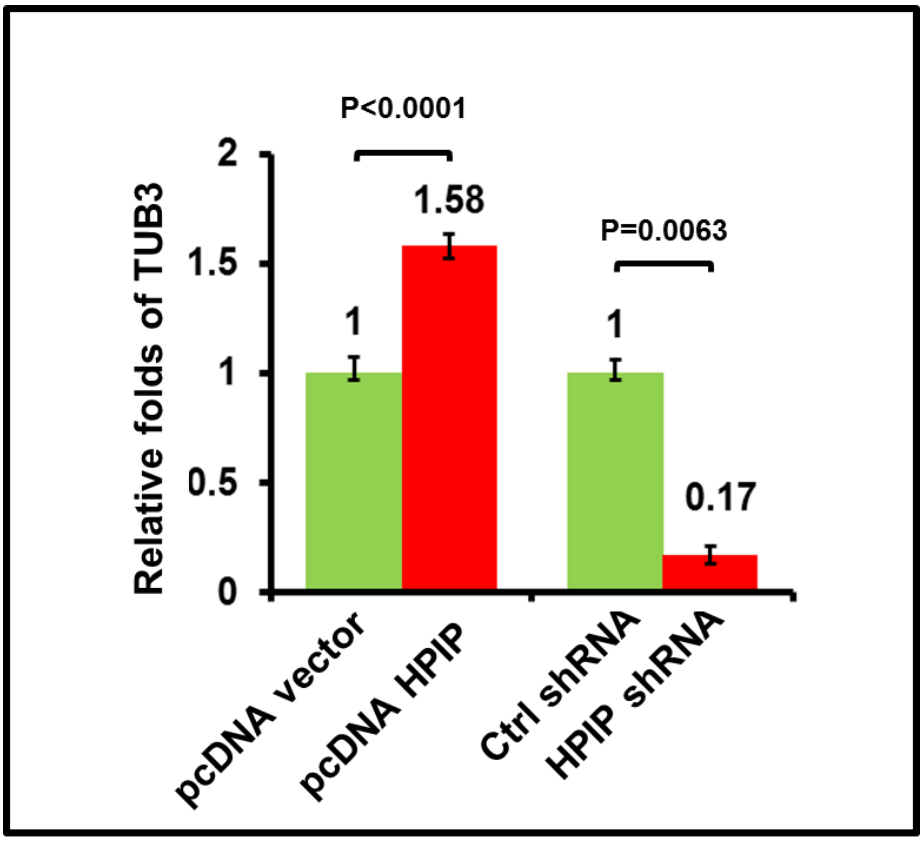

Figure 17. Effect of HPIP on β-tubulin III expression, as a measure of taxol resistance in MCF7 cells. Quantitative RT-PCR was carried out and results were analysed by $2^{\Delta\Delta Ct}$ method.

2.5 DISCUSSION

Acquired resistance of cancer cells to chemotherapy has become a major hindrance in effective treatment of breast cancer. Although tremendous effort has been made to understand the mechanism of such resistance, a clear picture of taxol resistance or strategy to evade cellular resistance to chemotherapy is far from reality. So far multiple factors has been implicated to play a role in taxol resistance. MAPs such as Stathmin, Tau and MAP4 are known to play a key role in taxol resistance by interfering with the taxol binding to microtubules. For example, high Tau expression is observed in taxol resistance in breast cancer (Rouzier *et al*., 2005). Tau protein binds to the microtubule at the same site as taxol, promotes polymerisation and stabilizes microtubules but with greater reversibility. However, Tau overexpression leads to enhanced polymerization but with reduced cell flexibility (Dye *et al.,* 1993). Stathmin, a p53 regulated protein, destabilises microtubules by causing microtubule catastrophe. Overexpression of stathmin is associated with decreased binding of paclitaxel and taxol resistance (Alli *et al.,* 2002). CLIP-170, a cytoplasmic linker protein of 170 kD binds to microtubules and causes microtubule rescue. However overexpression CLIP-170 causes microtubules to form thick ring like bundles and sensitizes cancer cells to taxol (Sun *et al.,* 2012). Several signalling proteins that are components of cell signalling pathways regulating cell cycle arrest and apoptosis has been implicated in taxol resistance. Taz, a component of Hippo-LATS pathway that regulates apoptosis, causes taxol resistance (Lai *et al.,* 2011). Nlp (ninein like protein), which is involved in centrosome maturation and spindle formation, when overexpressed promotes G2-M arrest and attenuates taxol-mediated apoptosis coupled with elevated levelsof anti-apoptotic protein, Bcl-2 (Zhao *et al.,* 2012).

HPIP is known to promote breast cancer (Manavathi *et al.,* 2006; Shostak *et al.,* 2014). HPIP has been associated with poor clinical outcome in patients with invasive breast cancer. HPIP is known to promote cell migration by altering focal adhesion dynamics (Bugide *et al*., 2014).

HPIP is known to bind to the microtubules and also activate AKT pathway when overexpressed HPIP MCF7 cells were treated with taxol (Manavathi *et al.,* 2006). A number of studies associate the activation of AKT pathway with taxol resistance (Yun *et al.,* 2015; McCubrey *et al.,* 2006). Thus, we hypothesized that HPIP can act as a microtubule associated protein similar to tau and stathmin, and can cause taxol binding. Being an upstream regulator of AKT/MAPK pathway (Manavathi *et al,* 2006; Wang *et al.,* 2008), HPIP can trigger anti-apoptotic signalling pathways to escape cell death.

Our findings from publicly available databases imply that HPIP is overexpressed in breast cancers patients that are resistant to taxol therapy compared to patients sensitive to taxol. It is also overexpressed in taxol resistant prostate cancer cell line, DU-145 and PC-3. Previous literature shows that proteins that have been reported to play a role in taxol resistance show variable expression in mammary cell lines, e.g., Taz (Lai *et al.,* 2011). We therefore, verified the expression of HPIP in breast cancer cell lines. Since, the duration of mitotic arrest and extent of cell death vary considerably among human non-transformed cells and cancer cells (Brito and Reider, 2009), we have further checked HPIP expression in both metastatic breast cancer cells (MCF7) and non-transformed cells (MCF10A). Similar to Tau (Rouzier *et al.,* 2005) and Nlp (Zhao *et al.,* 2012) that are found to be overexpressed in taxol resistant breast cancer, HPIP expression is found to be more in the cancerous MCF7 cells in western blot analysis. Concomitantly, MCF7 cells showed a greater cell viability on taxol treatment than non-cancerous MCF10A cells. Thus, HPIP overexpression is observed in taxol resistant breast cancer cells.

Taxanes have been more successful in treating estrogen receptor (ER) negative breast cancer patients than ER positive. Previous studies has reported that taxol resistance is mediated by an ER responsive pathway (Tabuchi *et al.,* 2008). Since HPIP is an ER interacting protein, there is a possibility of involvement of HPIP in taxol resistance. Therefore, we have utilised MCF7,

a cell line long established as a taxol resistant, estrogen receptor positive (ER+) breast cancer cell line as our model system and pursued our investigations. Previous studies have shown that the fate of the cells after taxol treatment depend on the concentration of the drug used. At low concentrations, paclitaxel stabilizes mitotic spindle and activates mitotic checkpoint leading to anaphase block and mitotic arrest. This prevents cell proliferation block and induces apoptosis. At higher concentrations, paclitaxel promotes microtubule bundle formation during interphase, which inhibits S phase entry, which in turn, prevents cell proliferation and induces necrosis (Yeung *et al.,* 1999**)**. We have therefore, determined the IC_{50} value of paclitaxel in HPIP silenced and overexpressed MCF7 cells and found that silencing of HPIP makes cells more sensitive to paclitaxel, whereas, overexpression leads to resistance. Thus, alterations in HPIP levels can lead to changes in sensitivity of the cells towards taxol.

The exact mechanism by which taxol exerts its effect is still unknown. Various reports show that, depending on the drug concentration used *in vitro*, cells can die at the G1 phase of the cell cycle, or arrest in mitosis and die or escape by mitotic slippage. Gascoigne and Taylor has proposed that fate of the cancer cell is dependent on two competing networks: the activation of caspase dependant cell apoptotic pathway and another pathway that degrades cyclin B1 and exit from mitosis (Gascoigne and Taylor, 2009). Denning and Hirose has proposed that chemotherapeutic drugs like taxol mediates apoptotic cell death by an evolutionarily conserved signalling pathway involving DEPDC1 and JNK to inhibit the anti-apoptotic Bcl-2 family proteins CED-9 and MCL1, resulting in caspase activation and apoptosis (Denning and Hirose, 2014). Thus, several signalling molecules that activates the apoptotic pathways have been found to effect taxol sensitivity in cancers. TAZ, a component of the emerging Hippo–LATS tumour suppressor pathway, which plays important roles in regulating cell proliferation and apoptosis in both drosophila and mammals, has been found to taxol resistance in breast cancer (Lai *et al.,* 2011). On the other hand, cancer cell lines overexpressing pro-apoptotic protein

BIM are found to be more sensitive to taxol (Li *et al.,* 2005). Paclitaxel-induced apoptosis is found to be BAK-dependent in breast tumour (Miller *et al.,* 2013). Interestingly, recent studies have shown that the hypoxic microenvironment of cancer tumours can oppose taxol-induced apoptosis and instead activates autophagy (Notte *et al.,* 2013, 2015). Although HPIP overexpression leads to taxol resistance, the IC_{50} value still remains low. This arises question whether HPIP causes taxol resistance by evading the apoptotic pathways. On carrying ut Annexin V assay, we found that HPIP indeed mediates taxol resistance by allowing the cells to escape apoptosis. Silencing of HPIP leads to a higher percentage of cells undergoing apoptosis.

We have further confirmed whether this apoptosis is a result of cell cycle arrest or not. Taxol is found to downregulate Wee1 kinase expression, which phosphorylates and inactivates cyclinB/Cdc2, and induce the activity of cyclin-dependent kinase inhibitor, $p21^{WAF/CIP1}$ (Choi and Yoo, 2012). Taxol resistance is also imparted by Timp-1 protein which decreases the stability of cyclinB1 (Wang *et al.*, 2010). Taxol resistance also occurs as a result of suppression of checkpoint genes, *Mad2* and *BubR1* that abolished checkpoint function (Sudo *et al.,* 2004). We found that on silencing HPIP, higher number of cells are undergoing G2/M arrest.

Previous reports shows that increased β-tubulin class III were associated with poor outcomes for cancer patients. Infact it is considered as a biomarker for taxol resistance (Roque *et al*., 2014). Overexpression of *TUBB3,* a brain-specific tubulin isotype, leads to reduced microtubule assembly and resistance to taxol. There are several proteins that are reported to confer taxol resistance also mediates overexpression of Class III β-Tubulin, e.g., mitotic centromere-associated kinesin (MCAK), a kinesin-related protein that destabilizes microtubules (Ganguly *et al.,* 2011). HPIP is also found to alter the expression of Class III β-tubulin. Overexpression of HPIP results in increase in Class III β-tubulin levels and vice versa.

Thus, in this study we have established a novel function of HPIP of conferring taxol resistance in breast cancer.

Our findings implicate that HPIP is not only an oncoprotein inducing cancer properties to cells but can also be an important determinant of taxol sensitivity of breast cancer cells. Also, in a recent report, focal adhesion kinase (FAK) was found to be up-regulated in taxol-resistant cancer cells. These resistant cells adhered nearly two-fold faster, had higher integrin expression and dramatically reduced focal adhesions, both in size and number (McGrail *et al.*, 2015). Thus we can draw a link between HPIP and FAK with respect to taxol resistance. Thus, like Tau and Stathmin, HPIP can bind to microtubules and cause taxol resistance or, can activate FAK to alter adhesion dynamics leading to resistance to chemotherapeutics and progression in cancer metastasis. Further investigations are, therefore, required to elucidate a functional mechanism for HPIP mediated taxol resistance in breast cancer.

Chapter 3

Mechanism of HPIP- mediated taxol resistance in breast cancer cells

3.1 HYPOTHESIS AND OBJECTIVE

After establishing the role of HPIP in taxol resistance to breast cancer cells, we next intend to examine the mechanism that underlie in this phenomenon. Being a microtubule binding protein, we hypothesize that the direct physical interaction between HPIP and microtubules might affect the taxol binding affinity towards microtubules. Both Abramovich *et al.* and Manavathi *et al.* have shown that HPIP interacts with microtubules (Abramovich *et al.*, 2002; Manavathi *et al.*, 2006). In fact, Abramovich *et al.* has identified the 190-218 aa region to be specifically interacting with microtubules. In this part of the study, we tried to validate whether this region is responsible for imparting taxol resistance.

3.2 INTRODUCTION

Microtubules are highly dynamic cytoskeletal structures made of α/β-tubulin heterodimers. As described earlier, the highly dynamic nature of microtubules is attributed to dynamic instability, in which the ends of the microtubules undergo cycles of slow growth and rapid shortening, as well as treadmilling, in which tubulin gets added at one end of a microtubule and net loss at the other end. Both these phenomena are crucial for cell signalling, migration, transport of proteins, vesicles, mitochondria and other organelles, and in mitosis. During mitosis, microtubules are responsible for the capture and alignment of chromosomes on the metaphase plate followed by their segregation to the two daughter cells at anaphase.

Taxanes are microtubule binding drugs and has been extensively used as a first line of chemotherapy against ovarian cancer, advanced breast cancer, lung cancer and Kaposi sarcoma. Taxol binds to a hydrophobic pocket in the central domain of β-tubulin, wherein it assumes a T-shaped or butterfly structure mimicking a part of the B9-B10 loop in the α-tubulin (Snyder *et al.*, 2001). This eight amino acid loop (residues 362-369) of α-tubulin designated as the stabilizing loop or L-loop promotes the lateral association between protofilaments. Also, the taxol binding site lies close to the M-loop which makes lateral contacts with the H3 helix of the adjacent β-tubulin monomer. On binding to this pocket, conformational changes occur in the microtubule lattice such that the M-loop, now makes stronger bonds (Fig 18; Nogales, 2000). Another possible mechanism is that taxol binding holds the GTPase and second globular domains of β-tubulin in an orientation favourable to maintain the straight protofilament conformation, which is otherwise be altered by hydrolysis of GTP (Amos and Löwe, 1999).

Several microtubule associated proteins have been implicated to cause taxol resistance, e.g., Tau, Stathmin and EB1. Tau binds to microtubules both from inside and outside. It contains a

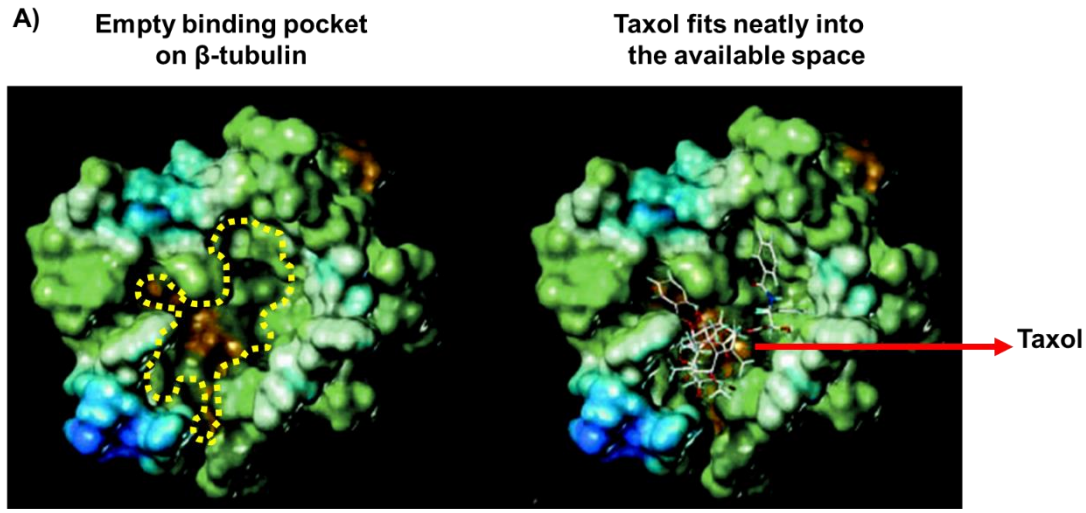

(Source: Snyder *et al.*, 2001)

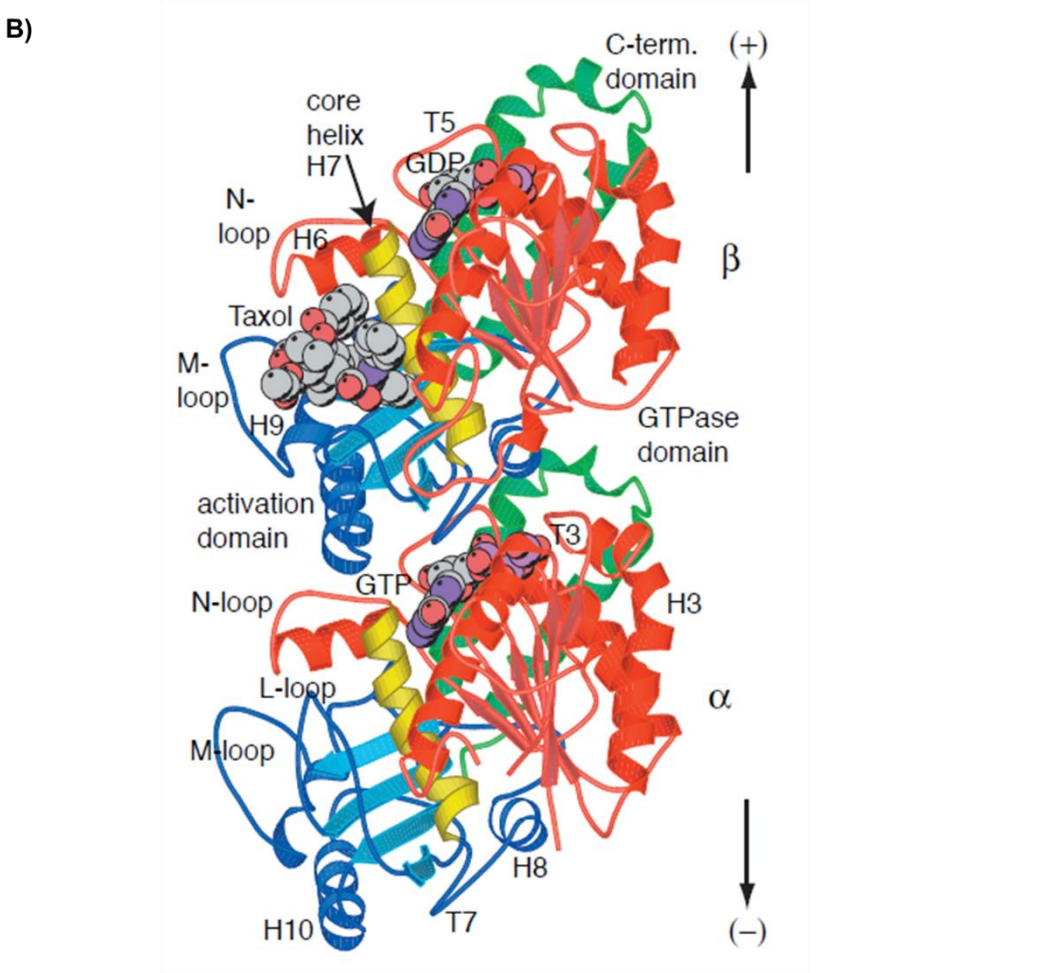

(Source: Amos and Schlieper, 2005)

Figure18. A) Structure of binding site of taxol on β-tubulin. The dotted line marks the empty hydrophobic pocket to which taxol binds. B) Ribbon diagram of αβ-tubulin heterodimer. Pink indicates the GTPase domains, blue indicates activation domains, yellow indicates the core helix that connects the two globular domains in each monomer, and green indicates the C-terminal domain on the external surface.

negatively charged N-terminal domain that projects out from the outer surface. It also contains a microtubule-binding domain with one to five copies of a semi-conserved, hydrophobic, proline-rich motif that binds to the internal surface of the microtubules. Atleast one of the repeating motif in tau overlaps with the taxol-binding site (Kar *et al*., 2003a), and shows sequence THVPGGGN similarity with the conserved TVVPGGDL of the L-loop of α-tubulin (Kar *et al*., 2003b). Under normal conditions, Tau binds to the microtubule at the same site as taxol, promotes polymerisation and stabilizes microtubules but with greater reversibility. Tau overexpression leads to competition for the binding site, enhanced polymerization and reduction in cells flexibility attributing to taxol resistance (Dye *et al.,* 1993).

End binding 1 (EB1) is reported to cause taxol sensitivity in breast cancer (Luo *et al.*, 2014). EB1 is a plus-end-tracking protein (+TIP) that is known to contain a single tubulin binding calponin homology (CH) domain in its N-terminal domain (Vitre *et al.*, 2008; Hayashi and Ikura, 2003). Although it is known to promote taxol binding *in vitro*, the exact molecular mechanism by which EB1 causes taxol sensitivity still remains elusive. It can be either by promoting taxol induced microtubule stabilisation or recruiting other factors e.g., CLIP-170 (Dixit *et al*., 2009).

Stathmin, a p53 regulated protein, binds exclusively to tubulin heterodimers and not microtubules (Orr *et al.,* 2003). It runs along a pair of tubulin heterodimers and its amino-terminal domain sequesters one of the α-tubulin subunits, preventing any further interactions thus leading to destabilisation of microtubules and causing microtubule catastrophe. It also increases the GTPase activity of tubulins by causing a conformational rotation between the GTPase and activation domains within each tubulin subunit (Wang *et al.,* 2007). Overexpression of stathmin is associated with decreased binding of paclitaxel and taxol resistance. (Alli *et al.,* 2002).

HPIP is a multi-nodal protein which plays a role as oncoprotein promoting tumor formation and focal adhesion dynamics (Manavathi *et al.*, 2006; Bugide *et al.*, 2014), activate erythroid differentiation in heamatopoietic cells (Manavathi *et al.*, 2012), germ cell proliferation (Yu *et al.*, 2012), embryonic development in embryonic stem cell (Shiraki *et al.*, 2014) and activates various cell signalling pathways, e.g., Akt-MAPK, PI3K-GSk3β pathways. Here, we report that HPIP is also responsible in determining taxol resistance in breast cancer cells. Thus, it is important to investigate the mechanism by which it causes taxol resistance.

Considering that taxol resistance has been implicated by a number of factors, HPIP can confer taxol resistance by directly interacting with microtubules or by activating cell signaling pathways that eventually activates anti-apoptotic proteins and evade cell death. HPIP was shown to co-localise in the cytoplasm and interact with microtubules (Abramovich *et al.*, 2002; Manavathi *et al.*, 2006). Abramovich *et al.* have reported that the 190-218 amino acid region is the microtubule binding domain of HPIP (Abramovich *et al*., 2002). This 28 amino acid sequence does not show homology with any of the known tubulin binding domains that competes for the taxol binding site, e.g., Tau repeats (Kar *et al.*, 2003b), human doublecortin DCX domain (Kim *et al*., 2003), CAP-Gly domain in CLIPs (Li *et al*., 2002), and calponin homology (CH) domain of EB1 (Hayashi and Ikura, 2003). However, all these domains shows one similar characteristic, i.e., they are all hydrophobic in nature and has binding sites either that of taxol or close to the hydrophobic pocket of β-tubulin. Hydropathy plot of HPIP sequence shows that the 190-218 residues shows maximum hydrophobicity (Fig 22A). Thus, we hypothesized that this region is capable of interacting with the hydrophobic pocket of β-tubulin and thereby, compete with taxol causing taxol resistance. If our hypothesis proves to be correct, an anti-peptide against this 190-218 region can in turn prevent HPIP from binding to microtubules rendering cancer cells sensitive to taxol. This can be used as a therapeutic for

treating cancer in combination with taxol. Thus, in this study we have tried to explore whether HPIP mechanically binds to microtubules and imparts taxol resistance.

3.3 METHODOLGY

3.3.1 Plasmid constructs

The microtubule domain deletion mutant of HPIP **(**HPIPΔMT) in T7-tagged mammalian expression vector, pcDNA 3.1 was generated by using the following strategy (Fig 19). First, we have amplified the regions immediately adjacent to the 190-218 region that is to be deleted, as two separate fragments. Using pcDNA-HPIP as template, we have PCR amplified the 1-190

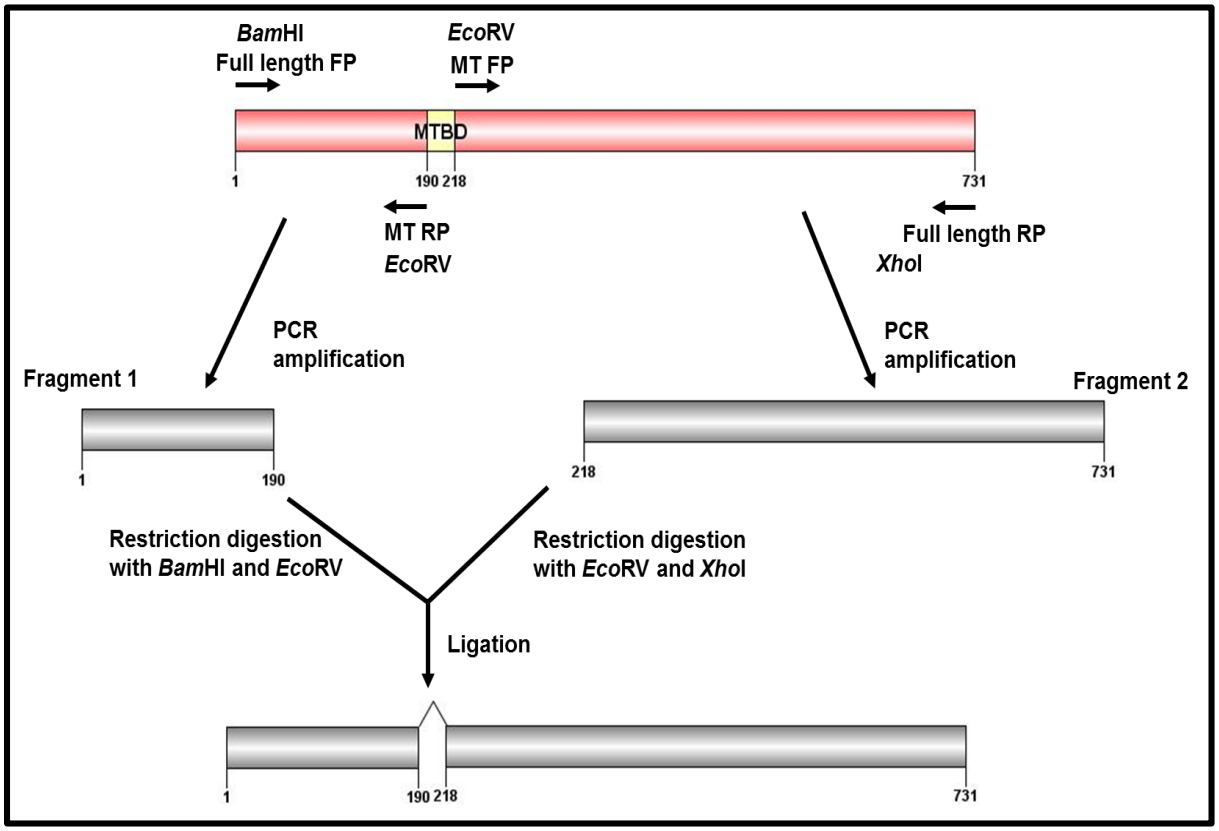

Figure 19. Strategy for cloning pcDNA- HPIPΔMT. The regions adjacent to 190-218 were amplified separately, ligated together and the resultant product was ligated into the pcDNA 3.1A vector.

S.No	Primer name	Sequence	restriction site
1.	WT-HPIP (1-731) Forward	5’ACTTCTCGAGAAATGGCCTCCTGC 3’	*Xho*I
2.	WT-HPIP (1-731) Reverse	5’TTAACGGGATCCTCAGCCCCGGTGGTGGT 3’	*Bam*HI
3	HPIPΔMT Reverse	5’GTAAGATATCGAAGAGCGTCCCT 3’	*Eco*RV
4	HPIPΔMT Forward	5’TTACGATATCATGGCCTCCTGCCC 3’	*Eco*RV
5	HPIP (1-160) Reverse	5’TTAACGGGATCCCCTCTCTAACTCTTGC 3’	*Bam*HI
6	HPIP (1-400) Reverse	5’TTAACGGGATCCGTCTCCAAAGAAGTGGCT 3’	*Bam*HI
7	HPIP (1-695) Reverse	5’TTAACGGGATCCGTCTCCAAAGAAGTGGCT 3’	*Bam*HI
8	HPIP (400-731) Forward	5’ACTTCTCGAGAACAGCGACGGCTGCTG 3’	*Xho*I

Table 2. List of primers used in this study

region of HPIP with WT-HPIP full length forward primer with *Bam*HI site and HPIPΔMT reverse primer. with *Eco*RV site. Similarly, the 218-731 region of HPIP was PCR amplified using WT-HPIP full length reverse primer with *Xho*I and HPIPΔMT forward primer with *Eco*RV site. The sequence of the primers have been catalogued in Table 2. The amplified fragments were digested with appropriate restriction enzymes separately and then ligated together to generate the HPIP- HPIPΔMT. The final product was then ligated into pcDNA 3.1C vector (Fig 19).

Name	Description	Insert size	Reference
BM 22	pcDNA3.1/T7-HPIP	2196 bp	Manavathi *et al*., 2006
BM 115	pGEX4T1-HPIP	2196 bp	In this study
BM 36	pcDNA HPIPΔMT	2166 bp	In this study
BM 107	pEGFP-HPIP	2196 bp	In this study
BM 110	pEGFP-HPIP (1-160)	480 bp	In this study
BM 111	pEGFP-HPIP (1-400)	1200 bp	In this study
BM 109	pEGFP-HPIP (1-695)	2085 bp	In this study
BM 113	pEGFP-HPIP (400-731)	993 bp	In this study
BM 119	pGFP-V-RS-HPIP shRNA 1	-	OriGene, USA
BM 120	pGFP-V-RS-HPIP shRNA 2	-	OriGene, USA
BM 123	pGFP-V-RS-control shRNA	-	OriGene, USA
BM 260	mCherry-Tubulin	1771 bp	Addgene, USA

Table 3. List of plasmids used in this study

For generating GST-tagged recombinant protein, the full-length HPIP sequence was released from pcDNA-HPIP plasmid by restriction digestion with *Bam*HI and *Xho*I (Fermentas, USA), and cloned into pGEX4T1 vector.

Size deletion mutants of HPIP were generated by polymerase chain reaction (PCR) amplification using pcDNA-HPIP as template using the primers mentioned in the Table 2. These fragments were then ligated into pEGFP-C1 vector after being digested with *Xho*I and *Bam*HI (Fig 24B). The mCherry-Tubulin was procured from Addgene, USA. *HPIP* gene specific 29-mer shRNA and nonspecific scrambled shRNA were procured from OriGene, USA. Plasmids used in this study has been listed in Table 3.

3.3.2 Cell culture

All the experiments were carried out either in MCF7 or HEK293T cells. These cells were procured from NCCS, Pune and cultured in a humidified atmosphere containing 5% CO_2 and maintained at 37^{o}C in Dulbecco's Modified Eagle's medium (DMEM) medium supplemented with 10% fetal bovine serum (FBS), 10 units/ml penicillin, and 10 µg/ml streptomycin.

3.3.3 *Transient transfection of cells*

Transient transfection was carried out using Lipofectamine™ 2000 (Invitrogen, USA) following the manufacturer's protocol. Cells were seeded onto plates in complete DMEM medium and allowed to grow till 70-80% growth confluency. Transfection complexes were prepared with plasmid DNA (µg) and Lipofectamine™ 2000 (µl) in a 1:1 ratio in 100 µl of Opti-MEM and incubated for 20 minutes at room temperature. Following incubation, transfection mix was added to culture plates containing serum and antibiotic- free DMEM medium. Cells were incubated in a humidified atmosphere containing 5% CO_2 at 37^{o}C for 6 hours following which the medium was replaced with fresh DMEM containing serum and antibiotics. Expression of transfected plasmids were verified after 48 hours either under the microscope or by western blotting.

3.3.4 Drug accumulation assay

Stabilization of microtubules by paclitaxel was studied by quantifying drug uptake by the cells. Cells sensitive to paclitaxel show a greater binding of the drug to the microtubules and this can be measured as fluorescent intensity of cells taking up drugs labelled with a fluorescent dye. Equal number of MCF7 cells were seeded in 60 mm culture dishes. Next day, the cells were transfected with control shRNA vector and HPIP- silencing shRNA plasmid respectively. After 48 hours of transfection, cells were incubated with 1 µM of fluorescent Oregon Green

paclitaxel (Molecular Probes Inc., USA) for 1 hour and were immediately analysed by FACS Calibre (BD Biosciences, USA).

3.3.5 Immunofluorescence microscopy

Cells were seeded on coverslips in 6-well plates. After completion of experimental procedures, the medium was removed and cells washed with the PBS buffer. Fixation was carried out with paraformaldehyde (4%) at room temperature for 20 minutes followed by washing with TBS thrice, 5 minutes each time, under shaking. Pre-chilled acetone and methanol (1:3) mixture was used to permeabilize cells for 20 minutes followed by washing with TBS thrice for 15 minutes each. This was followed with blocking with 3% BSA in TBS for 1 hour at room temperature followed by incubation with primary antibody (1:200 dilution) in 3% BSA at 4^{o}C overnight. Washings were carried out using TBS, TBS with triton-X (TBST) and TBS buffer, each time for 15 minutes, under shaking. Appropriate Alexa Fluor- tagged secondary antibody (Molecular Probes Inc., USA) in 3% BSA was added and incubated in dark at room temperature for 1 hour followed by washings with TBS buffer. Excess buffer was removed and the coverslips were mounted on glass slides with prolonged gold anti-fade reagent with DAPI (Invitrogen Life technologies, USA). The cover slip is incubated for 16 to 24 hours in dark at room temperature and edges are sealed with nail polish. Images were acquired at 20% magnification with Olympus F100 microscope (Olympus, USA).

3.3.6 Isolation of tubulins

Tubulin was isolated and purified from mammalian brain following a modified Weisenberg procedure (Andreu, 2007; Weisenberg, 1972). Bovine brains were homogenized in PMS buffer (10 mM sodium phosphate, 0.5 mM $MgCl_2$, and 0.24 M sucrose, pH 7.0) to remove cell membrane followed by successive ammonium sulphate fractionation of 32% and 43% saturation, respectively. Centrifugation at every step was carried out at 19000xg for 45 minutes,

4°C. The pellet was dissolved in PMG buffer (10 mM sodium phosphate, 0.5 mM $MgCl_2$, 0.1 mM GTP, pH 7.0) and subjected to batch DEAE sephadex anion exchange using 0.4M KCl-PMG buffer and finally eluting with 0.8 M KCl-PMG buffer. The elutant was saturated and precipitated with 43% ammonium sulphate. The pellet was dissolved in PMG buffer and gel exclusion chromatography was performed using Sephadex G25. Fractions of 0.5 ml were collected and precipitated with 40 mM $MgCl_2$. The fractions which showed rapid turbidity were considered as active tubulin, and were pooled and centrifuged followed with dialysis against tubulin polymerization buffer (10 mM sodium phosphate pH 6.5, 3.4 M glycerol, 1 mM GTP). Purified tubulin was stored in 50 µl aliquots at -80°C.

3.3.7 Recombinant protein purification

Recombinant His-tagged wild-type HPIP (WT-HPIP) and mutant HPIPΔMT (HPIP lacking microtubule binding domain 192-218 amino acids) were purified by affinity chromatography with TALON® metal affinity resin (Clontech, USA). Human Embryonic Kidney 293T cells (HEK293T) grown on 100 mm dishes were transfected with 10 µg each of pcDNA-HPIP and pcDNA-HPIPΔMT using Lipofectamine 2000 (Invitrogen, USA) following the manufacturer's protocol. After 48 hours post transfection, cells were lysed using Nonidet P-40 (NP-40 buffer; 150 mM NaCl, 1% NP-40, 50 mM Tris-Cl, pH 8.0) and centrifuged at 13000 rpm. The supernatant was incubated with TALON® beads for 1 hour under rotation at 4°C. The beads were pre-washed with equilibration buffer (50 mM sodium phosphate, 300 mM NaCl, pH 8.0). After incubation with supernatant, beads were washed thrice for 15 minutes with wash buffer (50 mM sodium phosphate, 500 mM NaCl, 10 mM imidazole, pH 7.0). Imidazole concentration was increased upto 40 mM to remove non-specifically bound proteins. Finally, bound proteins were eluted with buffer containing 50 mM sodium phosphate, 300 mM NaCl and 150 mM imidazole. The eluted protein was dialysed against BRB80 buffer (80 mM PIPES, 1 mM

EGTA, 1 mM $MgCl_2$, pH 6.9) The dialysed protein was concentrated in Amicon ultra tubes (Millipore, USA) with a molecular weight cut off (MWCO) of 30 kD following the manufacturer's protocol. The protein solution was centrifuged 3-4 times at 3000 rpm at 4°C for 10 minutes, each time adding 3-4 ml of BRB80 buffer. After adding glycerol (10%) to the purified protein, it was stored at -80°C for further use.

Recombinant GST and GST-HPIP were purified from pGEX4T1 and PGEX4T1-HPIP transformed E. *Coli* BL21 clones, respectively. Positive clones were induced with 1mM IPTG in late log phase at 30°C. Bacterial cultures were centrifuged and lysed with buffer containing 20% glucose, 10% glycerol, 50 mM tris pH 8, 2 mM DTT, 4 mM PMSF, 20 mM sodium fluoride and proteinase inhibitor cocktail. Lysate was further sonicated at 20% amplitude followed by centrifugation at 12000 rpm for 20 minutes at 4°C. The supernatant was incubated with GST-agarose beads (GE healthcare, USA) at 4°C and kept under rotation for 3 hours. These beads were extensively washed with NP-40 buffer (50 mM tris, 150 mM NaCl, 0.5% Np-40, 10% glycerol, 3 mM $MgCl_2$, 1 mM EDTA), and finally eluted with buffer containing 50 mM tris pH 9.5 and 10 mM glutathione. The protein purity was checked by running on SDS-PAGE and immunoblotting.

3.3.8 In vitro polymerisation Assay

Tubulin polymerization assay was performed in 100 µl volumes at 37°C in PEM buffer (80 mM PIPES, 1 mM EGTA, 1 mM $MgCl_2$, pH 6.9) using 1 mM GTP and 10 mg/ml of either purified goat brain tubulin or purified tubulin from Cytoskeleton Inc., USA. Polymerisation of tubulins with various concentrations of either wildtype HPIP or mutant HPIP-ΔMT in the presence and absence of paclitaxel was monitored spectrophotometrically at OD_{340} and readings were taken every 30 seconds for 30 minutes. Results are presented graphically as change in turbidity (percentage) over time (seconds).

3.3.9 Transmission electron microscopy (TEM)

For electron microscopy, the sample reaction of tubulin polymerization assay was used. After 30 min of incubation, the samples were fixed with prewarmed 2% glutaraldehyde overnight at 4^{o}C. The samples were diluted 25X and applied to carbon-coated electron microscopy grids (300 mesh). The grids were allowed to dry and washed with MiliQ water to remove excess sample. Subsequently, the grids were negatively stained with 2% phosphotungstate acid. The images were acquired using a Tecnai G2 transmission electron microscope (Fei, USA).

3.3.10 Immunoprecipitation

Cell lysates were prepared in nonidet P-40 (NP40) lysis buffer (20 mM Tris pH 8.0, 137 mM NaCl, 10% glycerol, 1% NP40, 2 mM EDTA and protease inhibitor cocktail). Approximately 1 mg of cell lysate was pre-cleared with agarose A/G beads and immune-precipitated with the indicated antibodies for overnight at 4°C. Agarose A/G beads were added (Santa Cruz Biotechnology, Texas, USA), incubated for 1 hr at 4°C under rotation. The beads were pelleted by brief centrifugation and washed at 4°C using NP40 lysis buffer. Finally, the beads were pelleted by centrifugation and dissolved in 2x SDS loading dye and then subjected to western blotting with respective antibodies.

3.3.11 Cell viability assay

Cells were seeded in 96-well plate (Corning, USA) at a density of 1x 10^5 and incubated at 37^{o}C. Cells in triplicate wells were treated with increasing concentrations of paclitaxel (Sigma) ranging from 0.01-5 µM and DMSO as vehicle control in a final volume of 100 µl for 48 hours. After drug treatment, 10 µl of WST-1 (Clonetech, USA) was added to each well and incubated for 30 minutes to hours at 37^{o}C, depending on colour development. The formation of formazan product was quantified by measuring absorbance at wavelength between 420-480 nm

(maximum absorbance at 440 nm) and at a reference wavelength of >600 nm. The 50% inhibitory concentration (IC_{50}) was calculated by using Sigma Plot software.

3.4 RESULTS

3.4.1 HPIP interferes with taxol binding to microtubules

Taxol diffuses into the microtubule lumen through small openings and binds to the internal wall of the microtubule, enhancing lateral contacts between protofilaments thereby restricting microtubule dissociation (Nogales, 2001). Therefore, we wanted to check whether HPIP can interfere with the binding of taxol to microtubule. This would directly affect the pharmacological accumulation of the drug. We have utilised a fluorescent labelled paclitaxel, Oregon Green® 488 Paclitaxel (Life technologies, USA; Fig 20A). Thus the fluorescence intensity is directly proportional to the amount of taxol bound to the microtubules (Rouzier *et al.,* 2005). Here, we have used two different HPIP targeting shRNA plasmid constructs for silencing HPIP in MCF7. We found that the HPIP silenced MCF7 cells when treated with Oregon Green® 488 Paclitaxel showed a bimodal distribution of fluorescence intensity compared to the control cells that showed unimodal distribution (Fig 20B). Thus, HPIP silenced cells showed an extra population of cells with high fluorescence intensity assuming that these represent the successfully transfected cells. A graphical representation showed that only 4.28% of the control cells showed high fluorescence whereas, percentage of MCF7 silenced with HPIP shRNA1 and HPIP shRNA2 with high fluorescence were 39.44% and 34.17% respectively (Fig 20C).

3.4.2 HPIP affects taxol-induced microtubule polymerisation and stability

Microtubules are highly dynamic structures undergoing reversible cycles of polymerisation and depolymerisation. This phenomenon is known as dynamic instability (Mitchison and

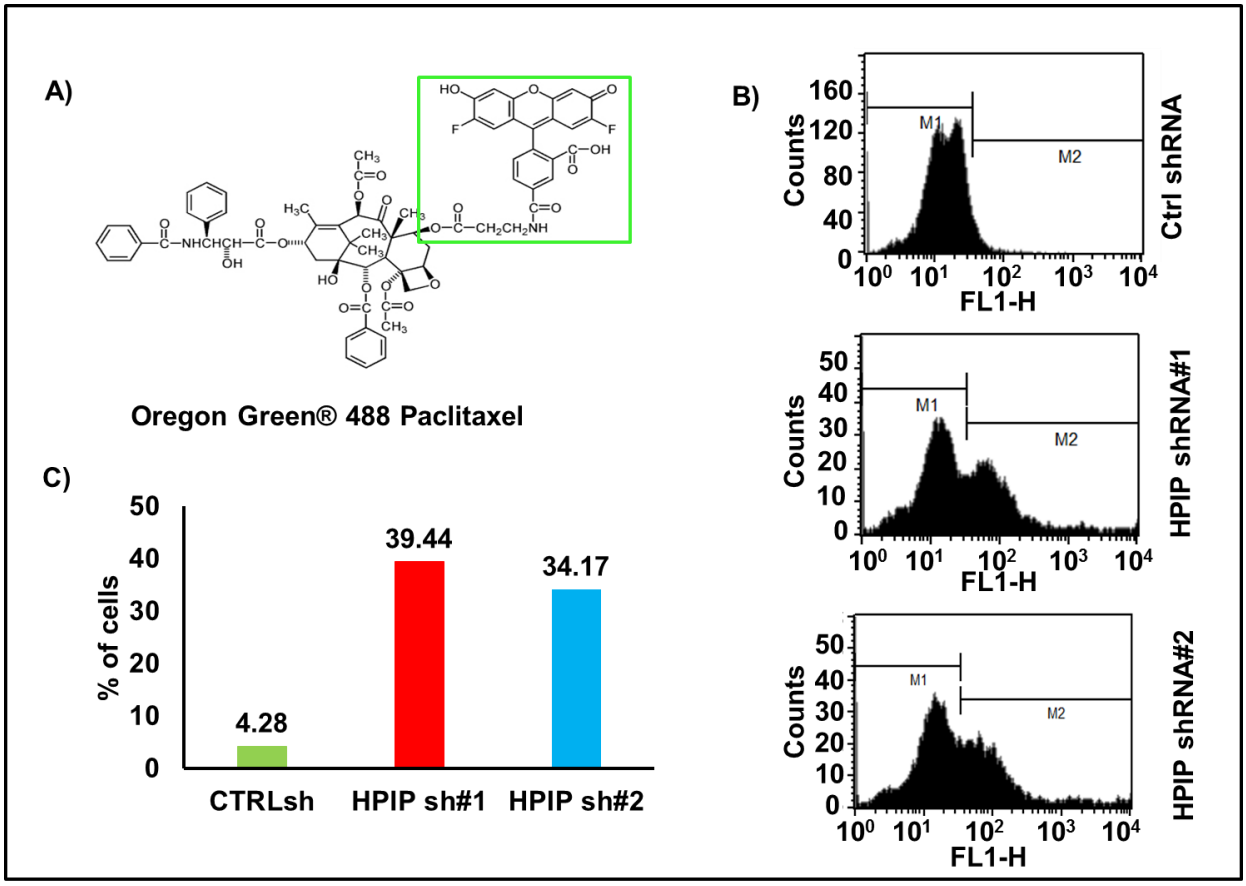

Figure 20. HPIP interferes with taxol binding to microtubules. A) Structure of Oregon green ® paclitaxel B) FACS analysis of transfected cells C) Percentage of cells showing high fluorescence.

Kirschner, 1984a). However, taxol lowers the critical tubulin concentration required to drive microtubule polymerisation and stabilises microtubule (De Brabander *et al.*, 1981), which finally results in mitotic arrest and apoptosis. We, next checked whether HPIP affects the taxol induced microtubule polymerisation and stabilization. We have carried out a spectrophotometric assay based on the fact that microtubules scatter to an extent that is proportional to the concentration of microtubule polymer (Shelanski *et al.*, 1973). Thus, tubulin polymerisation can be observed by monitoring the optical absorbance of the tubulin solution at 340 nm.

We have generated GST-tagged HPIP by cloning HPIP into pGEX4T1 vector (Fig 21A), and isolated and purified GST-HPIP recombinant protein using GST-sepharose beads (Fig 21B).

Initially, we had isolated and purified tubulins from mammalian brain following a modified Weisenberg procedure (Andreu, 2007; Weisenberg, 1972; Fig 21C). Thus, tubulin polymerisation was carried out with paclitaxel in presence and absence of GST-HPIP. As expected, the resulting polymerization curve represented the three phases of microtubule polymerization, namely nucleation, growth and steady state equilibrium. We observed that in the presence of GST-HPIP, the growth phase was reduced by ~16% indicating that HPIP interferes with the microtubule polymerisation activity of taxol (Fig 21D). Previous reports showed that microtubule associated proteins are capable of making morphological changes in the microtubule sheet, e.g., EB1 induces sheet closure as observed under electron microscopy (Vitre *et al.,* 2008). Therefore, we have subjected the tubulin polymerisation reaction mixture under TEM. Even at a resolution of 50 nm we failed to observe any structural changes in the microtubules as a result of HPIP.

3.4.3 Does 190-218 amino acid region of HPIP interact with microtubules?

Previously, HPIP is known to locate along with the microtubules (Manavathi *et al.,* 2006). Infact, Abamovich *et al.,* has mapped the microtubule binding region (MBD) to be between 190-218 amino acids of HPIP and claimed it to be sufficient to retain the protein into the cytoplasm (Abramovich *et al.,* 2002). ProtScale computation of hydrophobicity of HPIP using the Kyte and Doolittle scale revealed that the region of 190-218 amino acid shows highest hydrophobicity (Kyte and Doolittle, 1982; Fig 22A). We hypothesized that this leucine region of HPIP is capable of interacting with the hydrophobic pocket of the β-tubulin where taxol binds. This may lead to a competition for the binding site between HPIP and taxol accounting for the HPIP mediated taxol resistance. If our hypothesis is proved true then an anti-peptide targeting the 190-218 region would inhibit the binding of HPIP to the taxol binding site on tubulins. This, in turn, can sensitise the cells towards taxol. Therefore we have generated a

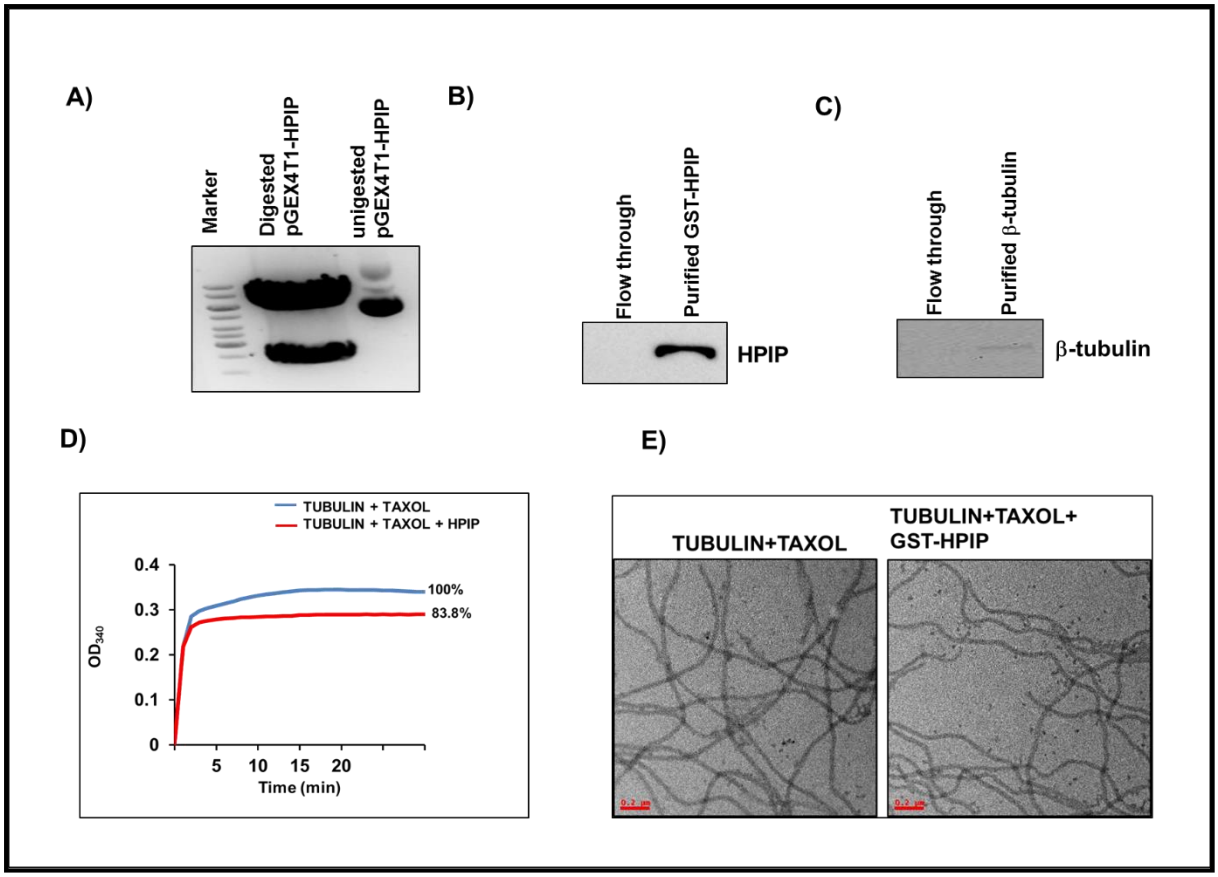

Figure 21. Effect of HPIP on taxol induced polymerization. A) Confirmation of HPIP insert in pGEX4T1 vector by restriction digestion with BamHI and XhoI on 1% agarose gel. B) SDS-PAGE showing purified GST-HPIP. C) Purification of tubulin from bovine brain and immunoblotting with anti –β tubulin antibody. D) *In vitro* tubulin polymerization assay with taxol in the presence and absence of GST-HPIP. E) Transmission electron microscopy of tubulin polymers.

MBD deletion mutant of HPIP (HPIPΔMT) and cloned into pcDNA 3.1 vector (Fig 22B). We have transfected both wildtype and mutant HPIP into HEK293T cells, and extracted and purified His-tagged WT-HPIP and His- tagged HPIPΔMT using metal TALON® beads (Fig. 22C). We have repeated *in vitro* tubulin polymerisation assay to check whether the mutant HPIP can reverse the effect of the wildtype HPIP on taxol induced tubulin polymerisation. Contradicting our expectations, the His- tagged HPIPΔMT had a similar effect as the His-tagged WT-HPIP. Mutant HPIP showed 35.56% whereas wildtype showed 43.46% reduction in taxol- induced microtubule polymerisation (Fig 22D).

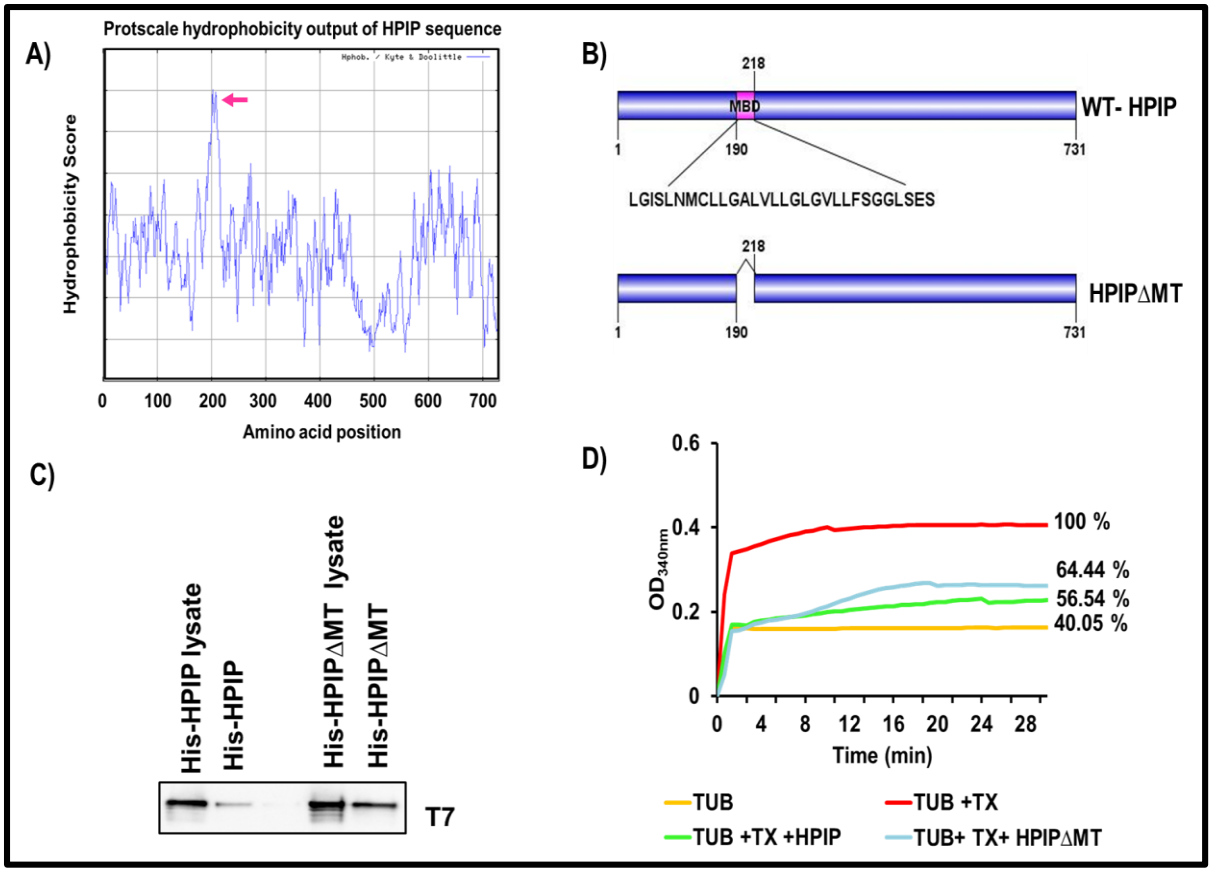

Figure 22. A) ProtScale hydropathy plot of HPIP protein sequence. B) Schematic representation of wild type HPIP (WT-HPIP) and microtubule binding domain (MBD) deleted mutant (HPIPΔMT). C) Expression and purification of His-tagged WT-HPIP and HPIPΔMT. D) *In vitro* tubulin polymerisation assay with taxol in the presence of WT-HPIP, HPIPΔMT or none.

To verify that the 190-218 amino acid region of HPIP is truly a microtubule binding region or not, we have checked the co-localisation of the wildtype and mutant HPIP. We have transfected pcDNA-HPIP and pcDNA-HPIPΔMT into MCF7 cells. Anti-rabbit His antibody was used to probe His-tagged proteins (Invitrogen, USA) and anti-rabbit α-tubulin antibody (Sigma, USA) was used to probe microtubules. After reprobing with appropriate secondary Alexa Fluor antibodies (Invitrogen, USA), the coverslips were observed under fluorescent microscope. The mutant HPIPΔMT was found to co-localise along with microtubules in a way similar to WT-HPIP (Fig 23A). Also, when wildtype or mutant his-tagged HPIP were incubated with MDA MB 231 cell lysates, mutant HPIP was found to interact and pull down tubulins along with it

similar to wildtype HPIP (Fig 23B). This makes the authenticity of the microtubule binding domain of HPIP (190-218 amino acids) highly debatable.

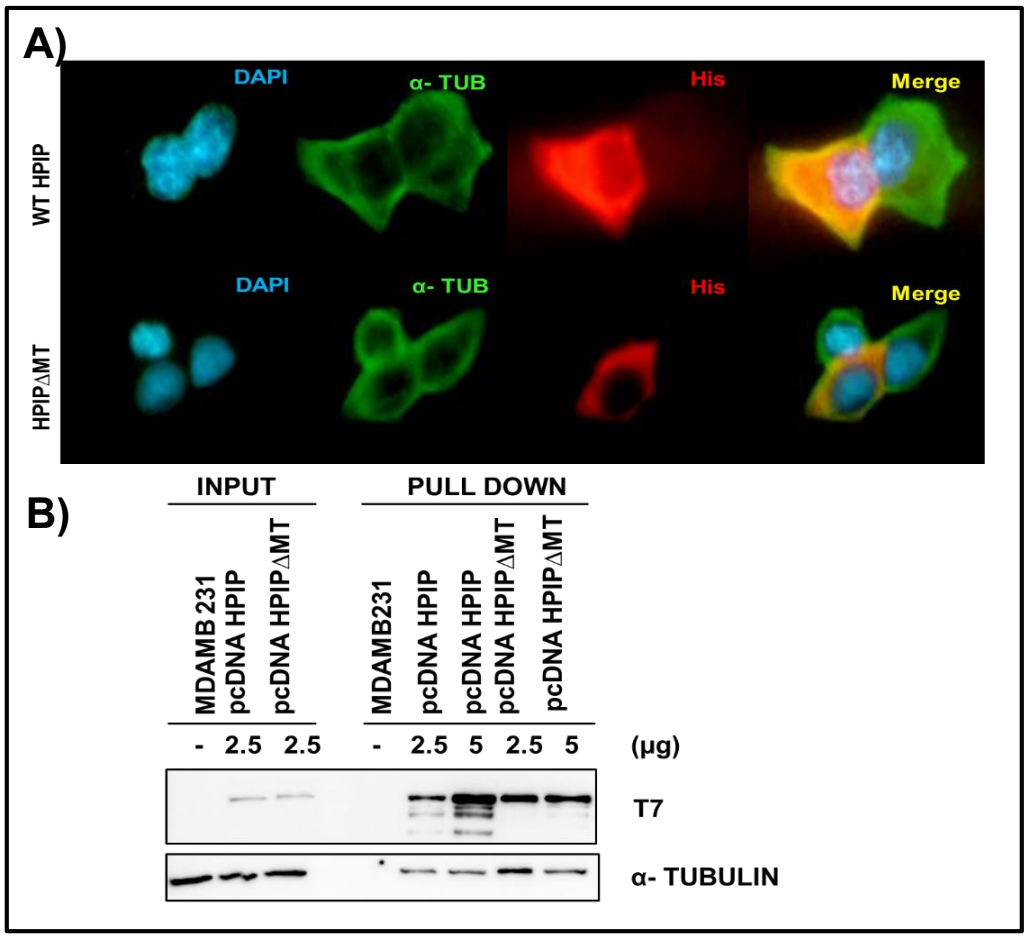

Figure 23: A) Co-localisation of WT-HPIP and HPIPΔMT along with α-tubulin in MCF7 cells. B) Pull down assay of tubulins by Ni-Talon beads bound with His-tagged WT-HPIP and HPIPΔMT

3.4.4 Identification of microtubule binding region of HPIP

Since our initial hypothesis that the 190-218 region of HPIP interacts with the taxol binding site failed, it became important that we map the region of HPIP that is involved in the nteraction between HPIP and microtubules. We have generated different GFP-tagged deletion mutants of HPIP, namely, 1-160, 1-400, 1-695 and 400-731 (Fig 24A). These clones were confirmed with restriction digestion with BamHI and XhoI followed with sequencing (Fig 24B). To map the region interacting with tubulins, we performed co-immunoprecipitation using HEK293T cell

lysate. We have co-transfected HEK293T cells with mcherry-tubulin C-18 plasmid along with the GFP tagged mutants of HPIP and immunoprecipitated GFP antibody and immunoblotted with α-tubulin. 10% input of cell lysated were also immuno blotted with GFP antibody to verify the transfection efficiency (Fig 24C). All the mutants expressed highly except for the C-terminal 400-731 amino acid plasmid, which showed low expression levels. Co-immunoprecipitation with GFP showed that all the mutants that retain the C-terminal were able to interact with tubulins (Fig 24D). Thus, we concluded that HPIP interacts with tubulins through its C-terminal domain.

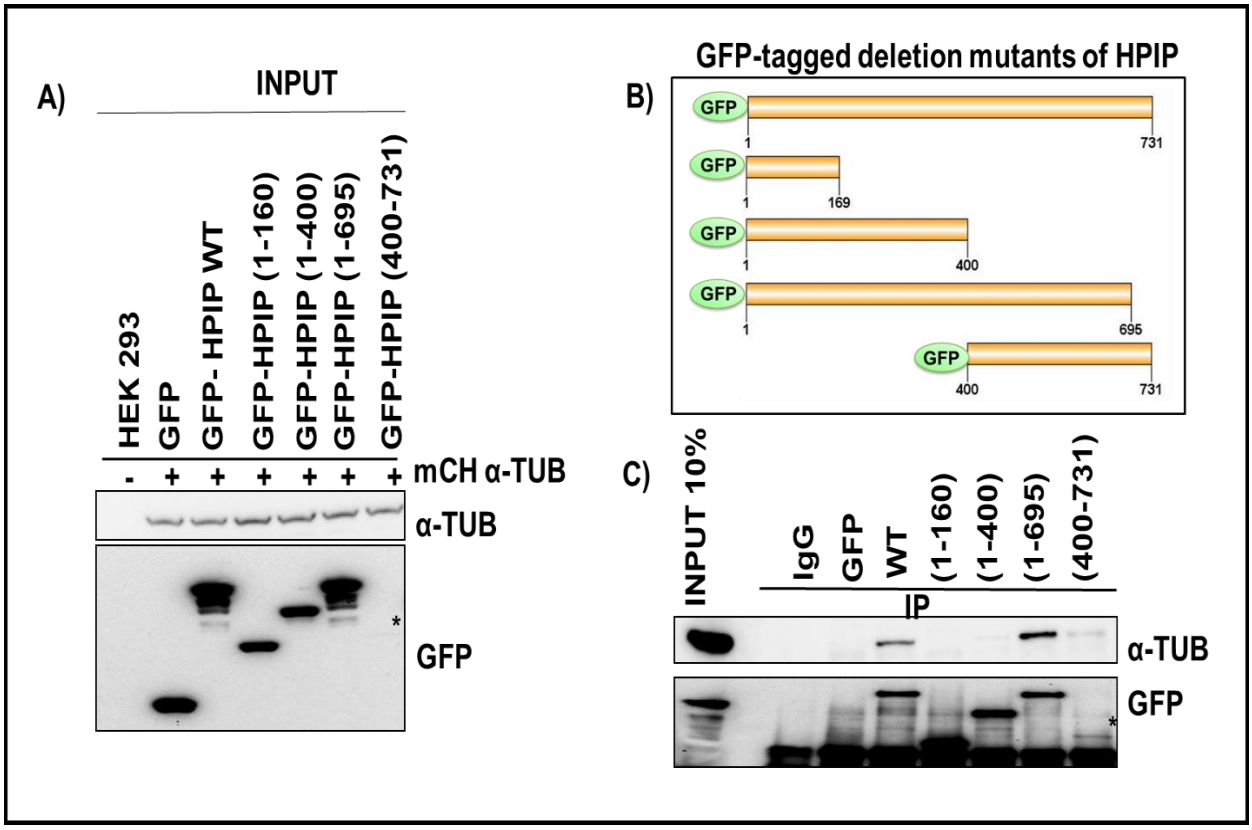

Figure 24. Identification of microtubule binding region of HPIP. A) HEK293T cells were co-transfected with mcherry-Tubulin-C18 and different size deletions lysates on SDS-PAGE and immunoblotting with specific proteins. B) Schematic diagram of the size deletion mutants generated during the course of the study. C) Cell extracts were immunoprecipitated with GFP antibody and immunoblotted first with anti- α-tubulin and then anti-GFP antibodies. Cell extracts immunoprecipitated with IgG antibody was used as control.

3.4.5 Role of C-terminal domain in taxol resistance

We have determined that the C-terminal domain (400-731) amino acid region of HPIP is crucial for interacting with microtubules. We, therefore, wanted to know if this region is involved in imparting taxol resistance in breast cancer. We have carried out cell viability assay with WST-1. We have used wildtype pEGFP-HPIP as a positive control and N-terminal pEGFP-HPIP (1-400) as a negative control. We have transfected MCF7 cells with wildtype pEGFP-HPIP, N-terminal pEGFP-HPIP (1-400) and C-terminal pEGFP-HPIP (400-731). After 24 hours of transfection, cells were seeded into 96 well plate and next day onwards cells were treated with increasing concentrations of taxol for 24 hours. We observed that the C-terminal region showed a better resistance and a higher cell viability than wildtype HPIP (Fig 25A). The IC_{50} value of taxol in C-terminal pEGFP-HPIP (400-731) transfected cells were 0.61 µM, whereas in peGFP-HPIP transfected cells it is 0.45 µM and 0.08 µM in N-terminal pEGFP-HPIP (1-400) transfected cells (Fig 25B). This proves that, the C-terminal region of HPIP from 400-731 amino acid region is important for interaction with microtubules and also responsible for causing taxol resistance.

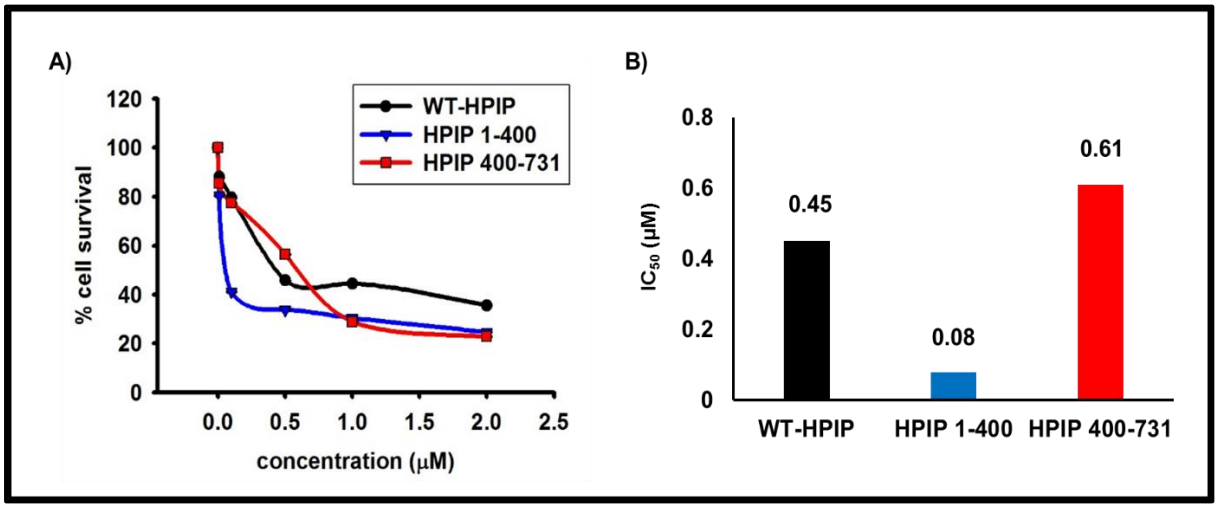

Figure 25. Effect of C-terminal domain of HPIP on taxol resistance. A) Cell viability assay of cells transfected with WT-HPIP, N-terminal (1-400 residues) of HPIP and C-terminal (400-731 residues) on treatment with increasing concentrations of paclitaxel. The percentage of cell survival was plotted as a function of drug concentration. B) The 50% inhibitory concentration (IC_{50}) was calculated with Sigma Plot software.

3.5 DISCUSSIONS

Various microtubule binding proteins when overexpressed in cancer cells have been implicated to confer taxol resistance, namely, Tau, EB1 and Stathmin. These proteins under normal conditions play important roles in cellular functioning. For instance, Tau is expressed abundantly in neuronal cells where it stabilizes microtubules as well as provides flexibility in the distal portions of axons (Scholz and Mandelkow, 2014). EB1 is a master regulator of microtubule plus ends and regulates dynamic instability. It is a cofactor or forms a scaffold for various other microtubule interacting proteins (Akhmanova and Steinmetz, 2008). STOPS are calmodulin binding proteins that functions in nerve cells and stabilise microtubules (Amos and Schlieper, 2005). All these proteins bind to microtubule by well-defined hydrophobic domains that seem to occupy a pocket in β-tubulin that corresponds to an extended loop (L-loop) in α-tubulin. These structures stabilise lateral contacts by holding the important M-loop in place (Amos, 2004).

HPIP is known to cause tumor progression, cell migration enhance focal adhesion dynamics and activation of cell signalling pathways. Previous literature shows that it has all the characteristics attributed to an oncoprotein. Various oncoproteins are known to cause resistance to chemotherapeutics. In this study, we have shown that HPIP is overexpressed in taxol resistant breast cancers. It confers resistance to taxol by promoting G2/M arrest followed by apoptosis. HPIP overexpression also leads to activation of AKT signalling on treatment with taxol. Previously, Abramovich *et al.* and Manavathi *et al.* have shown that HPIP is a microtubule interacting protein by immunofluorescence studies (Abramovich *et al*., 2000, 2002; Manavathi *et al.,* 2006). Fluorescence spectrophotometric studies and competitive binding experiments with [^{32}P]-GTP in our lab shows that HPIP binds to GTP (unpublished data by Manavathi *et al.*). Also, Abramovich *et al.* has reported that the 190-218 amino acid residues of HPIP are responsible for interacting with microtubules. Therefore, these data

suggests that HPIP not only interacts with microtubules but also plays a role in microtubule dynamics.

In this study we found that HPIP interferes with taxol binding with microtubules and also reduces the taxol induced microtubule polymerisation. Therefore, we investigated the role of the 190-218 amino acid region in interfering with taxol activity on microtubules. We hypothesized like other microtubule stabilizing proteins like Tau and STOPs, whether this region can occupy the hydrophobic site in β-tubulin. In this case, a peptide targeting this region can be used as a therapeutic supplementary along with taxol to treat breast cancer. We found that this region exhibits maximum hydrophobicity in HPIP. This region does not show homology with any known microtubule binding protein, neither does it possess any well-known domain or motif that binds to microtubules, e.g., Tau proline-rich repeats, EGGP motif of STOP protein, etc.

We have generated a mutant with the 190-218 residues deleted in HPIP protein. We observed that the mutant has an effect similar to the wildtype in reducing microtubule polymerisation and stabilisation induced by taxol. We have further verified whether this mutant interacts with microtubules. Our results contradict with that reported by Abramovich *et al.* and hence, we conclude that this domain is probably not the true microtubule binding domain of HPIP. This contradiction of results may be because, firstly, Abramovich *et al.* has shown the localisation of the microtubule binding domain of HPIP in the cytoplasm as a result of the GFP fluorescence, they didn't show any colocalisation with microtubule Secondly, they have concluded that the 190-218 residues bind to microtubule as a result of it lacking the NES and it being exported from the nucleus by the CRM1 receptor. They did not show any direct interaction. Here, we found that, even with the 190-218 residues deleted, the mutant still co-localise with microtubules and can pull down microtubules *in vitro* indicating direct interaction

with the microtubules. Further, when we have mapped the region binding to microtubules by co-immunoprecipitation with different deletion mutants of HPIP, the C-terminal region of HPIP (400-731 residues) interacts with microtubules, whereas, Abramovich *et al.* has reported the N-terminal region between 120-263 residues are important for microtubule binding (Abramovich *et al.*, 2002). We have shown that N-terminal region (1-400 residues) shows taxol sensitivity whereas, the C-terminal region (400-731 residues) shows better resistance than the wildtype full length HPIP. It has been reported that C-terminal domain is also important for other functions of HPIP, e.g., FAK interaction and activation (Bugide *et al.*, 2014). Further studies are required to elucidate the residues in the C-terminal region that interacts with microtubules.

Thus, HPIP is an important oncoprotein and can be a promising single gene marker of sensitivity to paclitaxel-containing chemotherapeutic regime. However, several questions still needs to be addressed, e.g., the cell signalling pathway that is triggered by HPIP as a result of taxol resistance and whether HPIP can show resistance to other chemotherapeutic drugs like vincristine and colchicine. Since, drug resistance is a multifactorial phenomenon in cancer, targeting HPIP alone may not be a good strategy to increase taxol resistance. Thus it's also important to identify other proteins interacting with HPIP that can also cause taxol resistance.

3.6 CONCLUSIONS

The conclusions drawn from this study can be summarised as given below.

- HPIP is overexpressed in breast cancer cell line, MCF7 which shows higher resistance to taxol when compared to non-transformed epithelial mammary cells, MCF10A.
- Alterations in HPIP can affect the cell's sensitivity to taxol. Silencing of HPIP in MCF7 cells makes it more sensitive to taxol while overexpression increases resistance.
- Taxol induced cell apoptosis is facilitated by silencing of HPIP in MCF7 cells.
- Increased cellular apoptosis in HPIP silenced MCF7 cells is a result of increased G2/M cell cycle arrest.
- Alteration in HPIP expression is associated with concomitant alterations in β-tubulin III expression. Overexpression leads to increased expression of β-tubulin III and vice versa.
- HPIP interferes with taxol binding to microtubules, therefore resulted in decreased accumulation of the drug in MCF7 cells.
- HPIP interferes with the stabilizing effect of taxol on microtubule polymerisation.
- The 190-218 amino acid region of HPIP, previously known to be the microtubule binding region, is found not to be the microtubule interaction region.
- The C-terminal region of HPIP is responsible for interacting with microtubules and causing taxol resistance

3.7 IMPORTANCE OF STUDY AND FUTURE PERSPECTIVE

Ever since taxol has been approved by FDA, USA, it has been used extensively for metastatic breast cancer, ovarian cancer, colon cancer and non-small cell lung cancer. Infact, taxane-based chemotherapy forms the first line therapy for metastatic breast cancer, especially, triple negative breast cancer (Mustacchi and Laurentiis, 2015). However, heterogeneity of the disease leads to resistance towards taxane therapy that results in recurrence of breast cancer, and in most cases it tends to be metastatic in nature. Over the last two decades, several new oncoproteins have been identified that were later found to cause taxol resistance as well. HPIP is one such protein. It was first identified as a PBX-interacting protein that inhibits PBX1-HOX complexes from binding to DNA (Abramovich *et al.,* 2000). Later, several others identified HPIP as an oncoprotein in breast cancer (Bugide *et al.,* 2014; Manavathi *et al.,* 2006; Wang *et al.,* 2008), hepatoma (Xu *et al*., 2013), colorectal cancer (Feng *et al.,* 2015), oral carcinoma (Okada *et al.,* 2015), pleomorphic sarcomas and leiomyosarcomas (Silveira *et al.,* 2013). Although its role in cancer has been established, its response to cancer therapy has not been studied. In this study, we have established that HPIP plays a crucial role in imparting taxol resistance to breast cancer cell, making it clinically important. We further identified the region of HPIP, i.e., the C-terminal region that imparts resistance towards taxol. However, further studies needs to be done to identify the amino acid residues in the C-terminal region that interacts with microtubules and impairs taxol from binding to microtubules. Xenograft studies with HPIP in mouse can further warrant our data and prove the importance of HPIP in taxol resistance *in vivo.* This can help us to design a peptide against HPIP that prevents HPIP from blocking taxol. This can be used clinically as a supplement in taxane-based chemotherapy. Although, we have elucidated that HPIP triggers the cellular apoptotic pathways, the exact mechanism by which it does still remains to be elucidated. This can also throw light in developing new taxane- based chemotherapy.

Bibliography

Abramovich, C., E.A. Chavez, P.M. Lansdorp, and R.K. Humphries. 2002. Functional characterization of multiple domains involved in the subcellular localization of the hematopoietic Pbx interacting protein (HPIP). *Oncogene*. 21:6766-6771.

Abramovich, C., W.F. Shen, N. Pineault, S. Imren, B. Montpetit, C. Largman, and R.K. Humphries. 2000. Functional cloning and characterization of a novel nonhomeodomain protein that inhibits the binding of PBX1-HOX complexes to DNA. *The Journal of biological chemistry*. 275:26172-26177.

Acquaviva, C., and J. Pines. 2006. The anaphase-promoting complex/cyclosome: APC/C. *Journal of cell science*. 119:2401-2404.

Ahn, J., M. Murphy, S. Kratowicz, A. Wang, A.J. Levine, and D.L. George. 1999. Down-regulation of the stathmin/Op18 and FKBP25 genes following p53 induction. *Oncogene*. 18:5954-5958.

Akhmanova, A., and M.O. Steinmetz. 2008. Tracking the ends: a dynamic protein network controls the fate of microtubule tips. *Nature reviews. Molecular cell biology*. 9:309-322.

Aldaz, H., L.M. Rice, T. Stearns, and D.A. Agard. 2005. Insights into microtubule nucleation from the crystal structure of human gamma-tubulin. *Nature*. 435:523-527.

Alli, E., J. Bash-Babula, J.M. Yang, and W.N. Hait. 2002. Effect of stathmin on the sensitivity to antimicrotubule drugs in human breast cancer. *Cancer research*. 62:6864-6869.

Alushin, G.M., G.C. Lander, E.H. Kellogg, R. Zhang, D. Baker, and E. Nogales. 2014. High-resolution microtubule structures reveal the structural transitions in alphabeta-tubulin upon GTP hydrolysis. *Cell*. 157:1117-1129.

Amos, L.A. 2004. Microtubule structure and its stabilisation. *Organic & biomolecular chemistry*. 2:2153-2160.

Amos, L.A., and J. Lowe. 1999. How Taxol stabilises microtubule structure. *Chemistry & biology*. 6:R65-69.

Amos, L.A., and D. Schlieper. 2005. Microtubules and maps. *Advances in protein chemistry*. 71:257-298.

Andre, F., C. Hatzis, K. Anderson, C. Sotiriou, C. Mazouni, J. Mejia, B. Wang, G.N. Hortobagyi, W.F. Symmans, and L. Pusztai. 2007. Microtubule-associated protein-tau is a bifunctional predictor of endocrine sensitivity and chemotherapy resistance in estrogen receptor-positive breast cancer. *Clinical cancer research : an official journal of the American Association for Cancer Research*. 13:2061-2067.

Andreu, J.M. 2007. Large scale purification of brain tubulin with the modified Weisenberg procedure. *Methods in molecular medicine*. 137:17-28.

Asthana, J., A. Kuchibhatla, S.C. Jana, K. Ray, and D. Panda. 2012. Dynein light chain 1 (LC8) association enhances microtubule stability and promotes microtubule bundling. *The Journal of biological chemistry*. 287:40793-40805.

Bagnoli, M., G.L. Beretta, L. Gatti, S. Pilotti, P. Alberti, E. Tarantino, M. Barbareschi, S. Canevari, D. Mezzanzanica, and P. Perego. 2013. Clinicopathological impact of ABCC1/MRP1 and ABCC4/MRP4 in epithelial ovarian carcinoma. *BioMed research international*. 2013:143202.

Balasubramani, M., C. Nakao, G.T. Uechi, J. Cardamone, K. Kamath, K.L. Leslie, R. Balachandran, L. Wilson, B.W. Day, and M.A. Jordan. 2011. Characterization and detection of cellular and proteomic alterations in stable stathmin-overexpressing, taxol-resistant BT549 breast cancer cells using offgel IEF/PAGE difference gel electrophoresis. *Mutation research*. 722:154-164.

Berrieman, H.K., M.J. Lind, and L. Cawkwell. 2004. Do beta-tubulin mutations have a role in resistance to chemotherapy? *The Lancet. Oncology*. 5:158-164.

Bhalla, K.N. 2003. Microtubule-targeted anticancer agents and apoptosis. *Oncogene*. 22:9075-9086.

Boggs, A.E., M.I. Vitolo, R.A. Whipple, M.S. Charpentier, O.G. Goloubeva, O.B. Ioffe, K.C. Tuttle, J. Slovic, Y. Lu, G.B. Mills, and S.S. Martin. 2015. alpha-Tubulin acetylation elevated in metastatic and basal-like breast cancer cells promotes microtentacle formation, adhesion, and invasive migration. *Cancer research*. 75:203-215.

Borisy, G.G., and E.W. Taylor. 1967. The mechanism of action of colchicine. Colchicine binding to sea urchin eggs and the mitotic apparatus. *The Journal of cell biology*. 34:535-548.

Borst, P., R. Evers, M. Kool, and J. Wijnholds. 2000. A family of drug transporters: the multidrug resistance-associated proteins. *Journal of the National Cancer Institute*. 92:1295-1302.

Brito, D.A., and C.L. Rieder. 2006. Mitotic checkpoint slippage in humans occurs via cyclin B destruction in the presence of an active checkpoint. *Current biology : CB*. 16:1194-1200.

Brito, D.A., and C.L. Rieder. 2009. The ability to survive mitosis in the presence of microtubule poisons differs significantly between human nontransformed (RPE-1) and cancer (U2OS, HeLa) cells. *Cell motility and the cytoskeleton*. 66:437-447.

Bugide, S., D. David, A. Nair, N. Kannan, V.S. Samanthapudi, J. Prabhakar, and B. Manavathi. 2014. Hematopoietic PBX-interacting protein (HPIP) is over expressed in breast infiltrative ductal carcinoma and regulates cell adhesion and migration through modulation of focal adhesion dynamics. *Oncogene*.

Carlier, M.F., T.L. Hill, and Y. Chen. 1984. Interference of GTP hydrolysis in the mechanism of microtubule assembly: an experimental study. *Proceedings of the National Academy of Sciences of the United States of America*. 81:771-775.

Cassimeris, L. 1993. Regulation of microtubule dynamic instability. *Cell motility and the cytoskeleton*. 26:275-281.

Cassimeris, L. 2002. The oncoprotein 18/stathmin family of microtubule destabilizers. *Current opinion in cell biology*. 14:18-24.

Channels, W.E., F.J. Nedelec, Y. Zheng, and P.A. Iglesias. 2008. Spatial regulation improves antiparallel microtubule overlap during mitotic spindle assembly. *Biophysical journal*. 94:2598-2609.

Choi, Y.H., and Y.H. Yoo. 2012. Taxol-induced growth arrest and apoptosis is associated with the upregulation of the Cdk inhibitor, p21WAF1/CIP1, in human breast cancer cells. *Oncology reports*. 28:2163-2169.

Cicchillitti, L., R. Penci, M. Di Michele, F. Filippetti, D. Rotilio, M.B. Donati, G. Scambia, and C. Ferlini. 2008. Proteomic characterization of cytoskeletal and mitochondrial class III beta-tubulin. *Molecular cancer therapeutics*. 7:2070-2079.

Clarke, P.R., and C. Zhang. 2008. Spatial and temporal coordination of mitosis by Ran GTPase. *Nature reviews. Molecular cell biology*. 9:464-477.

Cole, S.P., G. Bhardwaj, J.H. Gerlach, J.E. Mackie, C.E. Grant, K.C. Almquist, A.J. Stewart, E.U. Kurz, A.M. Duncan, and R.G. Deeley. 1992. Overexpression of a transporter gene in a multidrug-resistant human lung cancer cell line. *Science*. 258:1650-1654.

Credle, J.J., J.L. George, J. Wills, V. Duka, K. Shah, Y.C. Lee, O. Rodriguez, T. Simkins, M. Winter, D. Moechars, T. Steckler, J. Goudreau, D.I. Finkelstein, and A. Sidhu. 2015. GSK-3beta dysregulation contributes to parkinson's-like pathophysiology with associated region-specific phosphorylation and accumulation of tau and alpha-synuclein. *Cell death and differentiation*. 22:838-851.

D'Assoro, A.B., W.L. Lingle, and J.L. Salisbury. 2002. Centrosome amplification and the development of cancer. *Oncogene*. 21:6146-6153.

David-Pfeuty, T., H.P. Erickson, and D. Pantaloni. 1977. Guanosinetriphosphatase activity of tubulin associated with microtubule assembly. *Proceedings of the National Academy of Sciences of the United States of America*. 74:5372-5376.

De Brabander, M., G. Geuens, R. Nuydens, R. Willebrords, and J. De Mey. 1981. Taxol induces the assembly of free microtubules in living cells and blocks the organizing capacity of the centrosomes and kinetochores. *Proceedings of the National Academy of Sciences of the United States of America*. 78:5608-5612.

Dehmelt, L., and S. Halpain. 2005. The MAP2/Tau family of microtubule-associated proteins. *Genome biology*. 6:204.

Denning, D.P., and T. Hirose. 2014. Anti-tubulins DEPendably induce apoptosis. *Nature cell biology*. 16:741-743.

Dennis, K., M. Uittenbogaard, A. Chiaramello, and S.A. Moody. 2002. Cloning and characterization of the 5'-flanking region of the rat neuron-specific Class III beta-tubulin gene. *Gene*. 294:269-277.

Dephoure, N., C. Zhou, J. Villen, S.A. Beausoleil, C.E. Bakalarski, S.J. Elledge, and S.P. Gygi. 2008. A quantitative atlas of mitotic phosphorylation. *Proceedings of the National Academy of Sciences of the United States of America*. 105:10762-10767.

Derry, W.B., L. Wilson, and M.A. Jordan. 1995. Substoichiometric binding of taxol suppresses microtubule dynamics. *Biochemistry*. 34:2203-2211.

Diaz, J.F., J.M. Valpuesta, P. Chacon, G. Diakun, and J.M. Andreu. 1998. Changes in microtubule protofilament number induced by Taxol binding to an easily accessible site. Internal microtubule dynamics. *The Journal of biological chemistry*. 273:33803-33810.

Dixit, R., B. Barnett, J.E. Lazarus, M. Tokito, Y.E. Goldman, and E.L. Holzbaur. 2009. Microtubule plus-end tracking by CLIP-170 requires EB1. *Proceedings of the National Academy of Sciences of the United States of America*. 106:492-497.

Dogterom, M., and B. Yurke. 1997. Measurement of the force-velocity relation for growing microtubules. *Science*. 278:856-860.

Downing, K.H. 2000. Structural basis for the interaction of tubulin with proteins and drugs that affect microtubule dynamics. *Annual review of cell and developmental biology*. 16:89-111.

Downing, K.H., and E. Nogales. 1998. Tubulin and microtubule structure. *Current opinion in cell biology*. 10:16-22.

Dozier, J.H., L. Hiser, J.A. Davis, N.S. Thomas, M.A. Tucci, H.A. Benghuzzi, A. Frankfurter, J.J. Correia, and S. Lobert. 2003. Beta class II tubulin predominates in normal and tumor breast tissues. *Breast cancer research : BCR*. 5:R157-169.

Dutcher, S.K. 2003. Long-lost relatives reappear: identification of new members of the tubulin superfamily. *Current opinion in microbiology*. 6:634-640.

Dye, R.B., S.P. Fink, and R.C. Williams, Jr. 1993. Taxol-induced flexibility of microtubules and its reversal by MAP-2 and Tau. *The Journal of biological chemistry*. 268:6847-6850.

Ertych, N., A. Stolz, A. Stenzinger, W. Weichert, S. Kaulfuss, P. Burfeind, A. Aigner, L. Wordeman, and H. Bastians. 2014. Increased microtubule assembly rates influence chromosomal instability in colorectal cancer cells. *Nature cell biology*. 16:779-791.

Feng, Y., L. Li, X. Zhang, Y. Zhang, Y. Liang, J. Lv, Z. Fan, J. Guo, T. Hong, B. Ji, Q. Ji, G. Mei, L. Ding, S. Zhang, X. Xu, and Q. Ye. 2015a. HPIP is overexpressed in gastric cancer and promotes gastric cancer cell proliferation, migration and invasion. *Cancer science*.

Feng, Y., X. Xu, Y. Zhang, J. Ding, Y. Wang, X. Zhang, Z. Wu, L. Kang, Y. Liang, L. Zhou, S. Song, K. Zhao, and Q. Ye. 2015b. HPIP is upregulated in colorectal cancer and

regulates colorectal cancer cell proliferation, apoptosis and invasion. *Scientific reports*. 5:9429.

Ferlay, J., I. Soerjomataram, R. Dikshit, S. Eser, C. Mathers, M. Rebelo, D.M. Parkin, D. Forman, and F. Bray. 2015. Cancer incidence and mortality worldwide: sources, methods and major patterns in GLOBOCAN 2012. *International journal of cancer. Journal international du cancer*. 136:E359-386.

Fojo, T. 2007. Multiple paths to a drug resistance phenotype: mutations, translocations, deletions and amplification of coding genes or promoter regions, epigenetic changes and microRNAs. *Drug resistance updates : reviews and commentaries in antimicrobial and anticancer chemotherapy*. 10:59-67.

Freedman, H., J.T. Huzil, T. Luchko, R.F. Luduena, and J.A. Tuszynski. 2009. Identification and characterization of an intermediate taxol binding site within microtubule nanopores and a mechanism for tubulin isotype binding selectivity. *Journal of chemical information and modeling*. 49:424-436.

Ganguly, A., H. Yang, M. Pedroza, R. Bhattacharya, and F. Cabral. 2011. Mitotic centromere-associated kinesin (MCAK) mediates paclitaxel resistance. *The Journal of biological chemistry*. 286:36378-36384.

Gascoigne, K.E., and S.S. Taylor. 2009. How do anti-mitotic drugs kill cancer cells? *Journal of cell science*. 122:2579-2585.

Gonzalez-Angulo, A.M., F. Morales-Vasquez, and G.N. Hortobagyi. 2007. Overview of resistance to systemic therapy in patients with breast cancer. *Advances in experimental medicine and biology*. 608:1-22.

Gorbsky, G.J., P.J. Sammak, and G.G. Borisy. 1988. Microtubule dynamics and chromosome motion visualized in living anaphase cells. *The Journal of cell biology*. 106:1185-1192.

Hammond, J.W., D. Cai, and K.J. Verhey. 2008. Tubulin modifications and their cellular functions. *Current opinion in cell biology*. 20:71-76.

Hari, M., F. Loganzo, T. Annable, X. Tan, S. Musto, D.B. Morilla, J.H. Nettles, J.P. Snyder, and L.M. Greenberger. 2006. Paclitaxel-resistant cells have a mutation in the paclitaxel-binding region of beta-tubulin (Asp26Glu) and less stable microtubules. *Molecular cancer therapeutics*. 5:270-278.

Hasegawa, S., Y. Miyoshi, C. Egawa, M. Ishitobi, Y. Tamaki, M. Monden, and S. Noguchi. 2002. Mutational analysis of the class I beta-tubulin gene in human breast cancer. *International journal of cancer. Journal international du cancer*. 101:46-51.

Hayashi, I., and M. Ikura. 2003. Crystal structure of the amino-terminal microtubule-binding domain of end-binding protein 1 (EB1). *The Journal of biological chemistry*. 278:36430-36434.

Hoenger, A., E.P. Sablin, R.D. Vale, R.J. Fletterick, and R.A. Milligan. 1995. Three-dimensional structure of a tubulin-motor-protein complex. *Nature*. 376:271-274.

Honore, S., E. Pasquier, and D. Braguer. 2005. Understanding microtubule dynamics for improved cancer therapy. *Cellular and molecular life sciences : CMLS*. 62:3039-3056.

Inoue, S., and E.D. Salmon. 1995. Force generation by microtubule assembly/disassembly in mitosis and related movements. *Molecular biology of the cell*. 6:1619-1640.

Janke, C. 2014. The tubulin code: molecular components, readout mechanisms, and functions. *The Journal of cell biology*. 206:461-472.

Jordan, M.A., and L. Wilson. 2004. Microtubules as a target for anticancer drugs. *Nature reviews. Cancer*. 4:253-265.

Kalinina, E., R. Biswas, I. Berezniuk, A. Hermoso, F.X. Aviles, and L.D. Fricker. 2007. A novel subfamily of mouse cytosolic carboxypeptidases. *FASEB journal : official publication of the Federation of American Societies for Experimental Biology*. 21:836-850.

Kalinina, I., A. Nandi, P. Delivani, M.R. Chacon, A.H. Klemm, D. Ramunno-Johnson, A. Krull, B. Lindner, N. Pavin, and I.M. Tolic-Norrelykke. 2013. Pivoting of microtubules around the spindle pole accelerates kinetochore capture. *Nature cell biology*. 15:82-87.

Kamath, K., L. Wilson, F. Cabral, and M.A. Jordan. 2005. BetaIII-tubulin induces paclitaxel resistance in association with reduced effects on microtubule dynamic instability. *The Journal of biological chemistry*. 280:12902-12907.

Kar, S., J. Fan, M.J. Smith, M. Goedert, and L.A. Amos. 2003a. Repeat motifs of tau bind to the insides of microtubules in the absence of taxol. *The EMBO journal*. 22:70-77.

Kar, S., G.J. Florence, I. Paterson, and L.A. Amos. 2003b. Discodermolide interferes with the binding of tau protein to microtubules. *FEBS letters*. 539:34-36.

Karamese, M., S. Aksak, O.B. Gundogdu, and B. Unal. 2013. A new hypothesis about hematopoietic Pbx-interaction protein (HPIP): can it be a key factor in neurodegeneration in the post-menopausal period? *Medical hypotheses*. 81:470-476.

Kaur, R., G. Kaur, R.K. Gill, R. Soni, and J. Bariwal. 2014. Recent developments in tubulin polymerization inhibitors: An overview. *European journal of medicinal chemistry*. 87:89-124.

Kavallaris, M. 2010. Microtubules and resistance to tubulin-binding agents. *Nature reviews. Cancer*. 10:194-204.

Khongkow, P., A.R. Gomes, C. Gong, E.P. Man, J.W. Tsang, F. Zhao, L.J. Monteiro, R.C. Coombes, R.H. Medema, U.S. Khoo, and E.W. Lam. 2015. Paclitaxel targets FOXM1 to regulate KIF20A in mitotic catastrophe and breast cancer paclitaxel resistance. *Oncogene*.

Kim, M.H., T. Cierpicki, U. Derewenda, D. Krowarsch, Y. Feng, Y. Devedjiev, Z. Dauter, C.A. Walsh, J. Otlewski, J.H. Bushweller, and Z.S. Derewenda. 2003. The DCX-domain tandems of doublecortin and doublecortin-like kinase. *Nature structural biology*. 10:324-333.

Kiselyov, A., K.V. Balakin, S.E. Tkachenko, N. Savchuk, and A.V. Ivachtchenko. 2007. Recent progress in discovery and development of antimitotic agents. *Anti-cancer agents in medicinal chemistry*. 7:189-208.

Kisurina-Evgenieva, O., G. Mack, Q. Du, I. Macara, A. Khodjakov, and D.A. Compton. 2004. Multiple mechanisms regulate NuMA dynamics at spindle poles. *Journal of cell science*. 117:6391-6400.

Kline-Smith, S.L., and C.E. Walczak. 2004. Mitotic spindle assembly and chromosome segregation: refocusing on microtubule dynamics. *Molecular cell*. 15:317-327.

Koffa, M.D., C.M. Casanova, R. Santarella, T. Kocher, M. Wilm, and I.W. Mattaj. 2006. HURP is part of a Ran-dependent complex involved in spindle formation. *Current biology : CB*. 16:743-754.

Kumar, S., H. Mahdi, C. Bryant, J.P. Shah, G. Garg, and A. Munkarah. 2010. Clinical trials and progress with paclitaxel in ovarian cancer. *International journal of women's health*. 2:411-427.

Kyte, J., and R.F. Doolittle. 1982. A simple method for displaying the hydropathic character of a protein. *Journal of molecular biology*. 157:105-132.

Lai, D., K.C. Ho, Y. Hao, and X. Yang. 2011. Taxol resistance in breast cancer cells is mediated by the hippo pathway component TAZ and its downstream transcriptional targets Cyr61 and CTGF. *Cancer research*. 71:2728-2738.

Lee, J.J., and W.K. Kelly. 2009. Epothilones: tubulin polymerization as a novel target for prostate cancer therapy. *Nature clinical practice. Oncology*. 6:85-92.

Lesser, G.J., S.A. Grossman, S. Eller, and E.K. Rowinsky. 1995. The distribution of systemically administered [3H]-paclitaxel in rats: a quantitative autoradiographic study. *Cancer chemotherapy and pharmacology*. 37:173-178.

Li, R., T. Moudgil, H.J. Ross, and H.M. Hu. 2005. Apoptosis of non-small-cell lung cancer cell lines after paclitaxel treatment involves the BH3-only proapoptotic protein Bim. *Cell death and differentiation*. 12:292-303.

Li, S., J. Finley, Z.J. Liu, S.H. Qiu, H. Chen, C.H. Luan, M. Carson, J. Tsao, D. Johnson, G. Lin, J. Zhao, W. Thomas, L.A. Nagy, B. Sha, L.J. DeLucas, B.C. Wang, and M. Luo. 2002. Crystal structure of the cytoskeleton-associated protein glycine-rich (CAP-Gly) domain. *The Journal of biological chemistry*. 277:48596-48601.

Liu, Y., L. Chen, T.C. Ko, A.P. Fields, and E.A. Thompson. 2006. Evi1 is a survival factor which conveys resistance to both TGFbeta- and taxol-mediated cell death via PI3K/AKT. *Oncogene*. 25:3565-3575.

Lowe, J., H. Li, K.H. Downing, and E. Nogales. 2001. Refined structure of alpha beta-tubulin at 3.5 A resolution. *Journal of molecular biology*. 313:1045-1057.

Luduena, R.F. 1998. Multiple forms of tubulin: different gene products and covalent modifications. *International review of cytology*. 178:207-275.

Luo, Y., D. Li, J. Ran, B. Yan, J. Chen, X. Dong, Z. Liu, R. Liu, J. Zhou, and M. Liu. 2014. End-binding protein 1 stimulates paclitaxel sensitivity in breast cancer by promoting its actions toward microtubule assembly and stability. *Protein & cell*. 5:469-479.

MacNeal, P.S. 1978. Final report of the committee to study the future of the private practice of medicine. *Texas medicine*. 74:77-78.

Maeno, K., K. Ito, Y. Hama, K. Shingu, M. Kimura, M. Sano, H. Nakagomi, S. Tsuchiya, and M. Fujimori. 2003. Mutation of the class I beta-tubulin gene does not predict response to paclitaxel for breast cancer. *Cancer letters*. 198:89-97.

Manavathi, B., F. Acconcia, S.K. Rayala, and R. Kumar. 2006. An inherent role of microtubule network in the action of nuclear receptor. *Proceedings of the National Academy of Sciences of the United States of America*. 103:15981-15986.

Manavathi, B., D. Lo, S. Bugide, O. Dey, S. Imren, M.J. Weiss, and R.K. Humphries. 2012. Functional regulation of pre-B-cell leukemia homeobox interacting protein 1 (PBXIP1/HPIP) in erythroid differentiation. *The Journal of biological chemistry*. 287:5600-5614.

Margolis, R.L., C.T. Rauch, F. Pirollet, and D. Job. 1990. Specific association of STOP protein with microtubules in vitro and with stable microtubules in mitotic spindles of cultured cells. *The EMBO journal*. 9:4095-4102.

Margolis, R.L., and L. Wilson. 1978. Opposite end assembly and disassembly of microtubules at steady state in vitro. *Cell*. 13:1-8.

McCubrey, J.A., L.S. Steelman, S.L. Abrams, J.T. Lee, F. Chang, F.E. Bertrand, P.M. Navolanic, D.M. Terrian, R.A. Franklin, A.B. D'Assoro, J.L. Salisbury, M.C. Mazzarino, F. Stivala, and M. Libra. 2006. Roles of the RAF/MEK/ERK and PI3K/PTEN/AKT pathways in malignant transformation and drug resistance. *Advances in enzyme regulation*. 46:249-279.

McGrail, D.J., N.N. Khambhati, M.X. Qi, K.S. Patel, N. Ravikumar, C.P. Brandenburg, and M.R. Dawson. 2015. Alterations in Ovarian Cancer Cell Adhesion Drive Taxol Resistance by Increasing Microtubule Dynamics in a FAK-dependent Manner. *Scientific reports*. 5:9529.

McGrogan, B.T., B. Gilmartin, D.N. Carney, and A. McCann. 2008. Taxanes, microtubules and chemoresistant breast cancer. *Biochimica et biophysica acta*. 1785:96-132.

McNally, F. 2000. Capturing a ring of samurai. *Nature cell biology*. 2:E4-7.

Mialhe, A., L. Lafanechere, I. Treilleux, N. Peloux, C. Dumontet, A. Bremond, M.H. Panh, R. Payan, J. Wehland, R.L. Margolis, and D. Job. 2001. Tubulin detyrosination is a frequent occurrence in breast cancers of poor prognosis. *Cancer research*. 61:5024-5027.

Miceli, C., A. Tejada, A. Castaneda, and S.J. Mistry. 2013. Cell cycle inhibition therapy that targets stathmin in in vitro and in vivo models of breast cancer. *Cancer gene therapy*. 20:298-307.
Michaud, L.B., V. Valero, and G. Hortobagyi. 2000. Risks and benefits of taxanes in breast and ovarian cancer. *Drug safety*. 23:401-428.
Miller, A.V., M.A. Hicks, W. Nakajima, A.C. Richardson, J.J. Windle, and H. Harada. 2013. Paclitaxel-induced apoptosis is BAK-dependent, but BAX and BIM-independent in breast tumor. *PloS one*. 8:e60685.
Miller, M.L., and I. Ojima. 2001. Chemistry and chemical biology of taxane anticancer agents. *Chemical record*. 1:195-211.
Mitchison, T., and M. Kirschner. 1984a. Dynamic instability of microtubule growth. *Nature*. 312:237-242.
Mitchison, T., and M. Kirschner. 1984b. Microtubule assembly nucleated by isolated centrosomes. *Nature*. 312:232-237.
Mitchison, T.J. 1993. Localization of an exchangeable GTP binding site at the plus end of microtubules. *Science*. 261:1044-1047.
Monsarrat, B., E. Mariel, S. Cros, M. Gares, D. Guenard, F. Gueritte-Voegelein, and M. Wright. 1990. Taxol metabolism. Isolation and identification of three major metabolites of taxol in rat bile. *Drug metabolism and disposition: the biological fate of chemicals*. 18:895-901.
Moritz, M., M.B. Braunfeld, J.W. Sedat, B. Alberts, and D.A. Agard. 1995. Microtubule nucleation by gamma-tubulin-containing rings in the centrosome. *Nature*. 378:638-640.
Musacchio, A., and E.D. Salmon. 2007. The spindle-assembly checkpoint in space and time. *Nature reviews. Molecular cell biology*. 8:379-393.
Mustacchi, G., and M. De Laurentiis. 2015. The role of taxanes in triple-negative breast cancer: literature review. *Drug design, development and therapy*. 9:4303-4318.
Nettles, J.H., H. Li, B. Cornett, J.M. Krahn, J.P. Snyder, and K.H. Downing. 2004. The binding mode of epothilone A on alpha,beta-tubulin by electron crystallography. *Science*. 305:866-869.
Nogales, E. 1999. A structural view of microtubule dynamics. *Cellular and molecular life sciences : CMLS*. 56:133-142.
Nogales, E. 2000. Structural insights into microtubule function. *Annual review of biochemistry*. 69:277-302.
Notte, A., N. Ninane, T. Arnould, and C. Michiels. 2013. Hypoxia counteracts taxol-induced apoptosis in MDA-MB-231 breast cancer cells: role of autophagy and JNK activation. *Cell death & disease*. 4:e638.
Notte, A., M. Rebucci, M. Fransolet, E. Roegiers, M. Genin, C. Tellier, K. Watillon, A. Fattaccioli, T. Arnould, and C. Michiels. 2015. Taxol-induced unfolded protein response activation in breast cancer cells exposed to hypoxia: ATF4 activation regulates autophagy and inhibits apoptosis. *The international journal of biochemistry & cell biology*. 62:1-14.
O'Brien, E.T., W.A. Voter, and H.P. Erickson. 1987. GTP hydrolysis during microtubule assembly. *Biochemistry*. 26:4148-4156.
Ohta, S., K. Nishio, N. Kubota, T. Ohmori, Y. Funayama, T. Ohira, H. Nakajima, M. Adachi, and N. Saijo. 1994. Characterization of a taxol-resistant human small-cell lung cancer cell line. *Japanese journal of cancer research : Gann*. 85:290-297.
Okada, S., T. Irie, J. Tanaka, R. Yasuhara, G. Yamamoto, T. Isobe, C. Hokazono, T. Tachikawa, Y. Kohno, and K. Mishima. 2015. Potential role of hematopoietic pre-B-cell leukemia transcription factor-interacting protein in oral carcinogenesis. *Journal of*

oral pathology & medicine : official publication of the International Association of Oral Pathologists and the American Academy of Oral Pathology. 44:115-125.

Orr, G.A., P. Verdier-Pinard, H. McDaid, and S.B. Horwitz. 2003. Mechanisms of Taxol resistance related to microtubules. *Oncogene*. 22:7280-7295.

Panda, D., H.P. Miller, A. Banerjee, R.F. Luduena, and L. Wilson. 1994. Microtubule dynamics in vitro are regulated by the tubulin isotype composition. *Proceedings of the National Academy of Sciences of the United States of America*. 91:11358-11362.

Panda, D., H.P. Miller, and L. Wilson. 2002. Determination of the size and chemical nature of the stabilizing "cap" at microtubule ends using modulators of polymerization dynamics. *Biochemistry*. 41:1609-1617.

Peters, J.M. 2006. The anaphase promoting complex/cyclosome: a machine designed to destroy. *Nature reviews. Molecular cell biology*. 7:644-656.

Pilhofer, M., M.S. Ladinsky, A.W. McDowall, G. Petroni, and G.J. Jensen. 2011. Microtubules in bacteria: Ancient tubulins build a five-protofilament homolog of the eukaryotic cytoskeleton. *PLoS biology*. 9:e1001213.

Polager, S., and D. Ginsberg. 2003. E2F mediates sustained G2 arrest and down-regulation of Stathmin and AIM-1 expression in response to genotoxic stress. *The Journal of biological chemistry*. 278:1443-1449.

Poruchynsky, M.S., P. Giannakakou, Y. Ward, J.C. Bulinski, W.G. Telford, R.W. Robey, and T. Fojo. 2001. Accompanying protein alterations in malignant cells with a microtubule-polymerizing drug-resistance phenotype and a primary resistance mechanism. *Biochemical pharmacology*. 62:1469-1480.

Ramachandra, M., S.V. Ambudkar, D. Chen, C.A. Hrycyna, S. Dey, M.M. Gottesman, and I. Pastan. 1998. Human P-glycoprotein exhibits reduced affinity for substrates during a catalytic transition state. *Biochemistry*. 37:5010-5019.

Raspaglio, G., F. Filippetti, S. Prislei, R. Penci, I. De Maria, L. Cicchillitti, S. Mozzetti, G. Scambia, and C. Ferlini. 2008. Hypoxia induces class III beta-tubulin gene expression by HIF-1alpha binding to its 3' flanking region. *Gene*. 409:100-108.

Rodionov, V.I., and G.G. Borisy. 1997. Microtubule treadmilling in vivo. *Science*. 275:215-218.

Rohena, C.C., and S.L. Mooberry. 2014. Recent progress with microtubule stabilizers: new compounds, binding modes and cellular activities. *Natural product reports*. 31:335-355.

Roque, D.M., N. Buza, M. Glasgow, S. Bellone, I. Bortolomai, S. Gasparrini, E. Cocco, E. Ratner, D.A. Silasi, M. Azodi, T.J. Rutherford, P.E. Schwartz, and A.D. Santin. 2014. Class III beta-tubulin overexpression within the tumor microenvironment is a prognostic biomarker for poor overall survival in ovarian cancer patients treated with neoadjuvant carboplatin/paclitaxel. *Clinical & experimental metastasis*. 31:101-110.

Rouzier, R., R. Rajan, P. Wagner, K.R. Hess, D.L. Gold, J. Stec, M. Ayers, J.S. Ross, P. Zhang, T.A. Buchholz, H. Kuerer, M. Green, B. Arun, G.N. Hortobagyi, W.F. Symmans, and L. Pusztai. 2005. Microtubule-associated protein tau: a marker of paclitaxel sensitivity in breast cancer. *Proceedings of the National Academy of Sciences of the United States of America*. 102:8315-8320.

Sabbatini, P., and D.R. Spriggs. 2009. Epothilones: better or more of the same? *Journal of clinical oncology : official journal of the American Society of Clinical Oncology*. 27:3079-3081.

Safa, A.R. 2004. Identification and characterization of the binding sites of P-glycoprotein for multidrug resistance-related drugs and modulators. *Current medicinal chemistry. Anti-cancer agents*. 4:1-17.

Schiff, P.B., J. Fant, and S.B. Horwitz. 1979. Promotion of microtubule assembly in vitro by taxol. *Nature*. 277:665-667.

Scholz, T., and E. Mandelkow. 2014. Transport and diffusion of Tau protein in neurons. *Cellular and molecular life sciences : CMLS*. 71:3139-3150.

Seve, P., and C. Dumontet. 2008. Is class III beta-tubulin a predictive factor in patients receiving tubulin-binding agents? *The Lancet. Oncology*. 9:168-175.

Shalli, K., I. Brown, S.D. Heys, and A.C. Schofield. 2005. Alterations of beta-tubulin isotypes in breast cancer cells resistant to docetaxel. *FASEB journal : official publication of the Federation of American Societies for Experimental Biology*. 19:1299-1301.

Sharp, D.J., G.C. Rogers, and J.M. Scholey. 2000. Microtubule motors in mitosis. *Nature*. 407:41-47.

Shelanski, M.L. 1973. Chemistry of the filaments and tubules of brain. *The journal of histochemistry and cytochemistry : official journal of the Histochemistry Society*. 21:529-539.

Shiraki, N., S. Ogaki, and S. Kume. 2014. Profiling of embryonic stem cell differentiation. *The review of diabetic studies : RDS*. 11:102-114.

Shostak, K., F. Patrascu, S.I. Goktuna, P. Close, L. Borgs, L. Nguyen, F. Olivier, A. Rammal, H. Brinkhaus, M. Bentires-Alj, J.C. Marine, and A. Chariot. 2014. MDM2 restrains estrogen-mediated AKT activation by promoting TBK1-dependent HPIP degradation. *Cell death and differentiation*. 21:811-824.

Silveira, S.M., R.A. Villacis, F.A. Marchi, C. Barros Filho Mde, S.A. Drigo, C.S. Neto, A. Lopes, I.W. da Cunha, and S.R. Rogatto. 2013. Genomic signatures predict poor outcome in undifferentiated pleomorphic sarcomas and leiomyosarcomas. *PloS one*. 8:e67643.

Sirajuddin, M., L.M. Rice, and R.D. Vale. 2014. Regulation of microtubule motors by tubulin isotypes and post-translational modifications. *Nature cell biology*. 16:335-344.

Snyder, J.P., J.H. Nettles, B. Cornett, K.H. Downing, and E. Nogales. 2001. The binding conformation of Taxol in beta-tubulin: a model based on electron crystallographic density. *Proceedings of the National Academy of Sciences of the United States of America*. 98:5312-5316.

Soucek, K., A. Kamaid, A.D. Phung, L. Kubala, J.C. Bulinski, R.W. Harper, and J.P. Eiserich. 2006. Normal and prostate cancer cells display distinct molecular profiles of alpha-tubulin posttranslational modifications. *The Prostate*. 66:954-965.

Sparano, J.A. 2000. Taxanes for breast cancer: an evidence-based review of randomized phase II and phase III trials. *Clinical breast cancer*. 1:32-40; discussion 41-32.

Stearns, T., L. Evans, and M. Kirschner. 1991. Gamma-tubulin is a highly conserved component of the centrosome. *Cell*. 65:825-836.

Sudo, T., M. Nitta, H. Saya, and N.T. Ueno. 2004. Dependence of paclitaxel sensitivity on a functional spindle assembly checkpoint. *Cancer research*. 64:2502-2508.

Sui, H., and K.H. Downing. 2010. Structural basis of interprotofilament interaction and lateral deformation of microtubules. *Structure*. 18:1022-1031.

Sun, X., D. Li, Y. Yang, Y. Ren, J. Li, Z. Wang, B. Dong, M. Liu, and J. Zhou. 2012. Microtubule-binding protein CLIP-170 is a mediator of paclitaxel sensitivity. *The Journal of pathology*. 226:666-673.

Szakacs, G., J.K. Paterson, J.A. Ludwig, C. Booth-Genthe, and M.M. Gottesman. 2006. Targeting multidrug resistance in cancer. *Nature reviews. Drug discovery*. 5:219-234.

Szanto, A., E.E. Hellebrand, Z. Bognar, Z. Tucsek, A. Szabo, F. Gallyas, Jr., B. Sumegi, and G. Varbiro. 2009. PARP-1 inhibition-induced activation of PI-3-kinase-Akt pathway promotes resistance to taxol. *Biochemical pharmacology*. 77:1348-1357.

Tabuchi, Y., J. Matsuoka, M. Gunduz, T. Imada, R. Ono, M. Ito, T. Motoki, T. Yamatsuji, Y. Shirakawa, M. Takaoka, M. Haisa, N. Tanaka, J. Kurebayashi, V.C. Jordan, and Y. Naomoto. 2009. Resistance to paclitaxel therapy is related with Bcl-2 expression through an estrogen receptor mediated pathway in breast cancer. *International journal of oncology*. 34:313-319.

Tassin, A.M., and M. Bornens. 1999. Centrosome structure and microtubule nucleation in animal cells. *Biology of the cell / under the auspices of the European Cell Biology Organization*. 91:343-354.

Tilney, L.G., J. Bryan, D.J. Bush, K. Fujiwara, M.S. Mooseker, D.B. Murphy, and D.H. Snyder. 1973. Microtubules: evidence for 13 protofilaments. *The Journal of cell biology*. 59:267-275.

Uhlen, M., P. Oksvold, L. Fagerberg, E. Lundberg, K. Jonasson, M. Forsberg, M. Zwahlen, C. Kampf, K. Wester, S. Hober, H. Wernerus, L. Bjorling, and F. Ponten. 2010. Towards a knowledge-based Human Protein Atlas. *Nature biotechnology*. 28:1248-1250.

van Vuurden, D.G., E. Aronica, E. Hulleman, L.E. Wedekind, D. Biesmans, A. Malekzadeh, M. Bugiani, D. Geerts, D.P. Noske, W.P. Vandertop, G.J. Kaspers, J. Cloos, T. Wurdinger, and P.P. van der Stoop. 2014. Pre-B-cell leukemia homeobox interacting protein 1 is overexpressed in astrocytoma and promotes tumor cell growth and migration. *Neuro-oncology*. 16:946-959.

Verhey, K.J., and J. Gaertig. 2007. The tubulin code. *Cell cycle*. 6:2152-2160.

Vitre, B., F.M. Coquelle, C. Heichette, C. Garnier, D. Chretien, and I. Arnal. 2008. EB1 regulates microtubule dynamics and tubulin sheet closure in vitro. *Nature cell biology*. 10:415-421.

Voter, W.A., and H.P. Erickson. 1984. The kinetics of microtubule assembly. Evidence for a two-stage nucleation mechanism. *The Journal of biological chemistry*. 259:10430-10438.

Wade, R.H., and A.A. Hyman. 1997. Microtubule structure and dynamics. *Current opinion in cell biology*. 9:12-17.

Walczak, C.E. 2000. Microtubule dynamics and tubulin interacting proteins. *Current opinion in cell biology*. 12:52-56.

Walle, T., U.K. Walle, G.N. Kumar, and K.N. Bhalla. 1995. Taxol metabolism and disposition in cancer patients. *Drug metabolism and disposition: the biological fate of chemicals*. 23:506-512.

Wang, C., A. Cormier, B. Gigant, and M. Knossow. 2007. Insight into the GTPase activity of tubulin from complexes with stathmin-like domains. *Biochemistry*. 46:10595-10602.

Wang, H., B. Liu, C. Zhang, G. Peng, M. Liu, D. Li, F. Gu, Q. Chen, J.T. Dong, L. Fu, and J. Zhou. 2009. Parkin regulates paclitaxel sensitivity in breast cancer via a microtubule-dependent mechanism. *The Journal of pathology*. 218:76-85.

Wang, T., J.H. Lv, X.F. Zhang, C.J. Li, X. Han, and Y.J. Sun. 2010. Tissue inhibitor of metalloproteinase-1 protects MCF-7 breast cancer cells from paclitaxel-induced apoptosis by decreasing the stability of cyclin B1. *International journal of cancer. Journal international du cancer*. 126:362-370.

Wang, W., L. Cao, C. Wang, B. Gigant, and M. Knossow. 2015. Kinesin, 30 years later: Recent insights from structural studies. *Protein science : a publication of the Protein Society*. 24:1047-1056.

Wang, X., Z. Yang, H. Zhang, L. Ding, X. Li, C. Zhu, Y. Zheng, and Q. Ye. 2008. The estrogen receptor-interacting protein HPIP increases estrogen-responsive gene expression through activation of MAPK and AKT. *Biochimica et biophysica acta*. 1783:1220-1228.

Wang, Y., S. Yin, K. Blade, G. Cooper, D.R. Menick, and F. Cabral. 2006. Mutations at leucine 215 of beta-tubulin affect paclitaxel sensitivity by two distinct mechanisms. *Biochemistry*. 45:185-194.

Wani, M.C., H.L. Taylor, M.E. Wall, P. Coggon, and A.T. McPhail. 1971. Plant antitumor agents. VI. The isolation and structure of taxol, a novel antileukemic and antitumor agent from Taxus brevifolia. *Journal of the American Chemical Society*. 93:2325-2327.

Weisenberg, R.C. 1972. Microtubule formation in vitro in solutions containing low calcium concentrations. *Science*. 177:1104-1105.

Westermann, S., and K. Weber. 2003. Post-translational modifications regulate microtubule function. *Nature reviews. Molecular cell biology*. 4:938-947.

Wittmann, T., A. Hyman, and A. Desai. 2001. The spindle: a dynamic assembly of microtubules and motors. *Nature cell biology*. 3:E28-34.

Xiao, H., H. Wang, X. Zhang, Z. Tu, C. Bulinski, M. Khrapunovich-Baine, R. Hogue Angeletti, and S.B. Horwitz. 2012. Structural evidence for cooperative microtubule stabilization by Taxol and the endogenous dynamics regulator MAP4. *ACS chemical biology*. 7:744-752.

Xu, X., C. Jiang, S. Wang, Y. Tai, T. Wang, L. Kang, Z. Fan, S. Li, L. Li, J. Fu, J. Liu, Q. Ji, X. Wang, L. Wei, and Q. Ye. 2013. HPIP is upregulated in liver cancer and promotes hepatoma cell proliferation via activation of G2/M transition. *IUBMB life*. 65:873-882.

Yared, J.A., and K.H. Tkaczuk. 2012. Update on taxane development: new analogs and new formulations. *Drug design, development and therapy*. 6:371-384.

Yeung, T.K., C. Germond, X. Chen, and Z. Wang. 1999. The mode of action of taxol: apoptosis at low concentration and necrosis at high concentration. *Biochemical and biophysical research communications*. 263:398-404.

Yu, Y.H., F.P. Siao, L.C. Hsu, and P.H. Yen. 2012. TEX11 modulates germ cell proliferation by competing with estrogen receptor beta for the binding to HPIP. *Molecular endocrinology*. 26:630-642.

Yun, M., D. Lee, M.N. Park, E.O. Kim, E.J. Sohn, B.M. Kwon, and S.H. Kim. 2015. Cinnamaldehyde derivative (CB-PIC) sensitizes chemo-resistant cancer cells to drug-induced apoptosis via suppression of MDR1 and its upstream STAT3 and AKT signalling. *Cellular physiology and biochemistry : international journal of experimental cellular physiology, biochemistry, and pharmacology*. 35:1821-1830.

Zhai, Y., P.J. Kronebusch, and G.G. Borisy. 1995. Kinetochore microtubule dynamics and the metaphase-anaphase transition. *The Journal of cell biology*. 131:721-734.

Zhang, X., Q. Wang, M.T. Ling, Y.C. Wong, S.C. Leung, and X. Wang. 2007. Anti-apoptotic role of TWIST and its association with Akt pathway in mediating taxol resistance in nasopharyngeal carcinoma cells. *International journal of cancer. Journal international du cancer*. 120:1891-1898.

Zhao, W., Y. Song, B. Xu, and Q. Zhan. 2012. Overexpression of centrosomal protein Nlp confers breast carcinoma resistance to paclitaxel. *Cancer biology & therapy*. 13:156-163.

Zhou, J., and P. Giannakakou. 2005. Targeting microtubules for cancer chemotherapy. *Current medicinal chemistry. Anti-cancer agents*. 5:65-71.

Publications

THE JOURNAL OF BIOLOGICAL CHEMISTRY VOL. 287, NO. 8, pp. 5600–5614, February 17, 2012

Functional Regulation of Pre-B-cell Leukemia Homeobox Interacting Protein 1 (PBXIP1/HPIP) in Erythroid Differentiation*[S]

Received for publication, August 5, 2011, and in revised form, December 20, 2011 Published, JBC Papers in Press, December 20, 2011, DOI 10.1074/jbc.M111.289843

Bramanandam Manavathi[‡1], Dennis Lo[§2], Suresh Bugide[‡2], Oindrilla Dey[‡], Suzan Imren[§], Mitchell J. Weiss[¶], and R. Keith Humphries[§3]

From the [‡]Molecular and Cellular Oncology Laboratory, Department of Biochemistry, School of Life Sciences, University of Hyderabad, Hyderabad-500046, India, the [§]Terry Fox Laboratory, British Columbia Cancer Agency, Vancouver, British Columbia V5Z 1L3, Canada, the Department of Medicine, University of British Columbia, Vancouver, British Columbia V5Z 1L3, Canada, and the [¶]Division of Hematology, The Children's Hospital of Philadelphia, Philadelphia, Pennsylvania 19104

Background: HPIP is a pre-B-cell leukemia homeobox 1 (PBX1) interacting protein with unknown function in hematopoiesis.
Results: The *HPIP* gene is a target of GATA1 and CTCF and regulates erythroid differentiation involving PI3K/AKT-dependent mechanisms.
Conclusion: *HPIP* is a novel downstream target of GATA1 and serves as an essential regulator of erythroid differentiation.
Significance: A new regulator of erythroid differentiation is discovered. This finding may help in better understanding erythropoiesis.

Pre-B-cell leukemia homeobox interacting protein 1 or human PBX1 interacting protein (PBXIP1/HPIP) is a co-repressor of pre-B-cell leukemia homeobox 1 (PBX1) and is also known to regulate estrogen receptor functions by associating with the microtubule network. Despite its initial discovery in the context of hematopoietic cells, little is yet known about the role of HPIP in hematopoiesis. Here, we show that lentivirus-mediated overexpression of HPIP in human CD34$^+$ cells enhances hematopoietic colony formation *in vitro*, whereas HPIP knockdown leads to a reduction in the number of such colonies. Interestingly, erythroid colony number was significantly higher in HPIP-overexpressing cells. In addition, forced expression of HPIP in K562 cells, a multipotent erythro-megakaryoblastic leukemia cell line, led to an induction of erythroid differentiation. HPIP overexpression in both CD34$^+$ and K562 cells was associated with increased activation of the PI3K/AKT pathway, and corresponding treatment with a PI3K-specific inhibitor, LY-294002, caused a reduction in clonogenic progenitor number in HPIP-expressing CD34$^+$ cells and decreased K562 cell differentiation. Combined, these findings point to an important role of the PI3K/AKT pathway in mediating HPIP-induced effects on the growth and differentiation of hematopoietic cells. Interestingly, *HPIP* gene expression was found to be induced in K562 cells in response to erythroid differentiation signals such as DMSO and erythropoietin. The erythroid lineage-specific transcription factor GATA1 binds to the *HPIP* promoter and activates *HPIP* gene transcription in a CCCTC-binding factor (CTCF)-dependent manner. Co-immunoprecipitation and co-localization experiments revealed the association of CTCF with GATA1 indicating the recruitment of CTCF/GATA1 transcription factor complex onto the *HPIP* promoter. Together, this study provides evidence that *HPIP* is a target of GATA1 and CTCF in erythroid cells and plays an important role in erythroid differentiation by modulating the PI3K/AKT pathway.

The human hematopoietic system is composed of a heterogeneous population of cells that range in function from mature cells with limited proliferative potential to pluripotent stem cells known as hematopoietic stem cells (HSC)[4] with extensive proliferation, differentiation, and self-renewal capacities (1, 2). This process is governed by the interplay of a number of transcription factors and various signaling pathways, which altogether facilitate proper hematopoietic development (3, 4). Emerging evidence indicates that human leukemias, lymphomas, and possibly myelodysplastic syndromes are initiated at the level of HSCs and/or early multipotent progenitors that have been transformed due to genetic/chromosomal aberrations or deregulation of gene expression (5). Of several regulators of HSC, PBX transcription factors play an important role in the establishment and maintenance of definitive hematopoiesis, and PBX overexpression has been linked to leukemia development (6). PBX proteins mainly act as cofactors for HOX pro-

* This work was supported by Department of Science and Technology under Better Opportunities for Young Scientist in Chosen Areas of Science and Technology (to B. M.), a Terry Fox Foundation program project grant (to R. K. H.), the British Columbia Cancer Foundation, and in part by the Department of Science and Technology under the Fast-Track Program young investigator award (to B. M.).
[S] This article contains supplemental Figs. S1–S8.
[1] To whom correspondence may be addressed: Dept of Biochemistry, School of Life Sciences, University of Hyderabad, Hyderabad-500046, India. E-mail: manavathibsl@uohyd.ernet.in.
[2] Both authors contributed equally to this work.
[3] To whom correspondence may be addressed. E-mail: khumphri@bccrc.ca.

[4] The abbreviations used are: HSC, hematopoietic stem cell; PBX1, pre-B-cell leukemia homeobox 1; PBXIP1 or HPIP, pre-B-cell leukemia homeobox interacting protein 1; Epo, erythropoietin; q, quantitative; CFC, colony-forming cell assay; E/Meg, erythroid and megakaryocyte; 4-OHT, 4-hydroxytamoxifen; MTT, 3-(4,5-dimethylthiazol-2-yl)-2,5-diphenyltetrazolium bromide; CTCF, CCCTC-binding factor.

Derailed Estrogen Signaling and Breast Cancer: An Authentic Couple

Bramanandam Manavathi, Oindrilla Dey, Vijay Narsihma Reddy Gajulapalli, Raghavendra Singh Bhatia, Suresh Bugide, and Rakesh Kumar

Molecular and Cellular Oncology Laboratory (B.M., O.D., V.N.R.G., R.S.B., S.B.), Department of Biochemistry, School of Life Sciences, University of Hyderabad, Hyderabad 500046, India; Cancer Research Program (R.K.), Rajiv Gandhi Centre for Biotechnology, Thiruvananthapuram 695014, India; and Department of Biochemistry and Molecular Biology (R.K.), The George Washington University, Washington, D.C. 20052

Estrogen or 17β-estradiol, a steroid hormone, plays a critical role in the development of mammary gland via acting through specific receptors. In particular, estrogen receptor-α (ERα) acts as a transcription factor and/or a signal transducer while participating in the development of mammary gland and breast cancer. Accumulating evidence suggests that the transcriptional activity of ERα is altered by the action of nuclear receptor coregulators and might be responsible, at least in part, for the development of breast cancer. In addition, this process is driven by various posttranslational modifications of ERα, implicating active participation of the upstream receptor modifying enzymes in breast cancer progression. Emerging studies suggest that the biological outcome of breast cancer cells is also influenced by the cross talk between microRNA and ERα signaling, as well as by breast cancer stem cells. Thus, multiple regulatory controls of ERα render mammary epithelium at risk for transformation upon deregulation of normal homeostasis. Given the importance that ERα signaling has in breast cancer development, here we will highlight how the activity of ERα is controlled by various regulators in a spatial and temporal manner, impacting the progression of the disease. We will also discuss the possible therapeutic value of ERα modulators as alternative drug targets to retard the progression of breast cancer. (***Endocrine Reviews*** **34: 1–32, 2013)**

ISSN Print 0163-769X ISSN Online 1945-7189
Printed in U.S.A.

doi: 10.1210/er.2011-1057 Received November 30, 2011. Accepted July 9, 2012.
First Published Online September 4, 2012

I. Introduction

Breast cancer is heterogeneous in nature that originates from the mammary epithelial cells. Despite advances made in the understanding of the molecular and cellular events that underlie the disease, it remains the leading cause of cancer deaths among females worldwide (1). A woman's risk of breast cancer is influenced by her reproductive history, *i.e.*, lifetime exposure to reproduc-

Abbreviations: AIB1, Amplified in breast cancer-1; AKT, serine/threonine protein kinase; ALDH, aldehyde dehydrogenase; ATM, ataxia telangiectasia mutated; ATR, ataxia telangiectasia and rad3-related protein; BCAS3, breast carcinoma amplified sequence 3; BRCA1, breast cancer 1; BrCSC, breast cancer stem cell; BT-IC, breast tumor-initiating cell; CDK4, cyclin-dependent kinase; Ciz1, CDKN1A-interacting zinc finger protein 1; DACH1, dachshund homolog 1; DBC1, deleted in breast cancer 1; DNAPK, DNA-dependent protein kinase; E2, estrogen or 17β-estradiol; Efp, estrogen-responsive finger protein; EGFR, epidermal growth factor receptor; EMT, epithelial-mesenchymal transition; ER, estrogen receptor; ERE, estrogen response element; GPR30, G protein-coupled receptor 30; GREB1, growth regulation by estrogen in breast cancer 1; GSK3β, glycogen synthase kinase 3β; HAT, histone acetyl transferase; HDAC, histone deacetylase; HPIP, hematopoietic PBX-interacting protein 1; MaSC, mammary stem cell; miRNA, microRNA; MTA, metastasis-associated protein; MTA1s, MTA1 short form; NCOR1, nuclear receptor corepressor 1; NuRD, nucleosome remodeling and histone deacetylation complex; PAK1, serine/threonine p21-activated kinase; PELP1, proline, glutamic acid and leucine-rich protein; PHB, prohibitin; PI3K, phosphatidylinositol 3 kinase; PKA, protein kinase A; PR, progesterone receptor; PRMT1, protein arginine N-methyltransferase 1; REA, repressor of ER activity; SAFB, scaffold attachment factor B; SCID, severe combined immunodeficiency; SERM, selective ER modulator; SIRT1, sirtuin 1; S6K1, S6 kinase 1; SP, specificity protein; TFF1, trefoil factor 1; UTR, untranslated region.

Plagiarism report

Understanding the Role of HPIP in Taxol Resistance Using Breast Cancer As a Model System

by Oindrilla Dey

Understanding the Role of HPIP in Taxol Resistance Using Breast Cancer As a Model System

ORIGINALITY REPORT

18%	9%	16%	5%
SIMILARITY INDEX	INTERNET SOURCES	PUBLICATIONS	STUDENT PAPERS

PRIMARY SOURCES

1	McGrogan, B.T.. "Taxanes, microtubules and chemoresistant breast cancer", BBA - Reviews on Cancer, 200804 Publication	3%
2	www.ncbi.nlm.nih.gov Internet Source	2%
3	Maria Kavallaris. "Microtubules and resistance to tubulin-binding agents", Nature Reviews Cancer, 02/11/2010 Publication	1%
4	www.jbc.org Internet Source	<1%
5	Li, Zhaoming, Tian Tian, Xiaopeng Hu, Xudong Zhang, Feifei Nan, Yu Chang, Feng Lv, and Mingzhi Zhang. "Six1 mediates resistance to paclitaxel in breast cancer cells", Biochemical and Biophysical Research Communications, 2013. Publication	<1%
6	mitchison.med.harvard.edu Internet Source	<1%